(12) INTERNATIONAL APPLICATION PUBLISHED UNDER THE PATENT COOPERATION TREATY (PCT)

(19) World Intellectual Property Organization
International Bureau

(43) International Publication Date
28 March 2019 (28.03.2019)

WIPO | PCT

(10) International Publication Number
WO 2019/060921 A1

(51) International Patent Classification:
C12N 15/09 (2006.01) *D01F 4/02* (2006.01)
C07K 14/435 (2006.01) *D01D 5/24* (2006.01)
D01F 6/68 (2006.01)

(21) International Application Number:
PCT/US2018/052754

(22) International Filing Date:
25 September 2018 (25.09.2018)

(25) Filing Language: English

(26) Publication Language: English

(30) Priority Data:
62/563,022 25 September 2017 (25.09.2017) US

(71) Applicant: **BOLT THREADS, INC.** [US/US]; 5858 Horton Street, Suite 400, Emeryville, CA 94608 (US).

(72) Inventors: **BAKHTIARY DAVIJANI, Amir, Ahmad**; c/o Bolt Threads, Inc., 5858 Horton Street, Suite 400, Emeryville, CA 94608 (US). **TOM, Steven**; c/o Bolt Threads, Inc., 5858 Horton Street, Suite 400, Emeryville, CA 94608 (US). **BOULET-AUDET, Maxime**; c/o Bolt Threads, Inc., 5858 Horton Street, Suite 400, Emeryville, CA 94608 (US). **GUERETTE, Paul, Andre**; c/o Bolt Threads, Inc., 5858 Horton Street, Suite 400, Emeryville, CA 94608 (US). **WRAY, Lindsay**; c/o Bolt Threads, Inc., 5858 Horton Street, Suite 400, Emeryville, CA 94608 (US). **SUBLER, Nicole, Elizabeth**; c/o Bolt Threads, Inc., 5858 Horton Street, Suite 400, Emeryville, CA 94608 (US). **ZULFIQAR, Zoya, Nasir**; c/o Bolt Threads, Inc., 5858 Horton Street, Suite 400, Emeryville, CA 94608 (US). **LI, Hua**; c/o Bolt Threads, Inc., 5858 Horton Street, Suite 400, Emeryville, CA 94608 (US). **WANG, Jessica**; c/o Bolt Threads, Inc., 5858 Horton Street, Suite 400, Emeryville, CA 94608 (US).

(74) Agent: **HURT, Nicholas, S.** et al.; Fenwick & West LLP, Silicon Valley Center, 801 California Street, Mountain View, CA 94041 (US).

(81) Designated States *(unless otherwise indicated, for every kind of national protection available)*: AE, AG, AL, AM, AO, AT, AU, AZ, BA, BB, BG, BH, BN, BR, BW, BY, BZ, CA, CH, CL, CN, CO, CR, CU, CZ, DE, DJ, DK, DM, DO, DZ, EC, EE, EG, ES, FI, GB, GD, GE, GH, GM, GT, HN, HR, HU, ID, IL, IN, IR, IS, JO, JP, KE, KG, KH, KN, KP, KR, KW, KZ, LA, LC, LK, LR, LS, LU, LY, MA, MD, ME, MG, MK, MN, MW, MX, MY, MZ, NA, NG, NI, NO, NZ, OM, PA, PE, PG, PH, PL, PT, QA, RO, RS, RU, RW, SA, SC, SD, SE, SG, SK, SL, SM, ST, SV, SY, TH, TJ, TM, TN, TR, TT, TZ, UA, UG, US, UZ, VC, VN, ZA, ZM, ZW.

(84) Designated States *(unless otherwise indicated, for every kind of regional protection available)*: ARIPO (BW, GH, GM, KE, LR, LS, MW, MZ, NA, RW, SD, SL, ST, SZ, TZ, UG, ZM, ZW), Eurasian (AM, AZ, BY, KG, KZ, RU, TJ, TM), European (AL, AT, BE, BG, CH, CY, CZ, DE, DK, EE, ES, FI, FR, GB, GR, HR, HU, IE, IS, IT, LT, LU, LV, MC, MK, MT, NL, NO, PL, PT, RO, RS, SE, SI, SK, SM, TR), OAPI (BF, BJ, CF, CG, CI, CM, GA, GN, GQ, GW, KM, ML, MR, NE, SN, TD, TG).

Published:
— *with international search report (Art. 21(3))*
— *with sequence listing part of description (Rule 5.2(a))*

(54) Title: METHODS OF GENERATING HIGHLY-CRYSTALLINE RECOMBINANT SPIDER SILK PROTEIN FIBERS

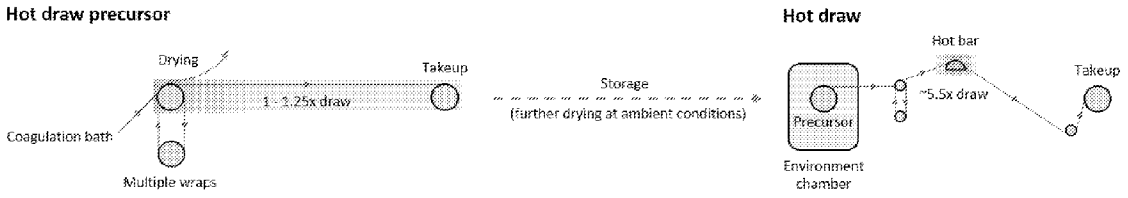


FIG. 2B

(57) Abstract: Provided herein are scalable methods of processing wet-spun fiber comprising recombinant spider silk polypeptides to generate a three-dimensional crystalline lattice of beta-sheet structures in the fiber.

WO 2019/060921 A1

Methods of Generating Highly-crystalline Recombinant Spider Silk Protein Fibers

Cross-Reference to Related Applications

[0001] This application claims the benefit of US Provisional Application No. 62/563,022, filed September 25, 2017, the contents of which are incorporated by reference in its entirety.

Sequence Listing

[0002] The instant application contains a Sequence Listing which has been submitted electronically in ASCII format and is hereby incorporated by reference in its entirety. Said ASCII copy, created on September 25, 2018, is named 41410WO_CRF_sequencelisting.txt and is 61,801 bytes in size.

Field of the Invention

[0003] The present invention relates to scalable methods of processing wet-spun fiber comprising recombinant spider silk polypeptides to generate a three-dimensional crystalline lattice of beta-sheet structures in the fiber.

Background of the Invention

[0004] Protein-based materials are of increasing interest as an alternative to petroleum-based products. To this end, considerable effort has been made to develop methods of making materials and fibers from regenerated protein sources derived from plants (e.g., zein, soy, wheat gluten) and animals (e.g. casein, keratin and collagen). Fiber made from regenerated protein dates back to the 1890s and has been made using various traditional wet-spinning techniques.

[0005] Because proteins typically form brittle structures, plasticizers such as polyols, lipids and sugars have been combined with regenerated protein sources to generate fibers and materials that are less susceptible to breaking and deformation. Plasticizers interact with the tertiary structures of proteins and can alter the physio-chemical properties of the proteins. For example, plasticizers may be used to lower the glass transition and melting temperature of a protein, thus allowing the protein to be manipulated and reformed into new tertiary structures while preventing degradation of the protein.

[0006] A substantial limitation in using regenerated and recombinant protein sources to create materials is variability in purity of the protein and the presence of impurities such as lipids and sugars which may act as plasticizers, thus producing materials with variable properties. Accordingly, innovations related to novel fibers or materials comprising proteins typically entail precise characterization of any plasticizers used and rheological analysis of the protein composition used to form the materials. *See e.g.* US 5,528,293; US 7,066,995; US 2014/0060383.

[0007] Silk proteins such as silk fibroin and spidroins have a complex secondary and tertiary structures which make them an ideal candidate for the creation of protein-based materials. Specifically, silk proteins form complex beta-sheet structures that are extremely stable and only denature at very high temperatures, far above the melting temperature of the protein.

[0008] While there has been significant work performed in generating fibers and materials from recombinant spider silk polypeptides using traditional spinning and molding processes (*see* US 7,057,023), much of this work has been proof-of-principle work that is not reproducible or scalable for mass commercialization. Specifically, none of the work has precisely characterized the recombinant spider silk polypeptide that is used as an input to these processes and the molecular structures formed by the recombinant spider silk polypeptide in the material that is output from the processes. Since impurities and ambient water bound to the protein may plasticize or otherwise interact with the recombinant spider silk polypeptides, failure to understand the impact of these components can produce materials with varying tertiary structures and mechanical properties. Accordingly, there is a need for processes of manufacturing materials from recombinant spider silk polypeptides which use the specific physio-chemical properties of recombinant spider silk polypeptide compositions to create fibers comprising stable and reproducible tertiary structures.

Summary of the Invention

[0009] Provided herein, according to some embodiments of the invention, is a drawn fiber comprising recombinant spider silk polypeptide, wherein the fiber is generated by: dissolving a powder comprising the recombinant spider silk polypeptide into a solvent to generate a spin dope; extruding the spin dope into a coagulation bath to form a precursor fiber; collecting the precursor fiber without drawing the precursor fiber; and drawing the precursor fiber over a hot surface to generate a drawn fiber, wherein the drawn fiber has a

crystallinity index of at least 4%, at least 5%, at least 6%, or at least 7% as measured using X-ray diffraction.

[0010] In some embodiments, the powder comprising the recombinant spider silk polypeptide is comprised of at least 60% recombinant spider silk polypeptide by weight. In some embodiments, the powder comprising the recombinant spider silk polypeptide is comprised of at least 70% recombinant spider silk polypeptide by weight. In some embodiments, the powder comprising the recombinant spider silk polypeptide is comprised of at least 80% recombinant spider silk polypeptide by weight.

[0011] In some embodiments, the drawn fiber is drawn over the hot surface at a draw ratio of at least 2X. In some embodiments, the drawn fiber is drawn over the hot surface at a draw ratio of at least 3X. In some embodiments, the drawn fiber is drawn over the hot surface at a draw ratio of at least 4X. In some embodiments, the drawn fiber is drawn over the hot surface at a draw ratio of at least 6X.

[0012] In some embodiments, the draw ratio is computed by determining the draw ratio at failure. In some embodiments, the draw ratio at failure comprises determining the distribution of maximum elongation at break of one or more precursor fibers using an apparatus designed to draw the fiber over a hot surface while increasing the draw ratio.

[0013] In some embodiments, the generation of the fiber further comprises drawing the drawn fiber over a hot surface one or more times.

[0014] In some embodiments, the drawing the drawn fibers over a hot surface one of more times comprises: determining a draw ratio at failure of the precursor fiber; and dividing the draw ratio at failure of the precursor fiber over the one or more times.

[0015] In some embodiments, the generation of the drawn fiber comprises annealing the precursor fiber prior to drawing the fiber. In some embodiments, annealing the precursor fiber comprises annealing the precursor fiber with alcohol vapor.

[0016] In some embodiments, the solvent is formic acid. In some embodiments, the solvent is NMMO.

[0017] In some embodiments, the drawn fiber has increased beta-sheet formation relative to the precursor fiber. In some embodiments, the drawn fiber has increased beta-sheet formation proportional to the draw ratio used to draw the fiber over the hot surface.

[0018] In some embodiments, the hot surface is at least 190 degrees Celsius. In some embodiments, the hot surface is at least 200 degrees Celsius. In some embodiments, the hot

surface is at least 20 degrees Celsius greater than the glass transition temperature of the precursor fiber.

[0019] In some embodiments, the recombinant spider silk polypeptide is 18B (SEQID NO: 1).

[0020] In some embodiments, the tenacity of the drawn fiber is greater than 20 cN/tex. In some embodiments, the tenacity of the drawn fiber is greater than 25 cN/tex. In some embodiments, the tenacity of the drawn fiber is greater than 26 cN/tex.

[0021] In some embodiments, the Herman orientation factor of the drawn fiber is approximately the same as native silk fiber. In some embodiments, the drawn fiber has more than 1.5 times, more than 2 times, or more than 2.5 times increased beta-sheet content as compared to air drawn fibers not drawn over a hot surface. In some embodiments, the drawn fiber has an increased 3D β-sheet content as compared to air drawn fibers not drawn over a hot surface.

Brief Description of the Drawings

[0022] The foregoing and other objects, features and advantages will be apparent from the following description of particular embodiments of the invention, as illustrated in the accompanying drawings in which like reference characters refer to the same parts throughout the different views. The drawings are not necessarily to scale, emphasis instead placed upon illustrating the principles of various embodiments of the invention.

[0023] Figure 1 depicts the tertiary structures formed in native silk fibroin and spidroin polypeptides.

[0024] Figure 2A depicts the drawing process used to generate "Air Draw" fibers according to one embodiment of the present invention.

[0025] Figure 2B depicts the drawing process used to generate "Hot Draw" fibers according to one embodiment of the present invention.

[0026] Figure 3A depicts the tenacity of Air Draw and Hot Draw fibers according to some embodiments.

[0027] Figure 3B depicts the initial modulus of Air Draw and Hot Draw fibers according to some embodiments.

[0028] Figure 4 depicts FTIR analysis corresponding to beta-sheet formation in Hot Draw fibers, precursor fibers and recombinant silk polypeptide powder according to some embodiments.

[0029] Figure 5 depicts the 2D X-ray diffraction patterns of the Precursor, Air Drawn and Hot drawn fibers according to a specific embodiment.

[0030] Figure 6A depicts the integrated scan from precursor fibers according to a specific embodiment.

[0031] Figure 6B depicts the integrated scan from Air Draw fibers according to a specific embodiment.

[0032] Figure 6C depicts the integrated scan from Hot Draw fibers according to a specific embodiment.

[0033] Figure 7A depicts azimuthal profiles of the fibers according to a specific embodiment.

[0034] Figure 7B depicts azimuthal profiles of the fibers according to a specific embodiment.

[0035] Figure 8 depicts a graph of tenacities measured from CDA-stored and annealed precursor fibers before and after post-hot draw annealing. A: hot drawn CDA-stored precursor. B: hot drawn CDA-stored precursor after annealing. C: hot drawn annealed precursor. D: hot drawn annealed precursor, annealed again after hot drawing.

[0036] Figure 9 depicts stress-strain curves corresponding to precursor and hot drawn *Bombyx mori* RSF fibers using a TexTechno Favimat+ at 65% relative humidity, according to ASTM standard D1776.

[0037] Figure 10 depicts a plot of the loss modulus and loss tangent curves for CDA-stored and annealed precursor fibers. The maxima indicating the glass transition temperature (Tg) is shown using arrows.

[0038] Figure 11 depicts a plot of complex viscosity and phase angle of 3 NMMO-based dopes as a function of frequency and temperature.

[0039] Figure 12 depicts radially integrated intensity through equatorial reflections generated from X-Ray diffraction of continuously hot drawn NMMO-based fibers.

[0040] Figure 13 depicts Azimuthally integrated intensity through the (120) reflection generated from X-Ray diffraction of continuously hot drawn NMMO-based fibers.

[0041] Figure 14 depicts Azimuthally integrated intensity through the (200) reflection generated from X-Ray diffraction of continuously hot drawn NMMO-based fibers.

[0042] Figure 15 depicts the draw ratio at failure of methanol vapor annealed and CDA-stored (unannealed) precursors drawn over a hot surface ranging from 120°C to 225°C.

[0043] Figure 16 depicts the draw ratio at failure for formic acid-based fibers spun with varying theoretical bath draw ratios and air draw ratios for fibers hot drawn at 200°C.

[0044] Figure 17 shows a plot of predicted continuous hot draw ratio vs. batch hot draw ratio at failure for formic-acid based precursors, illustrating a correspondence between the predicted and observed draw ratio at break.

Detailed Description of the Invention

[0045] The details of various embodiments of the invention are set forth in the description below. Other features, objects, and advantages of the invention will be apparent from the description. Unless otherwise defined herein, scientific and technical terms used in connection with the present invention shall have the meanings that are commonly understood by those of ordinary skill in the art. Further, unless otherwise required by context, singular terms shall include the plural and plural terms shall include the singular. The terms "a" and "an" includes plural references unless the context dictates otherwise. Generally, nomenclatures used in connection with, and techniques of, biochemistry, enzymology, molecular and cellular biology, microbiology, genetics and protein and nucleic acid chemistry and hybridization described herein are those well-known and commonly used in the art.

[0046] The following terms, unless otherwise indicated, shall be understood to have the following meanings:

[0047] The term "polynucleotide" or "nucleic acid molecule" refers to a polymeric form of nucleotides of at least 10 bases in length. The term includes DNA molecules (*e.g.*, cDNA or genomic or synthetic DNA) and RNA molecules (*e.g.*, mRNA or synthetic RNA), as well as analogs of DNA or RNA containing non-natural nucleotide analogs, non-native internucleoside bonds, or both. The nucleic acid can be in any topological conformation. For instance, the nucleic acid can be single-stranded, double-stranded, triple-stranded, quadruplexed, partially double-stranded, branched, hairpinned, circular, or in a padlocked conformation.

[0048] Unless otherwise indicated, and as an example for all sequences described herein under the general format "SEQ ID NO:", "nucleic acid comprising SEQ ID NO:1" refers to a nucleic acid, at least a portion of which has either (i) the sequence of SEQ ID NO:1, or (ii) a sequence complementary to SEQ ID NO:1. The choice between the two is dictated by the context. For instance, if the nucleic acid is used as a probe, the choice

between the two is dictated by the requirement that the probe be complementary to the desired target.

[0049] An "isolated" RNA, DNA or a mixed polymer is one which is substantially separated from other cellular components that naturally accompany the native polynucleotide in its natural host cell, *e.g.*, ribosomes, polymerases and genomic sequences with which it is naturally associated.

[0050] An "isolated" organic molecule (*e.g.*, a silk protein) is one which is substantially separated from the cellular components (membrane lipids, chromosomes, proteins) of the host cell from which it originated, or from the medium in which the host cell was cultured. The term does not require that the biomolecule has been separated from all other chemicals, although certain isolated biomolecules may be purified to near homogeneity.

[0051] The term "recombinant" refers to a biomolecule, *e.g.*, a gene or protein, that (1) has been removed from its naturally occurring environment, (2) is not associated with all or a portion of a polynucleotide in which the gene is found in nature, (3) is operatively linked to a polynucleotide which it is not linked to in nature, or (4) does not occur in nature. The term "recombinant" can be used in reference to cloned DNA isolates, chemically synthesized polynucleotide analogs, or polynucleotide analogs that are biologically synthesized by heterologous systems, as well as proteins and/or mRNAs encoded by such nucleic acids.

[0052] An endogenous nucleic acid sequence in the genome of an organism (or the encoded protein product of that sequence) is deemed "recombinant" herein if a heterologous sequence is placed adjacent to the endogenous nucleic acid sequence, such that the expression of this endogenous nucleic acid sequence is altered. In this context, a heterologous sequence is a sequence that is not naturally adjacent to the endogenous nucleic acid sequence, whether or not the heterologous sequence is itself endogenous (originating from the same host cell or progeny thereof) or exogenous (originating from a different host cell or progeny thereof). By way of example, a promoter sequence can be substituted (*e.g.*, by homologous recombination) for the native promoter of a gene in the genome of a host cell, such that this gene has an altered expression pattern. This gene would now become "recombinant" because it is separated from at least some of the sequences that naturally flank it.

[0053] A nucleic acid is also considered "recombinant" if it contains any modifications that do not naturally occur to the corresponding nucleic acid in a genome. For instance, an endogenous coding sequence is considered "recombinant" if it contains an insertion, deletion

or a point mutation introduced artificially, *e.g.*, by human intervention. A "recombinant nucleic acid" also includes a nucleic acid integrated into a host cell chromosome at a heterologous site and a nucleic acid construct present as an episome.

[0054] The term "peptide" as used herein refers to a short polypeptide, *e.g.*, one that is typically less than about 50 amino acids long and more typically less than about 30 amino acids long. The term as used herein encompasses analogs and mimetics that mimic structural and thus biological function.

[0055] The term "polypeptide" encompasses both naturally-occurring and non-naturally-occurring proteins, and fragments, mutants, derivatives and analogs thereof. A polypeptide may be monomeric or polymeric. Further, a polypeptide may comprise a number of different domains each of which has one or more distinct activities.

[0056] The term "isolated protein" or "isolated polypeptide" is a protein or polypeptide that by virtue of its origin or source of derivation (1) is not associated with naturally associated components that accompany it in its native state, (2) exists in a purity not found in nature, where purity can be adjudged with respect to the presence of other cellular material (*e.g.*, is free of other proteins from the same species) (3) is expressed by a cell from a different species, or (4) does not occur in nature (*e.g.*, it is a fragment of a polypeptide found in nature or it includes amino acid analogs or derivatives not found in nature or linkages other than standard peptide bonds). Thus, a polypeptide that is chemically synthesized or synthesized in a cellular system different from the cell from which it naturally originates will be "isolated" from its naturally associated components. A polypeptide or protein may also be rendered substantially free of naturally associated components by isolation, using protein purification techniques well known in the art. As thus defined, "isolated" does not necessarily require that the protein, polypeptide, peptide or oligopeptide so described has been physically removed from its native environment.

[0057] The term "polypeptide fragment" refers to a polypeptide that has a deletion, *e.g.*, an amino-terminal and/or carboxy-terminal deletion compared to a full-length polypeptide. In a preferred embodiment, the polypeptide fragment is a contiguous sequence in which the amino acid sequence of the fragment is identical to the corresponding positions in the naturally-occurring sequence. Fragments typically are at least 5, 6, 7, 8, 9 or 10 amino acids long, preferably at least 12, 14, 16 or 18 amino acids long, more preferably at least 20 amino acids long, more preferably at least 25, 30, 35, 40 or 45, amino acids, even more

preferably at least 50 or 60 amino acids long, and even more preferably at least 70 amino acids long.

[0058] A protein has "homology" or is "homologous" to a second protein if the nucleic acid sequence that encodes the protein has a similar sequence to the nucleic acid sequence that encodes the second protein. Alternatively, a protein has homology to a second protein if the two proteins have "similar" amino acid sequences. (Thus, the term "homologous proteins" is defined to mean that the two proteins have similar amino acid sequences.) As used herein, homology between two regions of amino acid sequence (especially with respect to predicted structural similarities) is interpreted as implying similarity in function.

[0059] When "homologous" is used in reference to proteins or peptides, it is recognized that residue positions that are not identical often differ by conservative amino acid substitutions. A "conservative amino acid substitution" is one in which an amino acid residue is substituted by another amino acid residue having a side chain (R group) with similar chemical properties (*e.g.*, charge or hydrophobicity). In general, a conservative amino acid substitution will not substantially change the functional properties of a protein. In cases where two or more amino acid sequences differ from each other by conservative substitutions, the percent sequence identity or degree of homology may be adjusted upwards to correct for the conservative nature of the substitution. Means for making this adjustment are well known to those of skill in the art. See, *e.g.*, Pearson, 1994, *Methods Mol. Biol.* 24:307-31 and 25:365-89 (herein incorporated by reference).

[0060] The twenty conventional amino acids and their abbreviations follow conventional usage. See *Immunology-A Synthesis* (Golub and Gren eds., Sinauer Associates, Sunderland, Mass., 2nd ed. 1991), which is incorporated herein by reference. Stereoisomers (*e.g.*, D-amino acids) of the twenty conventional amino acids, unnatural amino acids such as α-, α-disubstituted amino acids, N-alkyl amino acids, and other unconventional amino acids may also be suitable components for polypeptides of the present invention. Examples of unconventional amino acids include: 4-hydroxyproline, γ-carboxyglutamate, ε-N,N,N-trimethyllysine, ε-N-acetyllysine, O-phosphoserine, N-acetylserine, N-formylmethionine, 3-methylhistidine, 5-hydroxylysine, N-methylarginine, and other similar amino acids and imino acids (*e.g.*, 4-hydroxyproline). In the polypeptide notation used herein, the left-hand end corresponds to the amino terminal end and the right-hand end corresponds to the carboxy-terminal end, in accordance with standard usage and convention.

[0061] The following six groups each contain amino acids that are conservative substitutions for one another: 1) Serine (S), Threonine (T); 2) Aspartic Acid (D), Glutamic Acid (E); 3) Asparagine (N), Glutamine (Q); 4) Arginine (R), Lysine (K); 5) Isoleucine (I), Leucine (L), Methionine (M), Alanine (A), Valine (V), and 6) Phenylalanine (F), Tyrosine (Y), Tryptophan (W).

[0062] Sequence homology for polypeptides, which is sometimes also referred to as percent sequence identity, is typically measured using sequence analysis software. See, *e.g.*, the Sequence Analysis Software Package of the Genetics Computer Group (GCG), University of Wisconsin Biotechnology Center, 910 University Avenue, Madison, Wis. 53705. Protein analysis software matches similar sequences using a measure of homology assigned to various substitutions, deletions and other modifications, including conservative amino acid substitutions. For instance, GCG contains programs such as "Gap" and "Bestfit" which can be used with default parameters to determine sequence homology or sequence identity between closely related polypeptides, such as homologous polypeptides from different species of organisms or between a wild-type protein and a mutein thereof. See, *e.g.*, GCG Version 6.1.

[0063] A useful algorithm when comparing a particular polypeptide sequence to a database containing a large number of sequences from different organisms is the computer program BLAST (Altschul *et al.*, *J. Mol. Biol.* 215:403-410 (1990); Gish and States, *Nature Genet.* 3:266-272 (1993); Madden *et al.*, *Meth. Enzymol.* 266:131-141 (1996); Altschul *et al.*, *Nucleic Acids Res.* 25:3389-3402 (1997); Zhang and Madden, *Genome Res.* 7:649-656 (1997)), especially blastp or tblastn (Altschul *et al.*, *Nucleic Acids Res.* 25:3389-3402 (1997)).

[0064] Preferred parameters for BLASTp are: Expectation value: 10 (default); Filter: seg (default); Cost to open a gap: 11 (default); Cost to extend a gap: 1 (default); Max. alignments: 100 (default); Word size: 11 (default); No. of descriptions: 100 (default); Penalty Matrix: BLOWSUM62.

[0065] Preferred parameters for BLASTp are: Expectation value: 10 (default); Filter: seg (default); Cost to open a gap: 11 (default); Cost to extend a gap: 1 (default); Max. alignments: 100 (default); Word size: 11 (default); No. of descriptions: 100 (default); Penalty Matrix: BLOWSUM62.The length of polypeptide sequences compared for homology will generally be at least about 16 amino acid residues, usually at least about 20 residues, more usually at least about 24 residues, typically at least about 28 residues, and preferably more

than about 35 residues. When searching a database containing sequences from a large number of different organisms, it is preferable to compare amino acid sequences. Database searching using amino acid sequences can be measured by algorithms other than blastp known in the art. For instance, polypeptide sequences can be compared using FASTA, a program in GCG Version 6.1. FASTA provides alignments and percent sequence identity of the regions of the best overlap between the query and search sequences. Pearson, *Methods Enzymol.* 183:63-98 (1990) (incorporated by reference herein). For example, percent sequence identity between amino acid sequences can be determined using FASTA with its default parameters (a word size of 2 and the PAM250 scoring matrix), as provided in GCG Version 6.1, herein incorporated by reference.

[0066] Throughout this specification and claims, the word "comprise" or variations such as "comprises" or "comprising," will be understood to imply the inclusion of a stated integer or group of integers but not the exclusion of any other integer or group of integers.

[0067] The term "wet spinning" as used herein refers to a method of forming fibers from a polymer wherein the polymer is dissolved in solution and extruded into a substance that makes the dissolved polymer coagulate.

[0068] The term "coagulation bath" as used herein refers to a liquid bath comprising a substance that makes fibers coagulate.

[0069] The term "drawing" as used herein with reference to a fiber refers to the application of force to stretch a wet-spun fiber along its longitudinal axis after extrusion of the fiber into a coagulation bath. The term "undrawn fibers" refers to fibers that have been extruded into a coagulation bath but have not been subject to any drawing force. The term "draw ratio" is a term of art commonly defined as the ratio between the collection rate and the feeding rate. At constant volume, it can be determined from a ratio of the initial diameter (D_i) and final diameter (D_f) of the fiber (i.e., D_i / D_f).

[0070] The term "glass transition temperature" as used herein refers to the temperature at which a substance transitions from a hard, rigid or "glassy" state into a more pliable, "rubbery" state.

[0071] The term "melting temperature" as used herein refers to the temperature at which a substance transitions from a rubbery state to a less-ordered liquid phase. As used herein, the term melting temperature does not refer to the temperature at which recombinant proteins containing beta-sheets are denatured.

[0072] The term "plasticizer" as used herein refers to any molecule that interacts with a polypeptide sequence to prevent the polypeptide sequence from forming tertiary structures and bonds and/or increases the mobility of the polypeptide sequence to promote plasticity and flexibility. Some plasticizers enable the formation of structure. For example, water enables ß-sheet formation in silk.

[0073] Exemplary methods and materials are described below, although methods and materials similar or equivalent to those described herein can also be used in the practice of the present invention and will be apparent to those of skill in the art. All publications and other references mentioned herein are incorporated by reference in their entirety. In case of conflict, the present specification, including definitions, will control. The materials, methods, and examples are illustrative only and not intended to be limiting.

Overview

[0074] Provided herein are scalable methods of post-processing wet-spun fiber comprising recombinant silk proteins. These techniques discussed herein employ stable heat sources in conjunction with known quantities of plasticizers to draw fibers, resulting in an increase in the beta-sheet formation in the drawn fibers and the production of a three-dimensional lattice of beta-sheet structures. These techniques are designed to be scalable and therefore optimal for the large-scale production of recombinant silk fibers.

Recombinant Silk Proteins

[0075] The present disclosure describes embodiments of the invention including fibers synthesized from synthetic proteinaceous copolymers (i.e., recombinant polypeptides). Suitable proteinaceous co-polymers are discussed in U.S. Patent Publication No. 2016/0222174, published August 45, 2016, U.S. Patent Publication No. 2018/0111970, published April 26, 2018, and U.S. Patent Publication No. 2018/0057548, published March 1, 2018, each of which are incorporated by reference herein in its entirety.

[0076] In some embodiments, the synthetic proteinaceous copolymers are made from silk-like polypeptide sequences. In some embodiments, the silk-like polypeptide sequences are 1) block copolymer polypeptide compositions generated by mixing and matching repeat domains derived from silk polypeptide sequences and/or 2) recombinant expression of block copolymer polypeptides having sufficiently large size (approximately 40 kDa) to form useful molded body compositions by secretion from an industrially scalable microorganism. Large

(approximately 40 kDa to approximately 100 kDa) block copolymer polypeptides engineered from silk repeat domain fragments, including sequences from almost all published amino acid sequences of spider silk polypeptides, can be expressed in the modified microorganisms described herein. In some embodiments, silk polypeptide sequences are matched and designed to produce highly expressed and secreted polypeptides capable of molded body formation.

[0077] In some embodiments, block copolymers are engineered from a combinatorial mix of silk polypeptide domains across the silk polypeptide sequence space. In some embodiments, the block copolymers are made by expressing and secreting in scalable organisms (e.g., yeast, fungi, and gram positive bacteria). In some embodiments, the block copolymer polypeptide comprises 0 or more N-terminal domains (NTD), 1 or more repeat domains (REP), and 0 or more C-terminal domains (CTD). In some aspects of the embodiment, the block copolymer polypeptide is >100 amino acids of a single polypeptide chain. In some embodiments, the block copolymer polypeptide comprises a domain that is at least 80%, 81%, 82%, 83%, 84%, 85%, 86%, 87%, 88%, 89%, 90%, 91%, 92%, 93%, 94%, 95%, 96%, 97%, 98%, or 99% identical to a sequence of a block copolymer polypeptide as disclosed in International Publication No. WO/2015/042164, "Methods and Compositions for Synthesizing Improved Silk Fibers," incorporated by reference in its entirety.

[0078] Several types of native spider silks have been identified. The mechanical properties of each natively spun silk type are believed to be closely connected to the molecular composition of that silk. *See, e.g.*, Garb, J.E., et al., Untangling spider silk evolution with spidroin terminal domains, *BMC Evol. Biol.*, 10:243 (2010); Bittencourt, D., et al., Protein families, natural history and biotechnological aspects of spider silk, *Genet. Mol. Res.*, 11:3 (2012); Rising, A., et al., Spider silk proteins: recent advances in recombinant production, structure-function relationships and biomedical applications, *Cell. Mol. Life Sci.*, 68:2, pg. 169-184 (2011); and Humenik, M., et al., Spider silk: understanding the structure-function relationship of a natural fiber, *Prog. Mol. Biol. Transl. Sci.*, 103, pg. 131-85 (2011). For example:

[0079] Aciniform (AcSp) silks tend to have high toughness, a result of moderately high strength coupled with moderately high extensibility. AcSp silks are characterized by large block ("ensemble repeat") sizes that often incorporate motifs of poly serine and GPX. Tubuliform (TuSp or Cylindrical) silks tend to have large diameters, with modest strength and high extensibility. TuSp silks are characterized by their poly serine and poly threonine content, and short tracts of poly alanine. Major Ampullate (MaSp) silks tend to have high strength and modest extensibility. MaSp silks can be one of two subtypes: MaSp1 and

MaSp2. MaSp1 silks are generally less extensible than MaSp2 silks, and are characterized by poly alanine, GX, and GGX motifs. MaSp2 silks are characterized by poly alanine, GGX, and GPX motifs. Minor Ampullate (MiSp) silks tend to have modest strength and modest extensibility. MiSp silks are characterized by GGX, GA, and poly A motifs, and often contain spacer elements of approximately 100 amino acids. Flagelliform (Flag) silks tend to have very high extensibility and modest strength. Flag silks are usually characterized by GPG, GGX, and short spacer motifs.

[0080] The properties of each silk type can vary from species to species, and spiders leading distinct lifestyles (e.g. sedentary web spinners vs. vagabond hunters) or that are evolutionarily older may produce silks that differ in properties from the above descriptions (for descriptions of spider diversity and classification, see Hormiga, G., and Griswold, C.E., Systematics, phylogeny, and evolution of orb-weaving spiders, *Annu. Rev. Entomol.* 59, pg. 487-512 (2014); and Blackedge, T.A. et al., Reconstructing web evolution and spider diversification in the molecular era, *Proc. Natl. Acad. Sci. U.S.A.*, 106:13, pg. 5229-5234 (2009)). However, synthetic block copolymer polypeptides having sequence similarity and/or amino acid composition similarity to the repeat domains of native silk proteins can be used to manufacture on commercial scales consistent molded bodies that have properties that recapitulate the properties of corresponding molded bodies made from natural silk polypeptides.

[0081] In some embodiments, a list of putative silk sequences can be compiled by searching GenBank for relevant terms, e.g. “spidroin” “fibroin” “MaSp”, and those sequences can be pooled with additional sequences obtained through independent sequencing efforts. Sequences are then translated into amino acids, filtered for duplicate entries, and manually split into domains (NTD, REP, CTD). In some embodiments, candidate amino acid sequences are reverse translated into a DNA sequence optimized for expression in *Pichia (Komagataella) pastoris*. The DNA sequences are each cloned into an expression vector and transformed into *Pichia (Komagataella) pastoris*. In some embodiments, various silk domains demonstrating successful expression and secretion are subsequently assembled in combinatorial fashion to build silk molecules capable of molded body formation.

[0082] Silk polypeptides are characteristically composed of a repeat domain (REP) flanked by non-repetitive regions (e.g., C-terminal and N-terminal domains). In an embodiment, both the C-terminal and N-terminal domains are between 75-350 amino acids in length. The repeat domain exhibits a hierarchical architecture, as depicted in Figure 1. The repeat do-

main comprises a series of blocks (also called repeat units). The blocks are repeated, sometimes perfectly and sometimes imperfectly (making up a quasi-repeat domain), throughout the silk repeat domain. The length and composition of blocks varies among different silk types and across different species. Table 1A lists examples of block sequences from selected species and silk types, with further examples presented in Rising, A. et al., Spider silk proteins: recent advances in recombinant production, structure-function relationships and biomedical applications, *Cell Mol. Life Sci.*, 68:2, pg 169-184 (2011); and Gatesy, J. et al., Extreme diversity, conservation, and convergence of spider silk fibroin sequences, *Science*, 291:5513, pg. 2603-2605 (2001). In some cases, blocks may be arranged in a regular pattern, forming larger macro-repeats that appear multiple times (usually 2-8) in the repeat domain of the silk sequence. Repeated blocks inside a repeat domain or macro-repeat, and repeated macro-repeats within the repeat domain, may be separated by spacing elements. In some embodiments, block sequences comprise a glycine rich region followed by a polyA region. In some embodiments, short (~1-10) amino acid motifs appear multiple times inside of blocks. For the purpose of this invention, blocks from different natural silk polypeptides can be selected without reference to circular permutation (i.e., identified blocks that are otherwise similar between silk polypeptides may not align due to circular permutation). . The particular permutation selected for a given silk sequence can be dictated by convenience (usually starting with a G) more than anything else. Silk sequences obtained from the NCBI database can be partitioned into blocks and non-repetitive regions.

[0083] Fiber-forming block copolymer polypeptides from the blocks and/or macro-repeat domains, according to certain embodiments of the invention, is described in International Publication No. WO/2015/042164, incorporated by reference. Natural silk sequences obtained from a protein database such as GenBank or through *de novo* sequencing are broken up by domain (N-terminal domain, repeat domain, and C-terminal domain). The N-terminal domain and C-terminal domain sequences selected for the purpose of synthesis and assembly into fibers or molded bodies include natural amino acid sequence information and other modifications described herein. The repeat domain is decomposed into repeat sequences containing representative blocks, usually 1-8 depending upon the type of silk, that capture critical amino acid information while reducing the size of the DNA encoding the amino acids into a readily synthesizable fragment. In some embodiments, a properly formed block copolymer polypeptide comprises at least one repeat domain comprising at least 1 repeat sequence, and is optionally flanked by an N-terminal domain and/or a C-terminal domain.

[0084] In some embodiments, a repeat domain comprises at least one repeat sequence. In some embodiments, the repeat sequence is 150-300 amino acid residues. In some embodiments, the repeat sequence comprises a plurality of blocks. In some embodiments, the repeat sequence comprises a plurality of macro-repeats. In some embodiments, a block or a macro-repeat is split across multiple repeat sequences.

[0085] In some embodiments, the repeat sequence starts with a glycine, and cannot end with phenylalanine (F), tyrosine (Y), tryptophan (W), cysteine (C), histidine (H), asparagine (N), methionine (M), or aspartic acid (D) to satisfy DNA assembly requirements. In some embodiments, some of the repeat sequences can be altered as compared to native sequences. In some embodiments, the repeat sequences can be altered such as by addition of a serine to the C terminus of the polypeptide (to avoid terminating in F, Y, W, C, H, N, M, or D). In some embodiments, the repeat sequence can be modified by filling in an incomplete block with homologous sequence from another block. In some embodiments, the repeat sequence can be modified by rearranging the order of blocks or macrorepeats.

[0086] In some embodiments, non-repetitive N- and C-terminal domains can be selected for synthesis. In some embodiments, N-terminal domains can be by removal of the leading signal sequence, *e.g.*, as identified by SignalP (Peterson, T.N., et. Al., SignalP 4.0: discriminating signal peptides from transmembrane regions, *Nat. Methods*, 8:10, pg. 785-786 (2011).

[0087] In some embodiments, the N-terminal domain, repeat sequence, or C-terminal domain sequences can be derived from *Agelenopsis aperta, Aliatypus gulosus, Aphonopelma seemanni, Aptostichus sp. AS217, Aptostichus sp. AS220, Araneus diadematus, Araneus gemmoides, Araneus ventricosus, Argiope amoena, Argiope argentata, Argiope bruennichi, Argiope trifasciata, Atypoides riversi, Avicularia juruensis, Bothriocyrtum californicum, Deinopis Spinosa, Diguetia canities, Dolomedes tenebrosus, Euagrus chisoseus, Euprosthenops australis, Gasteracantha mammosa, Hypochilus thorelli, Kukulcania hibernalis, Latrodectus hesperus, Megahexura fulva, Metepeira grandiosa, Nephila antipodiana, Nephila clavata, Nephila clavipes, Nephila madagascariensis, Nephila pilipes, Nephilengys cruentata, Parawixia bistriata, Peucetia viridans, Plectreurys tristis, Poecilotheria regalis, Tetragnatha kauaiensis,* or *Uloborus diversus*.

[0088] In some embodiments, the silk polypeptide nucleotide coding sequence can be operatively linked to an alpha mating factor nucleotide coding sequence. In some embodiments, the silk polypeptide nucleotide coding sequence can be operatively linked to another endogenous or heterologous secretion signal coding sequence. In some

embodiments, the silk polypeptide nucleotide coding sequence can be operatively linked to a 3X FLAG nucleotide coding sequence. In some embodiments, the silk polypeptide nucleotide coding sequence is operatively linked to other affinity tags such as 6-8 His residues.

[0089] In some embodiments, the recombinant spider silk polypeptides are based on recombinant spider silk protein fragment sequences derived from MaSp2, such as from the species *Argiope bruennichi*. In some embodiments, the synthesized fiber contains protein molecules that include two to twenty repeat units, in which a molecular weight of each repeat unit is greater than about 20 kDa. Within each repeat unit of the copolymer are more than about 60 amino acid residues, often in the range 60 to 100 amino acids that are organized into a number of "quasi-repeat units." In some embodiments, the repeat unit of a polypeptide described in this disclosure has at least 95% sequence identity to a MaSp2 dragline silk protein sequence.

[0090] The repeat unit of the proteinaceous block copolymer that forms fibers with good mechanical properties can be synthesized using a portion of a silk polypeptide. These polypeptide repeat units contain alanine-rich regions and glycine-rich regions, and are 150 amino acids in length or longer. Some exemplary sequences that can be used as repeats in the proteinaceous block copolymers of this disclosure are provided in in co-owned PCT Publication WO 2015/042164, incorporated by reference in its entirety, and were demonstrated to express using a *Pichia* expression system.

[0091] In some embodiments, the spider silk protein comprises: at least two occurrences of a repeat unit, the repeat unit comprising: more than 150 amino acid residues and having a molecular weight of at least 10 kDa; an alanine-rich region with 6 or more consecutive amino acids, comprising an alanine content of at least 80%; a glycine-rich region with 12 or more consecutive amino acids, comprising a glycine content of at least 40% and an alanine content of less than 30%; and wherein the fiber comprises at least one property selected from the group consisting of a modulus of elasticity greater than 550 cN/tex, an extensibility of at least 10% and an ultimate tensile strength of at least 15 cN/tex.

[0092] In some embodiments, the quasi-repeat unit of the polypeptide can be described by the formula $\{GGY-[GPG-X_1]_{n1}-GPS-(A)_{n2}\}$ (SEQ ID NO: 3), where X_1 is independently selected from the group consisting of SGGQQ (SEQ ID NO; 4), GAGQQ (SEQ ID NO: 5), GQGPY (SEQ ID NO: 6), AGQQ (SEQ ID NO: 7) and SQ, n1 is a number from 4 to 8, and n2 is a number from 6 to 20. The repeat unit is composed of multiple quasi-repeat units. In additional embodiments, 3 "long" quasi repeats are followed by 3 "short" quasi-repeat units.

As mentioned above, short quasi- repeat units are those in which n1=4 or 5. Long quasi-repeat units are defined as those in which n1=6, 7 or 8. In some embodiments, all of the short quasi-repeats have the same X_1 motifs in the same positions within each quasi-repeat unit of a repeat unit. In some embodiments, no more than 3 quasi-repeat units out of 6 share the same X_1 motifs.

[0093] In additional embodiments, a repeat unit is composed of quasi-repeat units that do not use the same X_1 more than two occurrences in a row within a repeat unit. In additional embodiments, a repeat unit is composed of quasi-repeat units where at least 1, 2, 3, 4, 5, 6, 7, 8, 9, 10, 11, 12, 13, 14, 15, 16, 17, 18, 19 or 20 of the quasi-repeats do not use the same X_1 more than 2 times in a single quasi-repeat unit of the repeat unit.

[0094] In some embodiments, the recombinant polypeptide comprises the polypeptide sequence of SEQ ID NO: 1 (i.e., 18B). In some embodiments, the repeat unit is a polypeptide comprising SEQ ID NO: 2. These sequences are provided in Table 1:

Table 1: Exemplary polypeptides sequences of recombinant protein and repeat unit

SEQ ID	Polypeptide Sequence
SEQ ID NO: 1	GGYGPGAGQQGPGSGGQQGPGGQGPYGSGQQGPGGAGQQGPGGQGPYGPGAAAAAAAAAG GYGPGAGQQGPGGAGQQGPGSQGPGGQGPYGPGAGQQGPGSQGPGSGGQQGPGGQGPYGP SAAAAAAAAAGGYGPGAGQRSQGPGGQGPYGPGAGQQGPGSQGPGSGGQQGPGGQGPYGP SAAAAAAAAGGYGPGAGQQGPGSQGPGSGGQQGPGGQGPYGPGAAAAAAAVGGYGPGAGQ QGPGSQGPGSGGQQGPGGQGPYGPSAAAAAAAAGGYGPGAGQQGPGSQGPGSGGQQGPGG QGPYGPSAAAAAAAAGGYGPGAGQQGPGSGGQQGPGGQGPYGSGQQGPGGAGQQGPGGQG PYGPGAAAAAAAAAGGYGPGAGQQGPGGAGQQGPGSQGPGGQGPYGPGAGQQGPGSQGPG SGGQQGPGGQGPYGPSAAAAAAAAAGGYGPGAGQRSQGPGGQGPYGPGAGQQGPGSQGPG SGGQQGPGGQGPYGPSAAAAAAAAGGYGPGAGQQGPGSQGPGSGGQQGPGGQGPYGPGAA AAAAAVGGYGPGAGQQGPGSQGPGSGGQQGPGGQGPYGPSAAAAAAAAGGYGPGAGQQGP GSQGPGSGGQQGPGGQGPYGPSAAAAAAAAGGYGPGAGQQGPGSGGQQGPGGQGPYGSGQ QGPGGAGQQGPGGQGPYGPGAAAAAAAAAGGYGPGAGQQGPGGAGQQGPGSQGPGGQGPY GPGAGQQGPGSQGPGSGGQQGPGGQGPYGPSAAAAAAAAAGGYGPGAGQRSQGPGGQGPY GPGAGQQGPGSQGPGSGGQQGPGGQGPYGPSAAAAAAAAGGYGPGAGQQGPGSQGPGSGG QQGPGGQGPYGPGAAAAAAAVGGYGPGAGQQGPGSQGPGSGGQQGPGGQGPYGPSAAAAA AAAGGYGPGAGQQGPGSQGPGSGGQQGPGGQGPYGPSAAAAAAAA
SEQ ID NO: 2	GGYGPGAGQQGPGSGGQQGPGGQGPYGSGQQGPGGAGQQGPGGQGPYGPGAAAAAAAAAG GYGPGAGQQGPGGAGQQGPGSQGPGGQGPYGPGAGQQGPGSQGPGSGGQQGPGGQGPYGP SAAAAAAAAAGGYGPGAGQRSQGPGGQGPYGPGAGQQGPGSQGPGSGGQQGPGGQGPYGP SAAAAAAAAGGYGPGAGQQGPGSQGPGSGGQQGPGGQGPYGPGAAAAAAAVGGYGPGAGQ QGPGSQGPGSGGQQGPGGQGPYGPSAAAAAAAAGGYGPGAGQQGPGSQGPGSGGQQGPGG QGPYGPSAAAAAAAA

[0095] In some embodiments, the structure of fibers formed from the described recombinant spider silk polypeptides form beta-sheet structures, beta-turn structures, or alpha-helix structures. In some embodiments, the secondary, tertiary and quaternary protein structures of the formed fibers are described as having nanocrystalline beta-sheet regions, amorphous beta-turn regions, amorphous alpha helix regions, randomly spatially distributed nanocrystalline regions embedded in a non-crystalline matrix (i.e., a glassy matrix), or randomly oriented nanocrystalline regions embedded in a non-crystalline matrix. While not wishing to be bound by theory, the structural properties of the proteins within the spider silk are theorized to be related to fiber mechanical properties. Crystalline regions in a fiber have been linked with the tensile strength of a fiber, while the amorphous regions have been linked to the extensibility of a fiber. The major ampullate (MA) silks tend to have higher strengths and less extensibility than the flagelliform silks, and likewise, the MA silks have higher volume fraction of crystalline regions compared with flagelliform silks. Furthermore, theoretical models based on the molecular dynamics of crystalline and amorphous regions of spider silk proteins, support the assertion that the crystalline regions have been linked with the tensile strength of a fiber, while the amorphous regions have been linked to the extensibility of a fiber. Additionally, the theoretical modeling supports the importance of the secondary, tertiary and quaternary structure on the mechanical properties of RPFs. For instance, both the assembly of nano-crystal domains in a random, parallel and serial spatial distributions, and the strength of the interaction forces between entangled chains within the amorphous regions, and between the amorphous regions and the nano-crystalline regions, influenced the potential mechanical properties of the resulting fibers.

[0096] In some embodiments, the molecular weight of the silk protein may range from 20 kDa to 2000 kDa, or greater than 20 kDa, or greater than 10 kDa, or greater than 5 kDa, or from 5 to 400 kDa, or from 5 to 300 kDa, or from 5 to 200 kDa, or from 5 to 100 kDa, or from 5 to 50 kDa, or from 5 to 500 kDa, or from 5 to 1000 kDa, or from 5 to 2000 kDa, or from 10 to 400 kDa, or from 10 to 300 kDa, or from 10 to 200 kDa, or from 10 to 100 kDa, or from 10 to 50 kDa, or from 10 to 500 kDa, or from 10 to 1000 kDa, or from 10 to 2000 kDa, or from 20 to 400 kDa, or from 20 to 300 kDa, or from 20 to 200 kDa, or from 40 to 300 kDa, or from 40 to 500 kDa, or from 20 to 100 kDa, or from 20 to 50 kDa, or from 20 to 500 kDa, or from 20 to 1000 kDa, or from 20 to 2000 kDa.

Characterization of recombinant spider silk polypeptide powder impurities

[0097] Different recombinant spider silk polypeptides have different physiochemical properties such as melting temperature and glass transition temperature based on the strength and stability of the secondary and tertiary structures formed by the proteins. Figure 1 illustrates exemplary tertiary structures formed by silk polypeptides in native silk fiber (i.e. fiber produced by insects). Silk polypeptides form beta-sheet structures in a monomeric form. In the presence of other monomers, the silk polypeptides form a three-dimensional crystalline lattice of beta-sheet structures. The beta-sheet structures are separated from, and interspersed with, amorphous regions of polypeptide sequences.

[0098] Beta-sheet structures are extremely stable at high temperatures – the melting temperature of beta-sheets is approximately 257°C as measured by fast scanning calorimetry. *See* Cebe et al., Beating the Heat – Fast Scanning Melts Silk Beta-sheet Crystals, Nature Scientific Reports 3:1130 (2013). As beta-sheet structures are thought to stay intact above the glass transition temperature of silk polypeptides, it has been postulated that the structural transitions seen at the glass transition temperature of silk polypeptides are due to increased mobility of the amorphous regions between the beta-sheets.

[0099] Plasticizers lower the glass transition temperature and the melting temperature of silk proteins by increasing the mobility of the amorphous regions and potentially disrupting beta-sheet structure. Suitable plasticizers used for this purpose include water, polyalcohols (polyols) and urea. As hydrophilic portions of silk polypeptides can bind ambient water present in the air as humidity, bound ambient water may plasticize silk polypeptides.

[0100] In addition, in instances where recombinant spider silk polypeptides are produced by fermentation and recovered as recombinant spider silk polypeptide powder from the same, there may be impurities present in the recombinant spider silk polypeptide powder that act as plasticizers or otherwise inhibit the formation of tertiary structures. For example, residual lipids and sugars may act as plasticizers and thus influence the glass transition temperature of the protein by interfering with the formation of tertiary structures.

[0101] Various well-established methods may be used to assess the purity and relative composition of recombinant spider silk polypeptide powder. Size Exclusion Chromatography separates molecules based on their relative size and can be used to analyze the relative amounts of recombinant spider silk polypeptide in its aggregate and monomeric forms as well as the amount of high, low and intermediate molecular weight impurities in the recombinant spider silk polypeptide powder. Similarly, Rapid High Performance Liquid

Chromatography may be used to measure various compounds present in a solution such as monomeric forms of the recombinant spider silk polypeptide. Ion Exchange Liquid Chromatography may be used to assess the concentrations of various trace molecules in solution, including impurities such as lipids and sugars. Other methods of chromatography and quantification of various molecules such as mass spectrometry are well established in the art.

[0102] Depending on the embodiment, the recombinant spider silk polypeptide powder may have a purity calculated based on the amount of the recombinant spider silk polypeptide in is monomeric and aggregate forms by weight relative to the other components of the powder. In various instances, the purity can range from 50% by weight to 90% by weight, depending on the type of recombinant spider silk polypeptide and the techniques used to recover, separate and post-process the recombinant spider silk polypeptide powder.

Dope Rheology and Protein Structures

[0103] Rheology is commonly used in fiber spinning to analyze the physio-chemical characteristics of the material that is spun into fiber such as polymers. Different rheological characteristics may impact the ability to spin material into fibers and the mechanical characteristics of the spun fibers. Rheology can be also used to indirectly study the secondary, tertiary and quaternary structures formed by recombinant spider silk polypeptides under different temperatures and conditions. Depending on the embodiment, shear rheometers and/or extensional rheometers may be used to analyze different rheological properties by oscillatory and extensional rheology.

[0104] In some embodiments, small amplitude oscillatory shear (SAOS) rheology is used to measure various rheological properties including but not limited to the loss tangent (G''/G'), complex viscosity (η^*) and phase angle (δ). In these embodiments, a SAOS rheometer outputs a stress response as a function of oscillation frequency, ω, which can be broken down into elastic and viscous contributions. The elastic component, the solid-like behavior, is measured by the storage modulus (or elastic modulus), $G'(\omega)$, while the viscous component, the fluid-like behavior, is measured by loss modulus (or viscous modulus), $G''(\omega)$. The rheometer also measures the ratio of G''/G', called the loss tangent, or tan (δ), which describes the extent to which the complex fluid is liquid-like ($\tan(\delta) >> 1$) or solid-like ($\tan(\delta) << 1$). The rheometer outputs the values of the phase angle, δ, which spans from 90^o (ideal liquid) to 0^o (ideal solid). At G' and G'' crossover, δ is 45^o, and the material is

transitioning from being more liquid-like to more solid-like. In addition, the complex viscosity η^*, defined by $\eta^* = G^*(\omega)/\omega$, is also measured by the rheometer. In embodiments where the silk polypeptide is a recombinant silk protein that is wet spun into fiber, different rheological characteristics such as complex viscosity, loss tangent, and phase angle may be assessed based on a spin dope comprising the recombinant spider silk polypeptide dissolved into an appropriate solvent. Similarly, in embodiments where the silk polypeptide is melt spun into fiber, different rheological characteristics may be assessed based on a spin dope comprising the silk polypeptide and a plasticizer.

[0105] Depending on the embodiment, various rheology metrics may be used to determine whether a spin dope comprising recombinant spider silk polypeptide is suitable for wet spinning. For example, in some embodiments, a complex viscosity as measured at 10 Hz of less than 30 Pa s, less than 25 Pa s, less than 20 Pa s, less than 15 Pa s can indicate that a spin dope comprising recombinant spider silk polypeptide is not suitable for wet spinning. Similarly, in some embodiments, a complex viscosity as measured at 10 Hz of higher than 70 Pa s, higher than 75 Pa s, higher than 80 Pa s, higher than 85 Pa s can indicate that a spin dope comprising recombinant spider silk polypeptide is not suitable for wet spinning. In some embodiments, the phase angle of the spin dope comprising recombinant spider silk polypeptide may between 50-90°, 55-85°, 65-85°, 65-80°, 70-80°, 70-85°, 65-70°, or 50-65°.

[0106] In some embodiments, Differential Scanning Calorimetry is used to determine the glass transition temperature of the recombinant spider silk polypeptide and/or fiber containing the same. In a specific embodiment, Modulated Differential Scanning Calorimetry is used to measure the glass transition temperature.

[0107] Depending on the embodiment and the type of recombinant spider silk polypeptide, the glass transition temperature may have a range of values. However, a measured glass transition temperature that is much lower that is typically observed for a recombinant spider silk polypeptide in its solid form may indicate that impurities or the presence of other plasticizers.

[0108] In addition, Fourier Transform Infrared (FTIR) spectroscopy data may be combined with rheology data to provide both a direct characterization of tertiary structures in the recombinant silk powder and/or spin dope containing the same. FTIR can be used to quantify secondary structures in silk polypeptides and/or dope comprising the silk polypeptides as discussed below in the section entitled "Fourier Transform Infrared (FTIR) Spectroscopy."

[0109] Depending on the embodiment, FTIR may be used to quantify beta-sheet structures present in the recombinant spider silk polypeptide powder and/or spin dope containing the same. In addition, in some embodiments, FTIR may be used to quantify impurities such as sugars and lipids present in the recombinant spider silk polypeptide powder. However, various chaotropes and solubilizers used in different protein pre-processing methods may diminish the number of tertiary structures in recombinant spider silk polypeptide powder or spin dope containing the same. Accordingly, there may be no correspondence between the amount of beta-sheet structures in recombinant spider silk polypeptide powder before and after is it spun into fiber. Similarly, there may be little to no correspondence between the glass transition temperature of a powder before and after it is spun into fiber.

[0110] In some embodiments, rheological data characterizing the recombinant spider silk polypeptides may be combined with FTIR to analyze secondary and tertiary structures formed in by the polypeptides. In a specific embodiment, rheological data may be captured in conjunction with FTIR spectra. For exemplary methods of combining rheology and FTIR, *see* Boulet-Audet et al., Silk protein aggregation kinetics revealed by Rheo-IR, Acta Biomaterialia 10:776–784(2014), the entirety of which is herein incorporated by reference.

[0111] Similarly, various methods of characterizing impurities in the recombinant silk powder may be combined with rheological and /or FTIR data to analyze the relationship between the presence of impurities and the formation of secondary and tertiary structures.

Wet Spinning Recombinant Silk Proteins

[0112] Depending on the embodiment, the recombinant spider silk polypeptides may be wet-spun into fiber using various established methods. Exemplary methods of wet-spinning recombinant spider silk polypeptides are discussed in detail in US 7,057,023, the entirety of which is herein incorporated by reference.

[0113] In most wet spinning embodiments, recombinant spider silk polypeptides are dissolved to form a spin dope. Suitable solvents for use in a spin dope include but are not limited to formic acid, aqueous solutions (e.g., eADF4), dimethyl sulfoxide (DMSO), N, N-dimethylformamide (DMF), hexafluoroisopropanol (HFIP), hexafluoroacetone hydrate, trifluoroacetic acid, water, phosphoric acid and any combination thereof. Other suitable solvents are listed in Koeppel and Holland, Progress and Trends in Artificial Silk Spinning: A Systematic Review, ACS Biomater. Sci. Eng. 3:226−237 (2017), the entirety of which is

herein incorporated by reference. Depending on the solvent used, various salts may be added to the spin dope. In some embodiments, N-methyl morpholine N-oxide (NMMO) is used as a solvent for recombinant spider silk polypeptide.

[0114] In various embodiments, the concentration of solvent and recombinant silk protein in the spin dope may be varied based on the properties of the silk polypeptide and the type of solvent used. Concentrations may be adjusted in part based on rheological data such as the complex viscosity or the phase angle. In specific embodiments where formic acid is used to dissolve the 18B protein (SEQ ID NO: 1), suitable concentrations of recombinant silk protein by weight in the spin dope range from: 20-60% by weight, 20-50% by weight, 20-40% by weight, 30-40% by weight, 30-60% by weight, or 30-50% by weight. In embodiments where NMMO is used to dissolve the 18B protein, suitable concentrations of recombinant silk protein by weight in the spin dope range from 20-60% by weight, 20-50% by weight, 20-40% by weight, 30-40% by weight, 30-60% by weight, or 30-50% by weight.

[0115] In some embodiments, a plasticizer will be added to the spin dope. Suitable plasticizers include water, polyols (e.g glycerol), lactic acid, methyl hydroperoxide, ascorbic acid, 1,4-dihydroxybenzene (1,4 Benzenediol) Benzene-1,4-diol, phosphoric acid, ethylene glycol, propylene glycol, triethanolamine, acid acetate, propane-1,3-diol or any combination thereof.

[0116] In some embodiments, various agents may be added to the spin dope to alter the rheological characteristics of the spin dope such as elongational viscosity, shear viscosity and linear viscoelasticity. Suitable agents used to alter the elongational viscosity include polyethylene glycol (PEG), Tween, Sodium dodecyl sulfate, polyethylene oxide, or any combination thereof. Other suitable agents are well known in the art.

[0117] In various embodiments, the spin dope may be subject to mixing or agitation to ensure a homogeneous spin dope. Suitable methods of mixing the spin dope include but are not limited to centrifugal mixers, high-shear mixers, and twin screw mixing. Other mixing methods are well established in the art. In instances where NMMO is used as a solvent, the spin dope may be subject to heat during mixing to form a viscous solution. In some instances, the spin dope may be degassed using centrifugation.

[0118] In some embodiments, a pigment or dye may be added to the spin dope to perform "solution dying" of the fiber. Solution dying is an optimal method of dying fiber as it eliminates large amounts of wastewater involved in dying finished fibers and textiles. Dyes may form covalent or cationic bonds with the recombinant silk protein to provide a colorfast

fiber. Any type of dye and/or pigment may be used for solution dying including but not limited to cationic dyes, anionic dyes, zwitterionic dyes and dispersions of pigment.

[0119] Depending on the required initial denier of the extruded fiber, spin dope comprising the recombinant silk protein may be extruded through spinnerets with varying orifice sizes. In most embodiments, the orifice will range from 50-200 μm, 50-100 μm, 50-150 μm, 100-150 μm, 100-200 μm or 150-200 μm. In some embodiments, the ideal orifice size will be based on the final draw ratio of the fiber. For example, a higher initial denier of an extruded fiber may be subject to a higher draw ratio than a smaller initial denier extruded fiber.

[0120] In instances where NMMO is used as a solvent, an air gap may be used to separate the extrusion device from the coagulation bath. Depending on the embodiment, the air gap may range in size from 2-5 cm, 2-10 cm, 2-20 cm, 5-10 cm, 5-20 cm, or 10-30 cm.

[0121] In various embodiments, different coagulation baths may be used, alone or sequentially. In some embodiments, alcohol such as ethanol or methanol will be used as a coagulation agent to precipitate or otherwise coagulated the extruded spin dope. Suitable alcohols for this purpose include ethanol, methanol or any combination thereof. For example, suitable coagulation bath could contain 80% ethanol and 20% methanol; 60% ethanol and 40% methanol; 40% ethanol and 60% methanol; or 20% ethanol and 80% methanol.

[0122] In some embodiments, the coagulation bath will combine a coagulation agent with the solvent used to generate the spin dope. For example, in some embodiments, the coagulation bath will comprise an alcohol and formic acid. In a specific embodiment, the coagulation bath will comprise 90% ethanol and 10% formic acid.

[0123] In some embodiments, the coagulation bath will combine a coagulation agent with a plasticizer such as water or any of the plasticizers listed above. In a specific embodiment, the coagulation bath will comprise 90% ethanol and 10% H_20.

[0124] Depending on the embodiment, the fiber may be subject to any number of coagulation baths, in any order. In some embodiments, the fiber may be the following series of coagulation baths: a coagulation bath comprising the solvent used for dope spinning, a coagulation bath comprising only alcohol, and a coagulation bath comprising a plasticizer.

[0125] Depending on the embodiment, the total residence time in the one or more coagulation baths will range from 5-10 seconds, 5-50 seconds, 10-50 seconds, 10-25 seconds, 20-50 seconds, from 25-50 seconds, from 30-50 seconds, from 35-50 seconds, from 40-50 seconds, from 20-40 seconds, from 20-35 seconds, from 20-30 seconds, and/or from 30-40

seconds. In most embodiments, the residence time will be sufficient to eliminate most or all residual formic acid from the fiber.

[0126] In most embodiments of the present invention, the extruded fiber will not be subject to any drawing while it is transferred through the one or more coagulation baths. In other words, the extruded fiber will only be subject to the minimal amount of force necessary to move the fiber through the coagulation bath and collect fiber on the godets. Extruded fiber that is not subject to any drawing strain is herein referred to as "precursor fiber."

Drawing Undrawn Fiber Over a Hot Surface

[0127] Precursor fiber may be drawn in order to increase the orientation of the fiber and promote three-dimensional crystalline structure formed by intermolecular and intramolecular beta-sheets. The application of activation strain in drawing promotes molecules to align on the axis of the fiber. Polymeric molecules such as polypeptides are partially aligned when forced to flow through the spinneret hole.

[0128] In some embodiments, the precursor fiber may be annealed using alcohol prior to drawing. In specific embodiments, the precursor fiber may be annealed using alcohol vapor (e.g. methanol vapor). In these embodiments, the precursor fiber may be placed in a sealed container with alcohol for a period of time ranging from 1 hour to 24 hours, 1 hour to 6 hours, 1 hour to 12 hours, 1 hour to 24 hours, 2 hours to 6 hours, 4 hours to 12 hours, 6 hours to 18 hours, 6 hours to 24 hours, 12 hours to 24 hours, 12 hours to 48 hours.

[0129] In the present invention, the alignment is optimized by passing the precursor fiber over a uniform hot surface while the fiber is drawn. The term "hot surface" as used herein refers to a surface that has provides both a substantially uniform heat and a substantially uniform surface. Using a hot surface as a heat source eliminates variability seen using ambient heat sources, resulting in greater uniformity in results and consequent scalability of the process for commercial mass production of the fiber. In some embodiments, the hot surface will be a metal bar or surface. In other embodiments, the hot surface may be made of ceramic or other materials. Depending on the embodiment, the hot surface can be curved or otherwise configured to facilitate the fiber moving over the hot surface.

[0130] In embodiments of the present invention, the undrawn extruded fiber is simultaneously moved over the hot surface in contact with the hot surface as it is drawn. Depending on the embodiment, the temperature of the hot surface can range from 160-210°C, 180-210°C, 190-210°C, 195-210°C, 195-205°C, or 200-205°C.

[0131] Depending on the embodiment, the undrawn extruded fiber can be subject to different draw ratios while it is drawn over the hot surface. Depending on the embodiment, the draw ratio may range from 2 to 7. In some embodiments, the maximum stable draw ratio may depend on the temperature of the hot surface.

[0132] In some embodiments, the temperature of the hot surface is calculated as a function of the glass transition temperature of the undrawn extruded fiber. For example, the temperature of the hot surface can be calculated to be greater than 5°C, 10°C, 15°C, 20°C, or 25°C greater than the glass transition temperature of the recombinant silk protein powder and/or the undrawn extruded fiber.

[00133] In some embodiments, the maximum draw ratio is determined using an apparatus designed to calculate the draw ratio at which the fiber will break (herein referred to as "draw ratio at failure"). In one embodiment, the apparatus is constructed by attaching parallel steel rods to both the traveler and the end of a linear actuator and positioning the apparatus over a hot surface, the temperature of which could be controlled. In this embodiment, the position of the hot surface is adjustable such that it could be brought in and out of contact with the steel rods so that precursor fibers strung between the rods can be hot drawn at controlled temperatures and rates.

[00134] In a specific embodiment, the draw ratio at failure is determined by affixing the precursor fibers between the rods of the batch hot drawing apparatus and bringing the hot surface in contact with the mounted fibers, the linear actuator was used to increase the distance between the rods (thus drawing the fibers) in steps of 5 mm at a rate of 5 mm/s until all of the fibers were broken. In this embodiment, the number of unbroken fibers remaining after each draw step can be recorded, from which the percent elongation at break distribution is approximated.

[0135] Depending on the embodiment and the rate at which fiber is passed over the uniform hot surface (referred to herein as the "reel rate"), the hot surface can vary in length (i.e. the size in cm of the hot surface that the fiber is drawn over), thus changing the duration of time that the undrawn extruded fiber is subject to heat and deformation. In most embodiments, the width of the hot bar will be no less than 1 cm. However, in various embodiments the width of the hot surface can range from 1-50 cm, 1-2 cm, 1-3 cm, 1-5 cm, 5-38 cm, 38-50 cm. Depending on the embodiment, the reel rate can range from 1 to 60 meters a minute.

[0136] Depending on the reel rate and the length of the hot surface, the total residence time over the hot surface may vary. In most embodiments, the total residence time can range from 0.2 seconds to 3 seconds.

[0137] In addition, the undrawn fiber may be subject to varying force which provides different draw ratios. In most embodiments, the tensile force will be provided by godets as illustrated in Figures 2A and 2B. Depending on the embodiment, the godets will be positioned 40 cm to 300 cm (3 m) apart. In some embodiments, the godets will be placed such that the fiber that is passed over the hot surface is at an angle relative to the hot surface. For example, in instances where the hot surface is curved, the godets may be placed such that the fiber that is passed over the hot surface contact the hot surface and pivots over the hot surface at an angle of 20 to 60 degrees relative to the hot surface (*see* Figure 2B).

[0138] In various embodiments, the deformation rate (i.e., the amount of deformation that the fiber is subject to with heat and drawing) of the undrawn fiber can vary based on the above factors. Deformation rate may be calculated based on the rate that the undrawn fiber is fed to the hot surface and the rate that the fiber is collected from the hot surface. For example, the fiber may be fed to the hot surface at a rate of 1 meters/minute and collected from the hot surface at a rate of 5 meters/minute. In a specific embodiment, the deformation rate $\epsilon(t)$ is calculated using the following equation, where the rate that the fiber is fed to the hot surface is represented v_1, the rate that the fiber is collected from the hot surface is v_2 and the length the deformation takes place over is L_0:

Equation 1:

$$\epsilon(t) = \frac{v_2 - v_1}{L_0}$$

[0139] Depending on the embodiment, drawing over a hot surface may be performed in one step or multiple (i.e. two, three, or four) steps. Parameters such as the strain rate, the deformation rate, the reel rate, the temperature of the hot surface and the length of the hot surface may be varied or otherwise different at each step. Performing drawing over multiple steps may affect the overall strain rate of the fiber, which may enhance formation of crystalline beta-sheet structures.

[0140] In a specific embodiment, multi-step drawing may be used to achieve an overall draw ratio that is equivalent to the draw ratio at failure. In these embodiments, several drawing steps may be performed. Depending on the embodiment, in some instances, the draw ratio performed at the first drawing step may be larger than that performed at

subsequent drawing steps. Depending on the embodiment, the take-up rate may be increased over subsequent drawing steps such that the final take-up rate is 20-40 m/min, 20-50 m/min, 30-60 m/min, or 20-100 m/min.

Fourier Transform Infrared Spectroscopy

[0141] Fourier Transform Infrared (FTIR) spectra can be used to assess the secondary and tertiary structures of proteins present in polypeptide powder and/or fibers. Specifically, FTIR spectra can be used to determine the amount of beta-sheets present in the fibers that are subject to different spinning and post-processing conditions. Thus, FTIR spectra may be used to determine the relative amount of beta-sheet structures based on the different techniques. Alternately, the FTIR spectra may be compared to native insect silk.

[0142] Depending on the embodiment, FTIR spectra at different wavenumbers may be used to assess the different tertiary structures present in the fibers. In various embodiments, wavenumbers corresponding to Amide I and Amide II bands may be used to assess various protein structures such as turns, beta-sheets, alpha helices, and side chains. Wavenumbers corresponding to these structures are well known in the art.

[0143] In most embodiments, FTIR spectra at wavenumbers corresponding to beta-sheets will be used to assess the quantity of beta-sheet structures in the polypeptide powder and/or fiber. In a specific embodiment, FTIR spectra at 982-949 cm^{-1}(CH2 rocking (A)n), 1695-1690 cm-1 (Amide I) 1620-1625 cm^{-1} (Amide I), 1440-1445 cm^{-1} (asymmetric CH3 bending) and/or 1508 cm^{-1} (Amide II) are used to determine the amount of beta-sheets present. Depending on the embodiment, the different wavenumbers and ranges can measured to determine the amount of beta-sheets present. In some embodiments, the FTIR spectra at 982-949 $^{cm-1}$ is used in order to eliminate interference from overlapping peaks. Exemplary methods of obtaining spectra at these wavenumbers are discussed in detail in Boudet-Audet et al, Identification and classification of silks using infrared spectroscopy, Journal of Experimental Biology, 218:3138-3149 (2015), the entirety of which is herein incorporated by reference.

Three Dimensional Crystal Beta-Sheet Formation of Drawn Fibers

[0144] X-ray diffraction (XRD) may be used to determine the amount of repetitive crystalline structures in recombinant spider silk polypeptide fibers. As discussed above, in native spider silk, polypeptide sequences comprising beta-sheets aggregate to form a three-

dimensional lattice of beta-sheets. This lattice consists of hydrophobic interactions between different polypeptide sequences forming the beta-sheets. As the three-dimensional lattice is a crystalline structure, XRD may be used to determine the presence of crystalline structures in recombinant spider silk polypeptide fibers.

[0145] In some embodiments, XRD samples can be prepared by making a bundle of fibers. Depending on the embodiment and the fiber used, the bundle can have from approximately 50-100 individual filaments per bundle. In some embodiments, the fibers are aligned in a bundle such that they were all parallel and affixed to a frame with the fiber bundle axis perpendicular to the X-ray beam.

[0146] Depending on the embodiment, the XRD diffraction pattern can be collected using various wavelengths, beam spots, distance to detector center and recorders as is well known in the art of XRD. The diffraction pattern may be collected at multiple points along the fiber over varying durations. Multiple diffraction patterns may be recorded and averaged. In a specific embodiment, XRD diffraction patterns are collected 3 times for 10 seconds each at three different points along the fiber and the three repeats are averaged. Multiple images may also be taken at each point and averaged for better statistics and enhanced signal to noise ratio.

[0147] In most embodiments, radial profiles are constructed by integrating the intensity azimuthally over the desired range of azimuthal angles, φ, and plotting it as a function of the scattering angle, 2θ. An integrated scan is obtained by integrating azimuthally over φ=-90 to 90° and plotting that as a function of 2θ. The integrated scan contains information regarding the crystallinity. To extract crystallinity values from the integrated scan, the amorphous and crystalline peaks have to be fitted to the intensity profile. Crystallinity can be calculated with the following equation:

$$CI = \frac{\sum A_c}{\sum A_a + \sum A_c}$$

where A_c is the area of crystalline peaks and A_a is the area of amorphous peaks. Azimuthal profiles are obtained by integrating the intensity radially over a thin ring, and plotting it as a function of the azimuthal angle. The alignment of the fiber can be then obtained by measuring the full-width half maximum (FWHM) of the azimuthal peak fit. The

azimuthal profile of the (200) peak was integrated over 2θ=10.5° to 11.5°, and (120) peak was integrated over 2θ=13° to 13.8°. The Hermans orientation factor is defined as:

$$f = (3\langle\cos^2\phi_3\rangle - 1)/2$$

where $\langle\cos^2\varphi\rangle$ is:

$$\langle\cos^2\phi_3\rangle = 1 - A\langle\cos^2\phi_1\rangle - B\langle\cos^2\phi_2\rangle$$

where axis 1 is (200), axis 2 is (120) and axis 3 is the fiber axis (002). *See* Grubb, Fiber Morphology of Spider Silk: The Effects of Tensile Deformation, Macromolecules 30(10): 2860-2867 (1997). An orientation factor of f=1 indicates alignment of crystals parallel to the fiber axis, f=-0.5 indicates crystal alignment perpendicular to fiber axis, and f=0 indicates randomly oriented crystals.

Example 1: Purity of Recombinant 18B Polypeptide Powder

[0148] 18B polypeptide sequences (SEQID NO: 1) comprising the FLAG tag were produced through various lots of large-scale fermentation, recovered and dried in powders ("18B powder"). The various lots of 18B powder are indicated in the table below in the column entitled "Source Ref." The 18B powders were subject to various post-processing techniques. The various types of post-processing techniques are indicated below in the column labeled "Reprocess technique". 18B powders that were not post-processed are labeled "as is."

[0149] Two lots of 18B powder (labeled "FACU" in the "Reprocess Technique" column) were subject to post-processing by dissolving the recombinant spider silk polypeptide in formic acid and re-precipitating the recombinant 18B polypeptide powder using isopropyl alcohol. One lot of 18B Powder was subject to re-processing and precipitation using guanidine thiocyanate according to a first protocol (labeled "Gdn Reprocessed" in the "Reprocess Technique" column). One lot of 18B powder was subject to re-processing and precipitation using Guanidine thiocyanate according to a second protocol (labeled "Snow White" in the "Reprocess Technique" column). As discussed above, various other proteins from the same lots were left unprocessed as controls.

[0150] Data characterizing the relative amounts of high, low and intermediate molecular weight impurities, monomeric 18B and aggregate 18B in the 18B powder was collected using Size Exclusion Chromatography (SEC) as follows: 18B powder was dissolved in 5M Guanidine Thiocyanate and injected onto a Yarra SEC-3000 SEC-HPLC

column to separate constituents on the basis of molecular weight. Refractive index was used as the detection modality. 18B aggregates, 18B monomer, low molecular weight (1-8 kDa) impurities, intermediate molecular weight impurities (8-50 kDa) and high molecular weight impurities (110-150 kDa) were quantified. The relevant composition was reported as mass % and area%. BSA was used as a general protein standard with the assumption that >90% of all proteins demonstrate dn/dc values (the response factor of refractive index) within ~7% of each other. Poly(ethylene oxide) was used as a retention time standard, and a BSA calibrator was used as a check standard to ensure consistent performance of the method.

[0151] Table 2 (below) lists the area% of the different components quantified using SEC and the mass% of 18B in its aggregate and monomeric forms. As shown in the same table, the 1589 Snow White powder, 1851 Snow White powder and the 128-Gdn reprocessed powder showed the highest purity. 1589 and 1851 Snow White powder produced comparable purity levels. While one of the FACU processed powder showed better purity than the as-is powders, the other was roughly equivalent to the as-is powder. Different sources for the as-is powders yielded different purity levels, with 1707 as-is having the highest purity.

Table 2: Size Exclusion Chromatography

Source Ref	Reprocess technique	High MW Impurity [area %]	Aggregate [area %]	18B [area %]	IMW Impurity [area %]	LMW Impurity [area%]	Aggregate + 18B [area%]
125	as-is	4.16	6.60	49.80	31.43	8.02	56.40
126	as-is	2.56	5.71	52.61	29.47	9.66	58.32
134	as-is	2.65	5.12	52.08	34.41	5.74	58.12
125	FACU	1.71	9.02	50.27	33.14	5.86	59.28
126	FACU	1.35	6.32	70.94	18.75	2.63	77.26
1707	as-is	1.6	5.2	71.6	16.3	5.4	73.77
128	Gdn reprocessed	3.3	15.0	55.1	23.1	3.5	78.02
1589	Snow White	1.07	9.30	71.86	14.73	3.04	89.41
1851	Snow White	1.26	8.75	67.07	15.65	7.34	88.11

Example 2: FTIR Data from Recombinant 18B Protein Powder

[0152] For each of the above-described samples, FTIR data collection was performed using a Bruker Alpha spectrometer equipped with a diamond-attenuated total reflection accessory. Spectra of were collected with 32 scans at 4 cm^{-1} resolution from 4000 to 600 cm^{-1} by pressing ~10 mg of powder against the internal reflection crystal using an anvil.

Absorbance values offset by subtracting the average between 1900 and 1800 cm^{-1} without bands. Spectra were then normalized by dividing the average between 1350 and 1315 cm^{-1} corresponding to the isotropic side chain vibration bands before calculating the average absorbance of the spectral region of interest. For Aliphatic [2996-2822 cm^{-1}] a linear baseline was subtracted between the boundaries to remove the contribution of the neighboring amide A band while no baseline was subtracted from the C-O [1100-1000 cm^{-1}] and ß-sheet [982-949 cm^{-1}] regions.

[0153] Table 3 below lists the integrated peak area for different peaks. The aliphatic 2996-2822 cm^{-1} peak represents the absorption to the CH2 and CH3 stretching mode from hydrocarbon chains. The C-O peak at 1100-1000 cm^{-1} represents esters and hydroxyl groups from proteins and polysaccharides. The 982-949 cm^{-1} absorbance constitutes is assigned to the CH3 rocking mode of the (A)n within ß-sheets. For a detailed discussion of the different peak, *see* Moore, W. H. and S. Krimm, Vibrational Analysis of Peptides, Polypeptides, and Proteins .2. Beta-Poly(L-Alanine) and Beta-Poly(L-Alanine glycine), Biopolymers 15(12):2465-2483 (1976).

[0154] As discussed above, the ß-sheets in the powder are not aligned and therefore the samples do not represent ß-sheet formation in the spun fiber.

Table 3: FTIR Peak Areas for 18B Powder Samples with standard deviations

Source Ref	Reprocess type	Aliphatic [2996-2822 cm^{-1}]	C-O [1100-1000 cm^{-1}]	ß-sheet [982-949 cm^{-1}]
125	as-is	0.070±0.001	1.30±0.03	0.734 ± 0.001
126	as-is	0.074±0.001	1.08±0.01	0.687 ± 0.001
134	as-is	0.044±0.002	0.78±0.01	0.56 ± 0.02
125	FACU	0.052±0.002	1.01±0.03	0.72 ± 0.02
126	FACU	0.048±0.001	0.971±0.002	0.700 ± 0.006
1707	as-is	0.058±0.007	0.658±0.006	0.44 ± 0.01
128	Gdn reprocessed	0.73±0.003	1.20±0.01	0.70 ± 0.03
1589	Snow White	0.041±0.02	0.71± 0.01	0.54 ± 0.02

Example 3: Glass Transition Temperature of the Recombinant 18B Protein Powder

[0155] Modulated Differential Scanning Calorimetry (MDSC) was used to determine the glass transition temperature of the different samples. A DSC, TA Instruments Q2000 was used to generate thermograms. Prior to the measurement, the instrument was calibrated using indium and sapphire to verify heat flow and heat capacity respectively, followed by an empty

pan to verify the baseline. 5-10 mg of sample was pressed into a non-hermetically sealed aluminum pan and placed in the DSC cell along with an empty reference pan. The cell was purged with nitrogen at 20 ml/min for the duration of the experiment. Protein powder was heated at 125° C for 1 hour to remove excess water, followed by a modulated ramp (3° C/min +/- 0.6°C, 1 minute period) from -20°C to 220°C. The Tg (glass transition temperature) was then determined from the reversing heat capacity thermogram by finding the point on the curve halfway between the tangents extrapolated from the onset and offset of the transition.

[0156] The glass transition temperatures are tabulated below.

Table 4: Glass Transition Temperatures of 18B Powder Samples

Source Ref	Reprocess type	Tg [°C]
125	as-is	182.01
126	as-is	180.40
134	as-is	180.70
125	FACU	152.93
126	FACU	163.14
1707	as-is	177.08
128	Cinderella	177.75
1589	Snow White	176.18

Example 4: Spin Dope Preparation and Rheology of the Spin Dopes

[0157] The above-discussed samples of 18B powder were dissolved in formic acid and mixed using a Thinky Planetary Centrifugal Mixer 400ARE-TWIN at 1600 RPM to generate spin dopes. Prior to dissolution, the 18B powder was baked to reduce the moisture content of the powder down to less than 4% by weight.

[0158] A Malvern Kinexus Lab+ Rotational Rheometer was used to measure the complex viscosity and the phase angle of the spin dopes. Parameters were set to a temperature of 22°C, a frequency of 100-0.1 Hz, and a strain of 1%. An interval of 3 points/decade was used to determine an average value for a given frequency.

[0159] Table 5 below includes the concentration by weight of the 18B powder in the spin dope, the complex viscosity and the phase angle as measured at 10 Hz. Data was not collected for 125-FACU.

Table 5: 18B Powder Concentration in Spin Dope, Complex Viscosity and Phase Angle

Source ID	Process type	18B Powder Concentration by weight [%]	Complex Viscosity [Pa s]	Phase Angle [o]
125	as-is	35	36.1	59.91
126	as-is	35	63.45	55.93
134	as-is	36	64.65	63.28
126	FACU	38.5	37.12	78.70
1707	as-is	36	58.75	72.19
128	Cinderella	34.5	57.8	69.84
1589	Snow White	35.4	42.56	82.34
1851	Snow White	36	42.42	79.09

Example 5: Hot Draw and Air Draw

[0160] Figure 2A illustrates the method used to wet spin and process the control ("Air Draw") fibers. The spin dopes comprising the different 18B samples at the above concentrations by weight were extruded using a 125 μm spinneret at into room temperature (approximately 22°C) coagulation baths as listed below. The coagulation baths were also maintained at room temperature (approximately 22°C). The Air Draw fibers were then subject to a single wrap on a set of godets under minimal draw (i.e. a draw ratio of ~1X), the still-wet fibers were then drawn between two godets spaced at a distance of 2.1 m to a draw ratio of 7-8X at room temperature at a relative humidity of approximately 55-65%. The reel rate was 15-23 m/min. The Air Draw fiber was then wound on a take-up godet.

[0161] Figure 2B illustrates the method used to wet spin and process fiber that were subject to rapid deformation over a uniform hot surface ("Hot Draw"). Spin dopes comprising the different 18B samples were extruded using a 125 μm spinneret at room temperature (approximately 22°C) into coagulation baths as listed below. The coagulation baths were also maintained at room temperature (approximately 22°C). The Air Draw fibers were then subject to a single wrap on godets no drawn and then passed to a take-up godet under minimal draw (i.e. a ~1X draw). The still-wet fibers were then allowed to dry over a period of at least 12 hours. The dried fiber was then passed over a hot surface between two godets spaced at a distance of 60 cm at a draw ratio of approximately 5.5X at a relative humidity of approximately 55-65%. The hot surface was a steel bar with a "D" shaped curved profile heated to 200°C. The total length of the hot surface the fibers traveled over was 1cm. The fiber approaching and leaving the hot surface was at an angle of 10-30 degrees relative to the hot surface. The feed reel rate used was approximately 1 m/min and the take-

up reel rate was approximately 5.5 m/min. Total residence time over the hot surface was 0.6 seconds.

[0162] The Air Draw and Hot Draw fibers were tested to determine their tenacity and initial modulus. Testing was performed using a TexTechno Favimat+ single fiber tester with optional Robot 2 feed system. Single fibers were tested at 65% relative humidity according to ASTM Standard D1776 to measure tenacity and initial modulus.

[0163] Table 6 below lists the tenacity and initial modulus of Air Draw and Hot Draw fibers. Also tabulated is the percentage content by volume of formic acid, methanol and ethanol in the coagulation bath used. Figures 3A and 3B are bar graphs respectively illustrating the tenacity and initial modulus of the Air Draw and Hot Draw Fibers. As shown in the table and Figures 3A and 3B there was a significant difference observed in the tenacity.

Table 6: Tenacity and initial modulus of Air Draw and Hot Draw fibers

Source Ref	Process type	Formic acid coag bath content [vol%]	Ethanol coag bath content [vol%]2	Methanol coag bath content [vol%]	Air Draw Tenacity (cN/tex)	Hot Draw Tenacity (cN/tex)	Air Draw Initial Modulus (cN/tex)	Hot Draw Initial Modulus (cN/tex)
126	as-is	10	90	0	16.07	19.4	472.54	426
126	as-is	0	80	20		18.32		457.29
134	as-is	0	100	0	21.34	20.57	473.82	475.2
125	FACU	0	40	60		17.61		424
125	FACU	0	80	20	21.01	25.73	532.14	552
126	FACU	0	40	60	15.14	23.4	510	523
1707	as-is	0	40	60	20.38	28.3	463.3	614
128	Cinderella	0	40	60	20.84	27.8	510	626
1851	Snow White	0	40	60	25.1	30.36	549.32	697.98

Example 6: Measuring ß-sheet Content using FTIR

[0164] FTIR was performed on various Hot Draw fibers that were drawn at different draw ratios. Specifically, fibers generated using a formic acid dope comprising the 144 As-is powder described above at a concentration of 36% by weight. Dope was extruded through a 125 µm spinneret into a coagulation bath comprising 90% ethanol, 3.5-5.5% methanol and 4-6% isopropanol to form precursor fibers. The coagulation bath and spinneret were maintained at room temperature (approximately 22°C). Precursor fibers were subject to minimal draw (i.e. a draw ratio of ~1X) as they were passed through the coagulation bath and wound on a take-up godet. The precursor fibers were dried overnight prior to hot drawing.

[0165] The various fibers were subject to different draw ratios (1X, 1.25X, 2.5X, 3.75X, 4.5X, 4.95X) while being drawn over the hot surface to determine the effect, if any, on beta-sheet formation. The hot surface was a steel bar with a "D" shaped curved profile heated to 200°C. The total length of the hot surface the fibers travelled over was 1cm. The fiber approaching and leaving the hot surface was at an angle of 10-30 degrees relative to the hot surface. Godets used to draw the fibers were spaced 60 cm apart. The feed reel rate used was 1 m/min and the take-up reel rates were 1, 1.25, 2.5, 3.75, 4.5 and 4.95 m/min corresponding to the above-discussed draw ratios.

[0166] FTIR was performed on the hot drawn fibers using a Bruker Alpha spectrometer equipped with a diamond attenuated total reflection accessory preceded by a wire grid polarizer selecting mostly S (perpendicular) polarized light. Recombinant polypeptide powder and the precursor fiber were included as controls. To quantify the molecular alignment three spectra of each orientation (0 and 90° relative to the polarization electric field) were collected with 32 scans at 4 cm^{-1} resolution from 4000 to 600 cm^{-1}.

[0167] The average values for the peak corresponding to 982-949 cm^{-1} were calculated based on the following steps. Absorbance values offset subtracting the average between 1900 and 1800 cm^{-1} without bands. Spectra were then normalized by dividing the average between 1350 and 1315 cm^{-1} corresponding to the isotropic (non-oriented) side chain vibration bands. The ß-sheet band was integrated by averaging the absorbance values between 982 and 949 cm^{-1}. The Dichroic ratio ("R") was by dividing integrated values collected at 0° by the corresponding spectra at 90°. The second order parameter <P2> alignment metric was then calculated from R using <P2> = (R - 1 / R + 2). A value of 1 indicates a perfectly oriented vibration mode along the fiber axis while -0.5 represents a vibration mode perfectly orientated perpendicular. In contrast, non-oriented modes will produce <P2> near 0. To

measure the crystallinity independent of the orientation, we calculated the isotropic absorbance spectra $A_{iso} = (A0° + 2*A90°)/3$ before integrating the bands. This also enables the ß-sheet content comparison between samples with varying alignment levels.

Table 7: ß-sheet Content of Hot Draw and Control Fibers and Powders

Source Ref	**Process type**	**Powder or Fiber**	**Hot Draw or Precursor**	**Draw Ratio**	**<P2> ß-sheet ß 982-949 cm-1**	**A_{iso} ß-sheet ß 982-949 cm-1**
1589	Snow White	Powder	N/A	1.00	0	0.054± 0.02
144	As-is	Fiber	Precursor	1.00	0.012±0.013	0.611±0.011
144	As-is	Fiber	Hot Draw	1.00	0.040±0.004	0.658±0.011
144	As-is	Fiber	Hot Draw	1.25	0.022±0.004	0.648±0.002
144	As-is	Fiber	Hot Draw	2.50	0.032± 0.003	0.685±0.004
144	As-is	Fiber	Hot Draw	3.75	0.041± 0.006	0.683±0.009
144	As-is	Fiber	Hot Draw	4.50	0.073± 0.016	0.071±0.027
144	As-is	Fiber	Hot Draw	4.95	0.063±0.010	0.675±0.009
Tussah	Control	Fiber	Native	NA	0.27±0.02	0.330±0.001

[0168] Figure 4 illustrates the results observed using this process. There was a marked increase in the A_{iso} and P2 values in the Hot Draw fibers as compared to the undrawn fiber. The increase roughly corresponded to the draw ratio. Thus, the Hot Draw fibers exhibited increased beta-sheet formation relative to the precursor fiber and beta-sheet formation corresponded to the draw ratio applied while passing the precursor fiber over the hot surface.

Example 7: Glass Transition Temperature of the Hot Draw and Precursor Fibers

[0169] Modulated Differential Scanning Calorimetry (MDSC) was used to determine the glass transition temperature of fiber formed from a subset of the samples discussed above with respect to Example 6 and below with respect to Example 8. A DSC, TA Instruments Q2000 was used to generate thermograms. Prior to the measurement, the instrument was calibrated using indium and sapphire to verify heat flow and heat capacity respectively, followed by an empty pan to verify the baseline. 5-10 mg of sample was pressed into a non-hermetically sealed aluminum pan and placed in the DSC cell along with an empty reference pan. The cell was purged with nitrogen at 20 ml/min for the duration of the experiment. The sample was heated at 125°C for 1 hour to remove excess water, followed by a modulated ramp (3°C/min +/- 0.6°C, 1 minute period) from -20°C to 220°C. The Tg (glass transition temperature) was then determined from the reversing heat capacity thermogram by finding the point on the curve halfway between the tangents extrapolated from the onset and offset of the transition.

[0170] The glass transition temperatures are tabulated below:

Table 8: Glass Transition Temperatures of 18B Fiber Samples

Source Ref	Reprocess Type	Fiber or Powder	Precursor or Hot Draw	Draw Ratio	Glass transition temperature by DSC (deg C)
144	As-is	Fiber	Precursor	None (~1X)	169.43
144	As-is	Fiber	Hot Draw	4.95x	173.93
1851	Snow white	Fiber	Hot Draw	6X	171.05

Example 8: Measuring Crystallinity using X-ray Diffraction (XRD)

[0171] X-ray diffraction was performed on fibers generated using a formic acid dope comprising the 1851 Snow White powder described above at a concentration of 36% by weight. Dope was extruded through a 125 μm spinneret into a coagulation bath comprising 40% ethanol and 60% methanol to form precursor fibers. The coagulation bath and spinneret were maintained at room temperature (approximately 22°C).

[0172] As a control, Air Draw fibers were subject to a single wrap on a set of godets under minimal draw (i.e. a draw ratio of ~1X), the still-wet fibers were then drawn between two godets spaced at a distance of 2.1 m to a draw ratio of 7-8X at room temperature at a

relative humidity of approximately 55-65%. The take-up reel rate was approximately 15-23 m/min. The Air Draw fiber was then wound on a take-up godet.

[0173] For the Hot Draw fibers, precursor fibers were subject to minimal draw (i.e. a draw ratio of ~1X) as they were passed through the coagulation bath and wound on a take-up godet. The precursor fibers were dried for several weeks before hot drawing. The hot drawn fiber was drawn in three stages. At each stage, the hot drawn fiber was subjected to a different draw ratio. At the first stage, the draw ratio was 1.69X. At the second stage, the draw ratio was 1.91X. At the third stage, the draw ratio was 1.85X. The combined draw ratio from the three stages was 6X. During each stage, the hot surface used was a steel bar with a "D" shaped curved profile heated to 200°C. The total length of the hot surface the fibers traveled over was 1cm. The fiber pivots at an angle of 20 to 60 degrees over the hot surface (*see* Figure 2B).Godets used to draw the fibers were spaced 60 cm apart. The feed reel rate was 1 m/min and the take-up reel rates were 1.69, 1.91 and 1.85 corresponding to the above-discussed draw ratios.

[0174] Precursor, Air Draw and Hot Draw fibers were analyzed using X-ray diffraction. The XRD samples were prepared by making a bundle of fibers with approximately 100 individual filaments per bundle. The fibers were aligned in a bundle such that they were all parallel and affixed to a frame with the fiber bundle axis perpendicular to the X-ray beam. The XRD was carried out at the Stanford Synchrotron Radiation Lightsource beamline 4-2. The wavelength of the X-ray beam was 1.033 Å, with a beam spot size of 100 x 100 μm and a distance to detector center of 327.5 mm. The pattern was recorded using a Rayonix MX225HE detector. The sample to detector distance was 327.5 mm. The diffraction pattern was collected 3 times for 10 seconds each at three different points along the fiber. The three repeats were averaged. Multiple images were taken at each point and averaged for better statistics and enhanced signal to noise ratio.

[0175] Radial profiles were constructed by integrating the intensity azimuthally over the desired range of azimuthal angles, φ, and plotting it as a function of the scattering angle, 2θ. An integrated scan is obtained by integrating azimuthally over φ=-90 to 90° and plotting that as a function of 2θ. The integrated scan contains information regarding the crystallinity. To extract crystallinity values from the integrated scan, the amorphous and crystalline peaks have to be fitted to the intensity profile. Crystallinity can be calculated with the following equation:

$$CI = \frac{\sum A_c}{\sum A_a + \sum A_c}$$

where A_c is the area of crystalline peaks and A_a is the area of amorphous peaks. For consistency in peak fitting, a radial profile at φ=-66 to -60° was plotted and used to fit the amorphous profile. The amorphous halo in X-ray diffraction patterns is typically isotropic. As this slice did not contain crystalline peaks, the amorphous peak was fitted. The parameters for the amorphous fit were then used for fitting the integrated scan and the remaining peaks were fitted.

Azimuthal profiles are obtained by integrating the intensity radially over a thin ring and plotting it as a function of the azimuthal angle. The alignment of the fiber can be then obtained by measuring the full-width half maximum (FWHM) of the azimuthal peak fit. The azimuthal profile of the (200) peak was integrated over 2θ=10.5° to 11.5°, and (120) peak was integrated over 2θ=13° to 13.8°. The Hermans orientation factor is defined as:

$$f = (3\langle\cos^2\phi_3\rangle - 1)/2$$

where $\langle\cos^2\varphi\rangle$ is:

$$\langle\cos^2\phi_3\rangle = 1 - A\langle\cos^2\phi_1\rangle - B\langle\cos^2\phi_2\rangle$$

where axis 1 is (200), axis 2 is (120) and axis 3 is the fiber axis (002). *See* Grubb, Fiber Morphology of Spider Silk: The Effects of Tensile Deformation, Macromolecules 30(10): 2860-2867 (1997). An orientation factor of f=1 indicates alignment of crystals parallel to the fiber axis, f=-0.5 indicates crystal alignment perpendicular to the fiber axis, and f=0 indicates randomly oriented crystals.

[0176] The 2D diffraction patterns of the Precursor, Air Drawn and Hot drawn fibers are shown in Figure 5. The integrated scans were generated from the 2D diffraction patterns and fitted with at most 5 peaks. The crystalline peaks at ~11.2°, ~13.3° and ~15.6 correspond to the (200), (120) and (211) reflections of the β-sheets structure. The broad wide peak with the largest area under the curve at ~14.5° corresponds to the amorphous structure and the peak at ~7° is likely due to the crystal to crystal distance. Figures 6A, 6B and 6C depict the integrated scans from the precursor fibers, air draw fibers, and hot draw fibers, respectively fitted with the peaks described above. Figure 6A depicts the integrated scan from precursor fibers. Peak 2 in Figure 6A corresponds to the crystalline (120) reflection. Figure 6B depicts the integrated scan from Air Draw fibers. Peaks 2 and 3 in Figure 6B correspond to (120) and

(211) reflections, respectively. Figure 6C depicts the integrated scan from Hot Draw fibers. Peaks 3, 4 and 5 in Figure 6C correspond to (200), (120), and (211) reflections, respectively.

[0177] Using the area under the curve of each peak, the crystallinity was calculated and tabulated in Table 9. The precursor fiber had the lowest crystallinity of 1.5%. The air drawn fiber had a crystallinity of 2.8%, while the hot drawn fiber had the highest crystallinity of 7.5%. This indicates that the structure resulting from hot draw process has more than 2.5 times higher β-sheets compared to the fibers from the air draw process. In addition, the diffraction pattern of the air drawn fibers lack the (200) peak, while the (200) peak is clearly visible in the hot drawn fibers. This suggests that the hot drawn fibers have formed 3D β-sheets, while the air drawn fibers have mainly formed a 2D structure and lack the interlocking of protein side chains.

[0178] The azimuthal profiles of the fibers with are shown in Figures 7A and 7B, respectively. In addition to the precursor, Hot Draw and Air Draw fibers, Native Tussah silk (*A. pernyi*) was used analyzed as a reference sample. The main (200) and (120) peaks are fitted with an azimuthal fit with a Pearson VII peak and (211)/(201) subsidiary peaks fitted with a Gaussian peak as described in Grubb, Macromolecules 30(10): 2860-2867 (1997). The Full Width at Half Maximum (FWHM) of the crystalline peaks was calculated and tabulated in Table 9. The FWHM of the precursor fiber is large compared to the drawn fibers. The Herman orientation factors of the various fibers were also calculated and included in Table 9. The Herman orientation factor of the hot drawn fiber is slightly higher than that of the air drawn fiber. The (120) peak in this sample is meridional, while all other (200) and (120) peaks are equatorial.

Table 9. Structural parameters of Snow White fibers

Source	Process type	Fiber or Powder	Hot Draw or Precursor	Draw Ratio	Crystallinity Index (%)	FWHM at 11°	FWHM at 13.3°	Herman Orientation Factor
1851	Snow white	Fiber	Precursor	None	1.54±0.05	74±16	78±16*	NA
1851	Snow white	Fiber	Air Drawn	7X	2.84±0.02	22.7±0.1	18.0±0.3	0.89±0.01
1851	Snow white	Fiber	Hot Draw	6X	7.49±0.05	17.4±0.4	19.5±0.2	0.91±0.01
Control	Control	Fiber	Native Tussah Silk (*A. pernyi*)	None	31 ± 4.9	17.6±2.0	15.1±0.4	0.92±0.01

Experiment 9: Manipulating Precursor Fiber Crystallinity to Modulate Properties of Drawn Fiber

[00179] Various techniques of increasing fiber crystallinity before and after drawing fiber were performed. In order to produce the fibers, 18B powder that was not subjected to any reprocessing was used. The purity of the 18B powder was determined using the same methodology described above in Example 1 and the purity profile is included below in Table 10. The 18B powder was stored at 60°C under vacuum to reduce the water content to below 4 wt%.

Table 10: Purity profile of 18B powder as assessed by size exclusion chromatography.

Fraction	**Average SEC area %**	**Standard deviation of SEC area %**
High molecular weight impurities	2.55	0.76
18B aggregates	5.73	0.59
18B monomer	47.96	0.99
Intermediate molecular weight impurities	31.65	0.2
Low molecular weight impurities	12.12	2.15

[00180] The 18B powder was dissolved in 98% formic acid at a concentration of 36 wt% using a planetary centrifugal mixer (Thinky ARE-400TWIN) at 1600 revolutions per minute and 1600 rotations per minute. The dope was degassed by centrifugation at 15317 RCF for 30 minutes before loading into a syringe. The dope was extruded via syringe pump

at 40 µl/min through a spinneret with a 127 µm diameter capillary, through a 1 cm air gap, and into a coagulation bath of 100% reagent alcohol (88.5 – 92.5 vol% ethanol; 4 – 6 vol% isopropanol; 3.5 – 5.5 vol% methanol). The fiber was reeled through 1.5 m of bath at 1.7 m/min (corresponding to a residence time of 53 s), wrapped once around a godet at the same speed, and then collected on a take-up godet at 3 m/min.

[00181] To investigate the modulating effect of annealing prior to hot drawing fiber, finished spools ("precursor fibers") were stored either in a box purged with clean dry air ("CDA-stored") or a sealed box containing a beaker filled with ~200 ml of methanol ("annealed") before characterization or post-processing. Precursors were stored under CDA for times ranging from 16 hours to 2 weeks, or in methanol vapor for times ranging from 16 hours to 24 hours.

[00182] Hot drawing of CDA-stored and annealed precursor fibers was performed by passing the fiber over a hot surface (20 cm path length) at 200 °C at a feed rate of 1 m/min, and collecting on a take-up godet at 4.3 m/min. The distance between the feed and take-up godets was 40 cm.

[00183] To investigate the beta-sheet formation of the CDA-stored and annealed fibers before and after hot drawing the fibers, the glass transition temperature (Tg) was measured using a dynamic mechanical analyzer (TA Instruments Q800). To prepare the precursor fibers for DMA, sections of fiber were epoxied to paper frames with a 1 cm gauge length, the sides of which were removed after the fiber was clamped inside the instrument furnace. Samples were subjected to a temperature ramp (22 to 250 °C at 3°C/min) while simultaneously subjected to an oscillatory strain (20 µm at 1 Hz). The DMA furnace was purged with clean dry air for the duration of the experiment. The glass transition temperature was calculated from the resulting thermograms by finding the peak maxima of the loss tangent. Table 11 (below) shows that the glass transition temperature significantly increases with methanol annealing, demonstrating a higher-level of crystallinity and beta-sheet formation.

Table 11: Glass transition temperatures of CDA-stored and annealed precursor fibers

Precursor storage condition	**Average T_g (storage modulus inflection, °C)**	**95% confidence interval of average T_g (storage modulus inflection, °C)**	**n**
CDA	147	13	4
Methanol vapor	195	7	3

[00184] In addition, the mechanical properties of precursor and hot drawn fibers were measured using a TexTechno Favimat+ at 65% relative humidity, according to ASTM standard D1776. Table 12 lists the different mean tenacities measured from CDA-stored and annealed precursor fibers before and after post-hot draw annealing. Figure 8 includes a graph of the same. Data points shown in Figure 8 represent the measurement of a single filament. Diamonds represent the mean tenacity and the upper and lower 95% confidence intervals of the mean tenacity. A: hot drawn CDA-stored precursor. B: hot drawn CDA-stored precursor after annealing. C: hot drawn annealed precursor. D: hot drawn annealed precursor, annealed again after hot drawing. As shown by these data, annealing steps prior to and after hot draw increased the tenacity of the fiber, likely because of increased three-dimensional crystallinity and beta-sheet structure formation.

Table 12- Tenacities of Hot Drawn Fibers

Sample code	Mean tenacity (cN/tex)	95% CI of mean tenacity (cN/tex)	n
A	12.9	0.3	13
B	15.3	0.7	15
C	17.5	0.6	15
D	16.9	0.5	14

Example 10: Hot Drawn Reconstituted *Bombyx mori* Silk Fiber

[00185] To observe the effect of "hot drawing" the fiber on silks with different characteristics than recombinant spider silks, fibers were spun from reconstituted *Bombyx mori* (i.e. silkworm) silk. The reconstitution method broadly followed the steps detailed in Rockwood DN, et al. Materials fabrication from *Bombyx mori* silk fibroin, Nat Protoc. 2011;6(10):1612-31. As a first step, 20 to 49 g of *Bombyx mori* yarns were washed in 1.5 L of 0.5 wt% sodium carbonate solution for more than 8 hours at 37 °C. Fibers were then rinsed with demineralized water four times to remove the carbonate before freeze drying. Subsequently, the dried fiber was solubilized in 9.5 M lithium bromide at 200 to 300 mg/mL in a planetary centrifugal mixer (Thinky ARE-400TWIN) set to 1600 RPM for 15 minutes. The solution was centrifuged at 2500 RPM to remove air bubbles before filtering through a 1.3 µm syringe filter. The solution was then transferred to a 30 kDa dialysis cassette to wash the lithium bromide until the permeate conductivity dropped below 50 µS/cm. The dialyzed solution was then flash frozen using liquid nitrogen before freeze drying to sublimate the water off of the silk. The *B. mori* reconstituted silk fibroin (RSF) foam was crushed using a mortar and pestle until forming a fine powder for dope mixing.

[00186] Prior to dope preparation, *B. mori* RSF was stored at 60 °C under vacuum to reduce water content to below 4 wt%. Powder was dissolved in 98% formic acid at a concentration of 36 wt% using a planetary centrifugal mixer (Thinky ARE-400TWIN) at 1600 RPM. The dope was degassed by centrifugation at 15317 RCF for 30 minutes before loading into a syringe.

[00187] Dope was extruded via syringe pump at 40 µl/min through a spinneret with a 127 µm diameter capillary, through a 1 cm air gap, and into a coagulation bath of 100% reagent alcohol (88.5 – 92.5 vol% ethanol; 4 – 6 vol% isopropanol; 3.5 – 5.5% methanol). The fiber was reeled through 1.5 m of bath at 1.7 m/min corresponding to a residence time of 53 s and wrapped once around a godet at the same speed. Precursor fibers were then collected on a take-up godet at 3 m/min. Finished spools were stored either in a box purged with clean dry air ("CDA-stored") or a sealed box containing a beaker filled with ~200 ml of methanol ("annealed") before characterization or post-processing. Precursors were stored under CDA for times ranging from 16 hours to 2 weeks, or in methanol vapor for times ranging from 16 hours to 24 hours.

[00188] Precursor fibers were continuously hot drawn by passing the fiber over a hot surface (20 cm path length) at 200 °C at a feed rate of 1.5 m/min, and collecting on a take-up

godet at 4.8 m/min for a draw ratio of 3.2X. The distance between the feed and take-up godets was 40 cm.

[00189] The mechanical properties of precursor and hot drawn fibers were measured using a TexTechno Favimat+ at 65% relative humidity, according to ASTM standard D1776. Table 13 below lists the mechanical properties of the fibers. Data is presented as the average value ± the 95% confidence interval of the mean. Stress-strain curves corresponding to this data are shown in Figure 9. As shown by this data, the methanol annealed fibers had a higher tenacity, likely due to enhanced formation of beta-sheet and three-dimensional crystalline structures.

Table 13: Tenacity, linear density (LD), and elongation at break for formic acid dope spun *Bombyx mori* precursor fibers and continuously hot drawn fibers

	n	LD dTex	95% CI	Tenacity cN/Tex	95% CI	Initial modulus cN/Tex	95% CI	Elongation at break %	95%CI
F5131_ *Bombyx mori* RSF As-is (precursor)	15	103	6	11.0	0.8	316	333	149	18
F5139_ *Bombyx mori* RSF As-is (hot drawn_3.2x)	24	68	3	22.1	0.7	653	670	16	3
F5140_ *Bombyx mori* RSF Annealed (hot drawn_3.2x)	22	65	3	25.0	0.8	868	889	11	2

[00190] The glass transition temperature (T_g) of CDA-stored and annealed precursor fibers was measured using a dynamic mechanical analyzer (TA Instruments Q800). To prepare the precursor fibers for DMA, sections of fiber were epoxied to paper frames with a 1 cm gauge length, the sides of which were removed after the fiber was clamped inside the instrument furnace. Samples were subjected to a temperature ramp from 22 to 250 °C at 3°C/min under an oscillatory strain of 20 μm at 1 Hz. The DMA furnace was purged with clean dry air for the duration of the experiment. The glass transition temperature was calculated from the resulting thermograms by finding the maxima of the loss tangent. Figure 10 includes plots of the loss modulus and loss tangent curves, the calculated glass transition temperature (Tg) is shown using arrows. Table 14 (below) includes the calculated glass transition temperature for the different samples. As with fibers created using 18B powder, a higher glass transition temperature was observed in annealed reconstituted *Bombyx mori* fibers.

Table 14 – Glass transition temperature of annealed and precursor *Bombyx mori* RSF fibers

	N	Storage modulus (degC)		Loss modulus peak (degC)		Tan delta peak (degC)	
Treatment		AVG	95% CI	AVG	95% CI	AVG	95% CI
Bombyx mori RSF As-is (precursor)	2	163.3	6.2	160.5	6.0	180.9	N/A
Bombyx mori RSF Annealed (precursor)	2	202.3	38.5	202.3	45.1	224.8	14.6

.

Example 11 – Fibers spun using N-methyl morpholine N-oxide (NMMO) as a dope solvent

[00191] N-methyl morpholine N-oxide was used as a dope solvent to determine whether the same properties could be observed using a different dope solvent. 18B powder with the same purity profile referenced in Example 9 was stored at 60°C under vacuum to reduce water content to below 4 wt%. A mixture containing 24 wt% 18B powder, 75 wt% NMMO monohydrate, and 1 wt% propyl gallate was mixed with an anchor impeller at 250 RPM in a glass reactor heated to 100 °C via oil bath for 90 minutes until a viscous solution was formed. The reactor was purged with nitrogen at 5 SCFM for the duration of mixing. After dissolution, the dope was degassed by stirring at 25 – 50 rpm and applying vacuum starting at 200 torr and increasing to 50 torr over the course of 16 minutes. The dope was then harvested from the reactor and further degassed via centrifugation at 15317 RCF, reheated at 80 °C for 30 minutes, and centrifuged a final time at 15317 RCF. Dope was stored at 80 °C until it was used for spinning.

[00192] The rheological properties of NMMO-based dopes were measured using a rotational rheometer (Malvern Panalytical Kinexus lab+) configured with a cone (2°, 20 mm diameter) and plate geometry. To measure the frequency response at a single temperature, dope samples were heated to 80 °C and subjected to a 1% oscillatory strain as the frequency ranged from 100 – 0.1 Hz, with 3 samples taken per decade. To measure the temperature response, dope samples were subjected to a 1% oscillatory strain at 10 Hz as the temperature was increased from 70 °C to 100 °C. Figure 11 shows that the complex viscosity and phase angle of NMMO-based dopes as a function of frequency and temperature. Data is shown from three independent repeat dope preparations. Table 15 below includes the mean values calculated from the repeat dope preparations at 85 °C.

Table 15 – Mean Complex Viscosity and Phase Angle of NMMO-based 18B Dopes at 85 °C and 10 Hz

	Mean	95% CI of mean	n
Complex viscosity (Pa·s)	100	25	3
Phase angle (°)	60	4	3

[00193] To generate fiber, dope was loaded in a syringe pump (Teledyne Isco 260D) equipped with a temperature control jacket connected to a recirculating oil heater. Dope was pumped through a custom-built jacketed extrusion line and spinneret, both of which were also connected to the oil heater. The oil temperature was maintained at 85 °C for the duration of spinning. Dope was extruded at 40 µl/min through a spinneret with a 125 µm diameter capillary, through a 5 cm air gap, and into a coagulation bath of 100% reagent alcohol (88.5 – 92.5 vol% ethanol; 4 – 6 vol% isopropanol; 3.5 – 5.5 vol% methanol). The fiber was reeled through the 1.5 m coagulation bath at 7 m/min (corresponding to a residence time of 12.8 s) and then wrapped 5 times around a set of godets onto which methanol was dripped at an average rate of 15 ml/min via a peristaltic pump. The total path length of the wraps around the first set of godets was 5 m. From there, the fiber was passed through a 1.5 m wash bath containing 80 vol% methanol and 20 vol% DI water at 10 m/min, corresponding to a residence time of 9 s. The fiber was then wrapped 5 times around another set of godets onto which a mixture of 75 vol% methanol and 25 vol% DI water was dripped at an average rate of 7 ml/min via peristaltic pump. The total path length of the wraps around the second set of godets was 3.3 m. Finally, the fiber was collected on a take-up godet at a rate of 10.5 m/min. Spools were stored at 22 °C and ambient relative humidity before characterization and post-processing.

[00194] NMMO-based precursor fibers were drawn by hand (referred to as "manual hot draw") by bringing them in contact with a hot surface (20 cm length) at 200 °C and stretching them at a draw ratio of approximately 3.4x. In addition, NMMO-based precursor fibers were continuously hot drawn in two stages by passing the fiber over a hot surface (20 cm path length) at 200 °C at a feed rate of 1.5 m/min, and collecting on a take-up godet at 3 m/min, followed by another draw step at a feed rate of 1.5 m/min and collecting on a take-up godet at 2.8 m/min, resulting in a total draw ratio of 3.73 m/min. The length between the feed and take-up godets was 40 cm.

[00195] The mechanical properties of hot drawn NMMO-based fibers were measured using a TexTechno Favimat+ at 65% relative humidity, according to ASTM standard D1776.

Table 16 (below) lists the tenacity, linear density, and percent elongation at break for manually and continuously hot drawn NMMO-based fibers. Fibers were generated from independent dope preparation/spinning runs (denoted by spool). Data is presented as the average value ± the 95% confidence interval of the average.

Table 16 – Mechanical Properties of NMMO-based fibers

Spool	Hot draw method	Tenacity (cN/tex)	Linear density (dtex)	Elongation at break (%)	n
[064]_F6	Manual	19.5 ± 0.8	3.8 ± 0.4	17 ± 2	23
[064]_F6	Continuous	17.9 ± 0.4	3.5 ± 0.1	26 ± 2	20
[065]_F2	Manual	18 ± 1	3.7 ± 0.2	18 ± 3	25
[065]_F2	Continuous	19.5 ± 0.4	3.7 ± 0.1	22 ± 2	18
[066]_F2	Manual	17 ± 1	3.7 ± 0.3	18 ± 4	25

[00196] X-ray diffraction was performed in order to measure crystallinity of the fibers. To prepare samples for XRD, fibers were bundled (~10-20 filaments/bundle) and affixed to a frame. XRD was performed on beamline 4-2 at the Stanford Synchrotron Radiation Lightsource with a beam energy of 15.5 keV (0.799 Å), spot size of 100 x 100 µm, and a sample to detector distance of 327.5 mm. Diffraction patterns were collected using a Rayonix MX225-HE detector with a 10 second exposure time. Three exposures were taken at 3 different points along the fiber bundle. Data was analyzed as described above with respect to Example 8. Figures E-G include the integrated radial and azimuthal intensity profiles generated from XRD of continuously hot drawn NMMO-based fibers. Figure 12 depicts radially integrated intensity through equatorial reflections. Figure 13 depicts Azimuthally integrated intensity through the (120) reflection. Figure 14 depicts Azimuthally integrated intensity through the (200) reflection. Table 17 includes the estimated percent crystallinity and Herman's orientation factor for continuously hot drawn NMMO-based fibers. Data is presented as the average ± the standard deviation of 3 exposures at 3 different locations on the fiber bundle.

Table 17 – Crystallinity of hot drawn NMMO-based fibers

Sample	Estimated crystallinity (%)	Herman's orientation factor
Continuously hot drawn NMMO-based fiber	6.70 ± 0.09	0.79 ± 0.00

Example 12 – Elevated Take-up Throughput Hot Draw Process

[00197] Elevated uptake speeds are beneficial in that they allow for rapid processing of precursor fiber. To investigate the effects of various uptake speeds on the hot draw process, precursor fiber was spun using NMMO-based dope as described above in Example 11. Precursor fibers were then continuously hot drawn by passing the fiber over a hot surface (20 cm path length) in three stages with the feed rate, take-up rate, and hot surface temperature or each stage as follows: stage 1: 10.5 m/min, 26.3 m/min (2.5x), 200 °C; stage 2: 26.3 m/min, 34 m/min (1.3x), 220 °C; stage 3: 34 m/min, 37 m/min (1.08x), 220 °C. The total draw ratio was thus 3.52x. The length between the feed and take-up godets for each stage was 40 cm.

[00198] The mechanical properties of hot drawn NMMO-based fibers were measured using a TexTechno Favimat+ at 65% relative humidity, according to ASTM standard D1776. Table 18 (below) includes tenacity, linear density, and elongation at break of the fibers produced from the elevated take-up throughput hot draw process.

Table 18 – Tenacity, linear density, and elongation at break of the fibers produced from the elevated take-up throughput hot draw process.

	Tenacity (cN/tex)	Linear density (dtex)	Elongation at break (%)
Mean	15.9	3.7	29
Standard deviation	0.9	0.5	5
95% confidence interval of mean	0.1	0.06	0.6
n	305	305	305

Example 13 – Batch mode Hot Drawing Precursor Fibers

[00199] An apparatus for performing hot draw in a batch manner was constructed by attaching parallel steel rods to both the traveler and the end of a linear actuator (Zaber T-LSR450D) and positioning the apparatus over a hot surface, the temperature of which could be controlled. The position of the hot surface was adjustable such that it could be brought in and out of contact with the steel rods. In this way, precursor fibers strung between the rods could be hot drawn at controlled temperatures and rates.

[00200] Formic acid-based precursor fibers were spun as described Example 9 from 18B powder of the same purity profile described therein. Precursor fibers were affixed between the rods of the batch hot drawing apparatus using Kapton tape. The length of the

fibers between the rods exposed to the hot surface was 2.5 cm. After bringing the hot surface in contact with the mounted fibers, the linear actuator was used to increase the distance between the rods (thus drawing the fibers) in steps of 5 mm at a rate of 5 mm/s until all of the fibers were broken. During this process, the number of unbroken fibers remaining after each draw step was recorded, from which the percent elongation at break distribution could be approximated.

[00201] To study the effects of precursor processing history on hot draw behavior, batch hot draw was performed on both methanol vapor annealed and CDA-stored precursors (the preparation of which is described in Example 9*)* as the temperature of the hot surface ranged from 120 °C to 225 °C. Figure 15 depicts the draw ratio at failure of these fibers over various temperatures.

[00202] In addition, batch hot draw was performed at 200 °C on formic acid-based fibers spun with varying theoretical bath draw ratios and air draw ratios. Theoretical bath draw ratios are calculated by dividing the rate at which the fiber is reeled from the coagulation bath by the theoretical jet velocity, which in turn is defined as the rate of change of the length of a cylinder whose diameter equals the diameter of the spinneret capillary and whose volume as a function of time is equal to the volumetric flow rate of dope through the capillary. For these fibers, the theoretical bath draw ratios ranged from 0.5x - 4x and the air draw ratios ranged from 1.1x – 6.3x. Figure 16 depicts the draw ratio at failure for these fibers. As shown in Figure 16, the draw ratio at failure decreased in proportion to estimated air draw ratio of the fibers. However, the fibers with a higher theoretical bath draw had much higher draw ratios at failure.

[00203] Using batch hot draw, the percent elongation at break distribution of fibers spun with varying theoretical bath draws and air draws was determined. The same fibers were also continuously hot drawn as described in Example 9, and their maximum stable continuous hot draw ratio was determined. The maximum stable continuous hot draw ratio was defined as the hot draw ratio at which at least 5 m of hot drawn fiber could be collected without breaking. The maximum stable continuous hot draw ratio of each fiber was then plotted against the corresponding average draw ratio at break (determined from the percent elongation at break distribution from batch hot draw) and a linear model was fit to the data. In this way, the maximum stable continuous hot draw ratio of a precursor with arbitrary processing history may be predicted by using a small (~1 m) amount of precursor to perform batch hot draw, rather than using a larger (~10 m) amount of precursor to naively optimize for

the maximum stable continuous hot draw ratio in continuous hot drawing. Figure 17 depicts the correspondence between the predicted and observed draw ratio at break.

Claims

1. A drawn fiber comprising silk polypeptide, wherein the fiber is generated by:
dissolving a powder comprising the silk polypeptide into a solvent to generate a spin dope;
extruding the spin dope into a coagulation bath to form a precursor fiber;
collecting the precursor fiber without drawing the precursor fiber; and
drawing the precursor fiber over a hot surface to generate a drawn fiber,
wherein the drawn fiber has a crystallinity index of at least 6% as measured using X-ray diffraction.

2. The drawn fiber of claim 1, wherein said silk polypeptide is a recombinant silk polypeptide.

3. The drawn fiber of claim 2, wherein said recombinant silk polypeptide comprises two or more repeat units of a proteinaceous block copolymer.

4. The drawn fiber of claim 1, wherein said silk polypeptide is a recombinant spider silk polypeptide.

5. The drawn fiber of claim 4, wherein the recombinant spider silk polypeptide is 18B (SEQID NO: 1).

6. The drawn fiber of any one of claims 1-5, wherein the powder comprising the silk polypeptide is comprised of at least 60% silk polypeptide by weight.

7. The drawn fiber of claim 6, wherein the powder comprising the silk polypeptide is comprised of at least 70% silk polypeptide by weight.

8. The drawn fiber of claim 7, wherein the powder comprising the silk polypeptide is comprised of at least 80% silk polypeptide by weight.

9. The drawn fiber of any of claims 1-8, wherein the drawn fiber is drawn over the hot surface at a draw ratio of at least 2X.

10. The drawn fiber of claim 9, wherein the drawn fiber is drawn over the hot surface at a draw ratio of at least 3X.

11. The drawn fiber of claim 10, wherein the drawn fiber is drawn over the hot surface at a draw ratio of at least 4X.

12. The drawn fiber of claim 11, wherein the drawn fiber is drawn over the hot surface at a draw ratio of at least 6X.

13. The drawn fiber of any of claims 9-12, wherein the draw ratio is computed by determining the draw ratio at failure.

14. The drawn fiber of claim 13, wherein determining the draw ratio at failure comprises determining the distribution of maximum elongation at break of one or more precursor fibers using an apparatus designed to draw the fiber over a hot surface while increasing the draw ratio.

15. The drawn fiber of any of claims 1-14, wherein the generation of the fiber further comprises drawing the drawn fiber over a hot surface one or more times.

16. The drawn fiber of claim 15, wherein the sum of the draw ratios at each drawing step is approximately equal to or less than the draw ratio at failure of the precursor fiber.

17. The drawn fiber of claim 15 or 16, wherein the generation of the fiber comprises:
determining a draw ratio at failure of the precursor fiber; and
distributing the draw ratio at failure of the precursor fiber over each of said drawing steps.

18. The drawn fiber of any of claims 1-17, wherein generating the fiber further comprises annealing the precursor fiber prior to drawing the fiber.

19. The drawn fiber of claim 18, wherein annealing the precursor fiber comprises annealing the precursor fiber with alcohol vapor.

20. The drawn fiber of any of claims 1-19, wherein the solvent comprises formic acid.

21. The drawn fiber of any of claims 1-19, wherein the solvent comprises NMMO.

22. The drawn fiber of claim 21, wherein the solvent comprises 20% to 60% by weight NMMO.

23. The drawn fiber of claim 21 or 22, wherein generating said fiber comprises heating said spin dope before said step of extruding the spin dope into said coagulation bath.

24. The drawn fiber of any one of claims 21-23, wherein extruding the spin dope into said coagulation bath comprises extruding the spin dope through an air in the range of 2 to 20 cm.

25. The drawn fiber of any of claims 1-24, wherein the drawn fiber has increased beta-sheet formation relative to the precursor fiber.

26. The drawn fiber of claim 25, wherein the drawn fiber has increased beta-sheet formation relative to the precursor fiber proportional to the draw ratio used to draw the fiber over the hot surface.

27. The drawn fiber of any of claims 1-26, wherein the hot surface is at least 190 degrees Celsius.

28. The drawn fiber of claim 27, wherein the hot surface is at least 200 degrees Celsius.

29. The drawn fiber of any of claims 1-28, wherein the hot surface is at least 20 degrees Celsius greater than the glass transition temperature of the precursor fiber.

30. The drawn fiber of any of claims 1-29, wherein the tenacity of the drawn fiber is greater than 20 cN/tex.

31. The drawn fiber of claim 30, wherein the tenacity of the drawn fiber is greater than 25 cN/tex.

32. The drawn fiber of claim 31 , wherein the tenacity of the drawn fiber is greater than 26 cN/tex.

33. The drawn fiber of any of claims 1-32, wherein the Herman orientation factor of the drawn fiber is approximately the same as native silk fiber.

34. The drawn fiber of any of claims 1-33, wherein the drawn fiber has a crystallinity index of at least 7% as measured using X-ray diffraction.

35. The drawn fiber of any of claims 1-34, wherein the drawn fiber has more than 1.5 times, more than 2 times, or more than 2.5 times increased beta-sheet content as compared to air drawn fibers subject to identical drawing conditions except not drawn over a hot surface.

36. The drawn fiber of any of claims 1-35, wherein the drawn fiber has an increased 3D β-sheet content as compared to air drawn fibers subject to identical drawing conditions except not drawn over a hot surface.

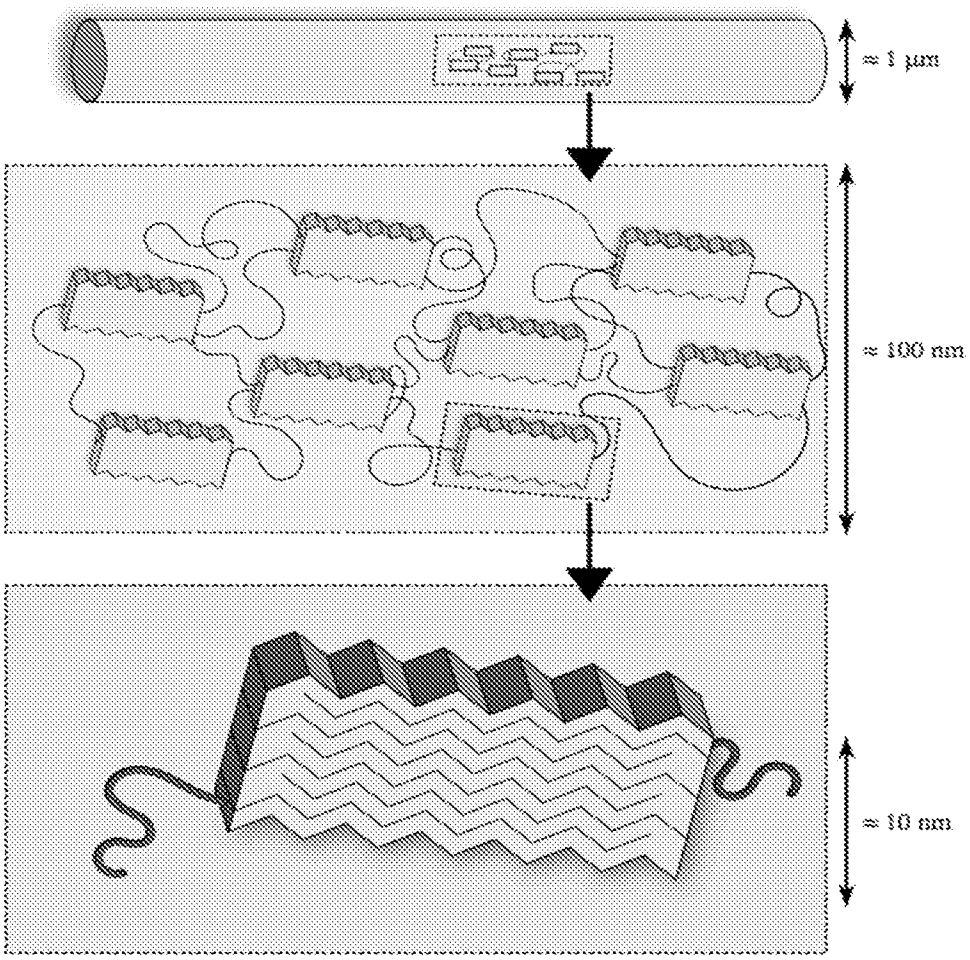


FIG. 1

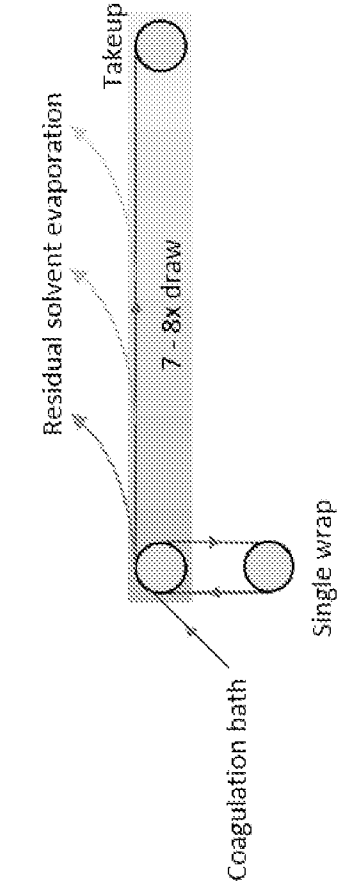

Air draw
Residual solvent evaporation
Takeup
7 - 8x draw
Single wrap
Coagulation bath

FIG. 2A

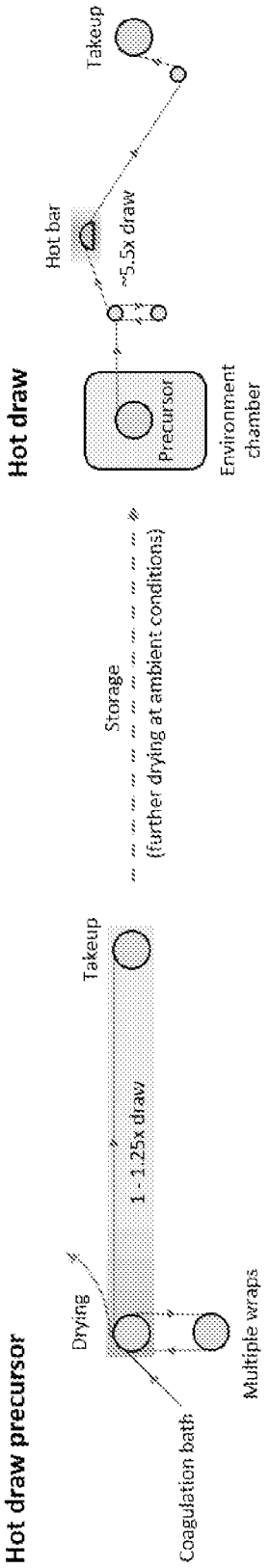

Hot draw
Takeup
Hot bar
~5.5x draw
Precursor
Environment chamber
Storage
(further drying at ambient conditions)
Hot draw precursor
Takeup
Drying
1 - 1.25x draw
Multiple wraps
Coagulation bath

FIG. 2B

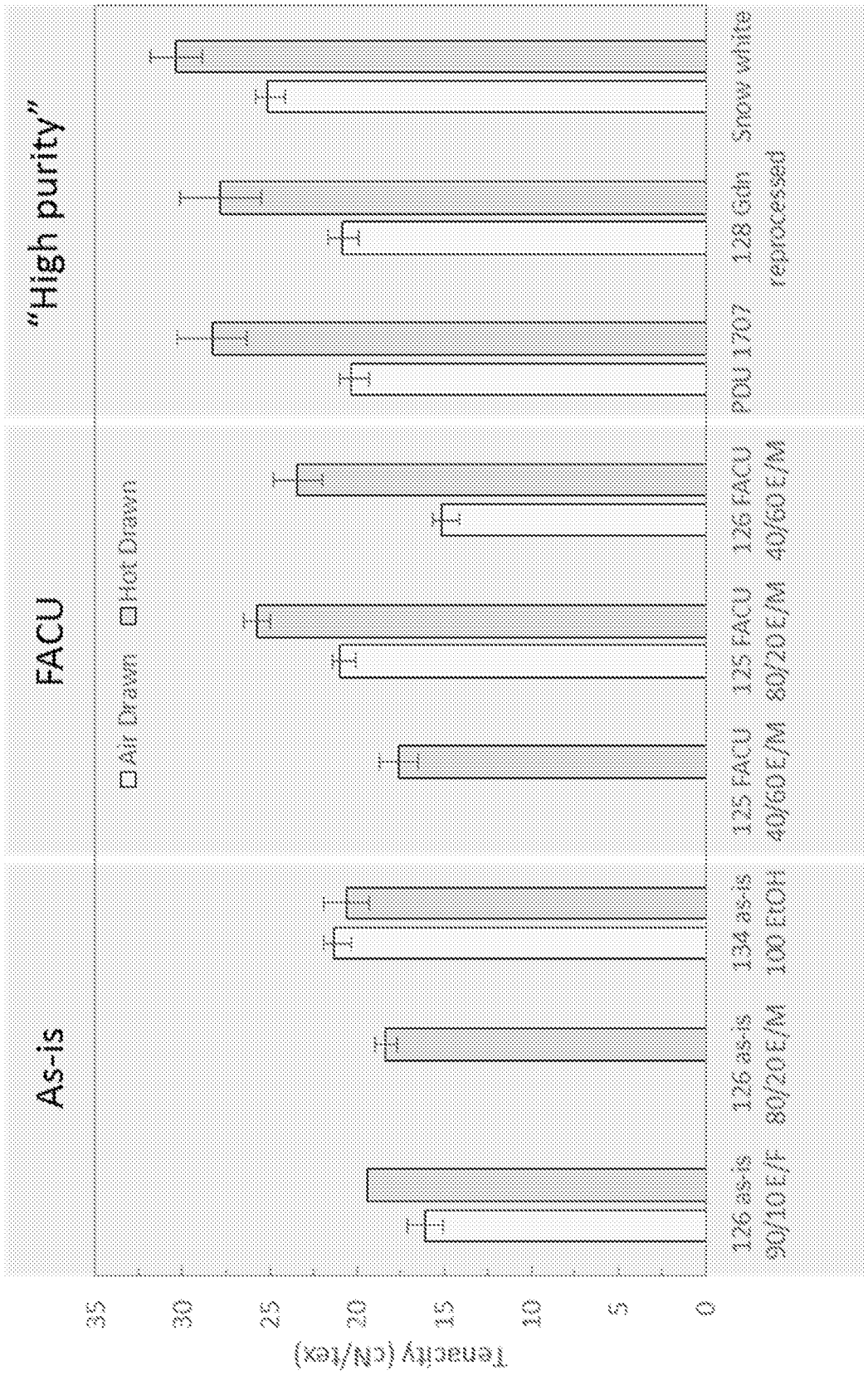

As-is
FACU
"High purity"
Air Drawn
Hot Drawn
Tenacity (cN/tex)
35
30
25
20
15
10
5
0
126 as-is 90/10 E/F
126 as-is 80/20 E/M
134 as-is 100 EtOH
125 FACU 40/60 E/M
125 FACU 80/20 E/M
126 FACU 40/60 E/M
PDM 1707
128 Odn reprocessed
Snow white

FIG. 3A

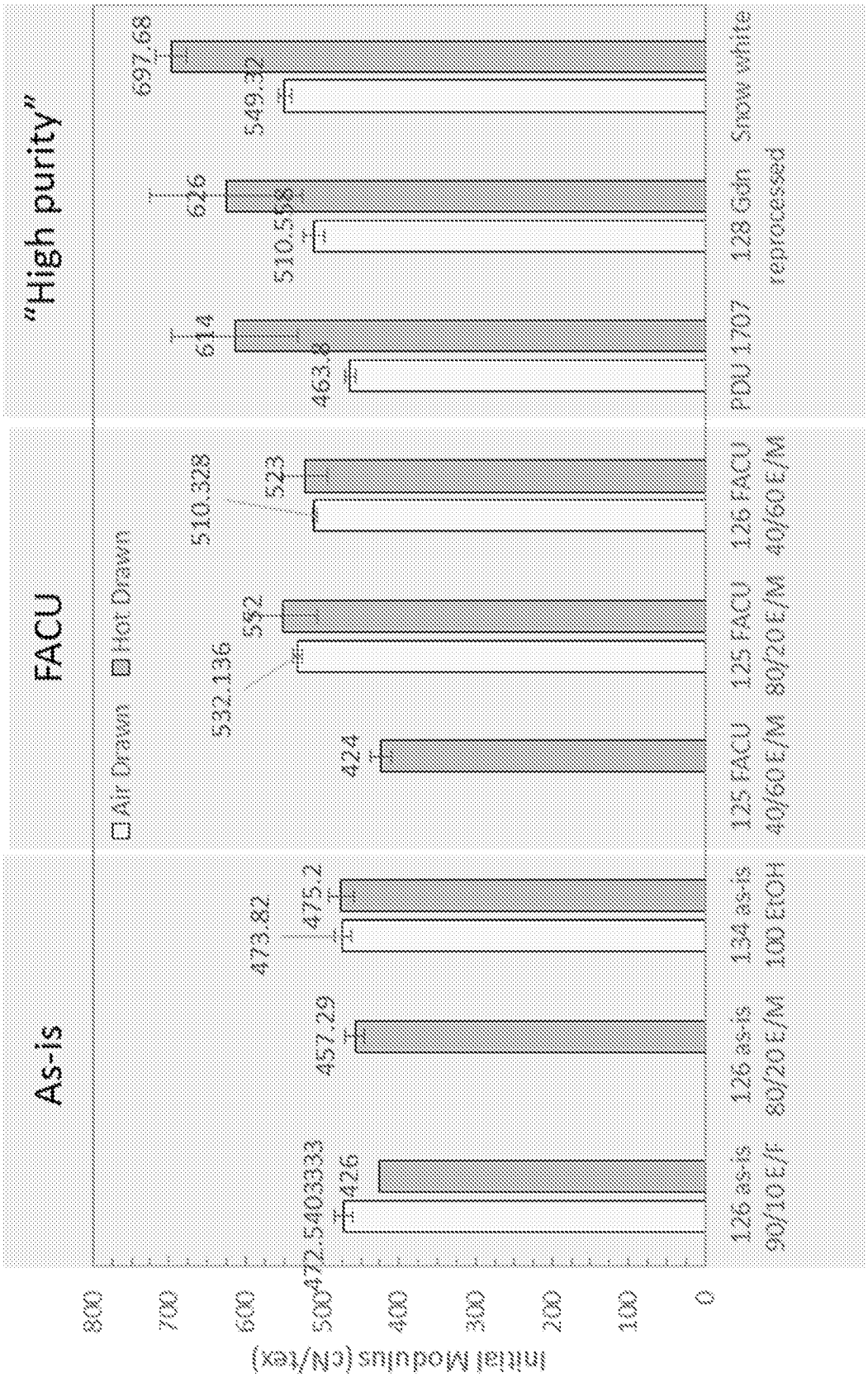

As-is
FACU
"High purity"
Air Drawn
Hot Drawn
Initial Modulus (cN/tex)
800
700
600
500
400
300
200
100
0
472.54
426
473.82
457.29
475.2
424
532.136
562
510.328
523
614
463.8
646
510.568
697.68
549.32
126 as-is
90/10 E/P
126 as-is
80/20 E/M
134 as-is
100 EtOH
125 FACU
40/60 E/M
125 FACU
80/20 E/M
126 FACU
40/60 E/M
PDU 1707
128 Gen
repurposed
Snow white

FIG. 3B

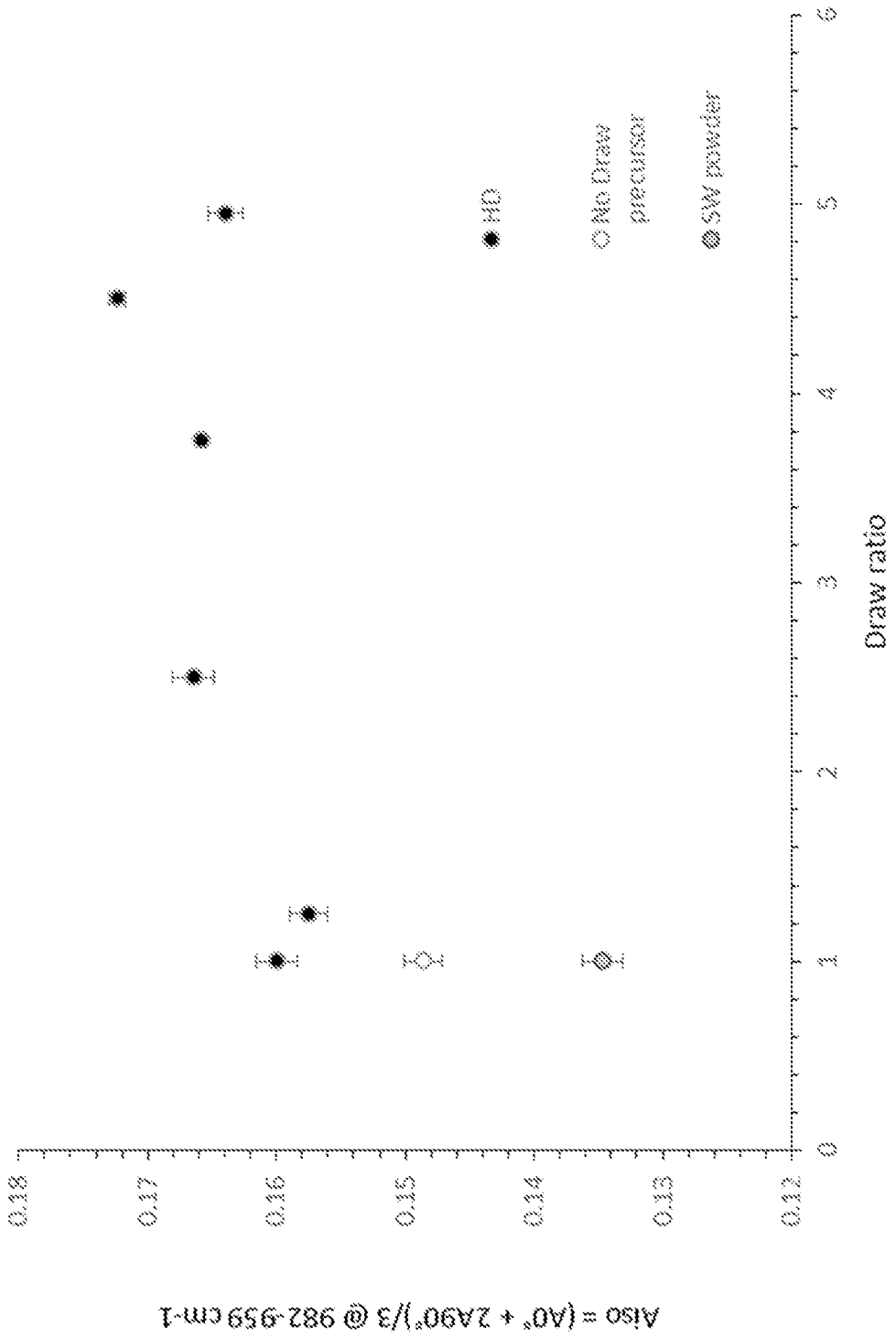

Aiso = (A0° + 2A90°)/3 @ 982-959 cm-1
0.18
0.17
0.16
0.15
0.14
0.13
0.12
0
1
2
3
4
5
6
Draw ratio
HD
No Draw precursor
SW powder

FIG. 4

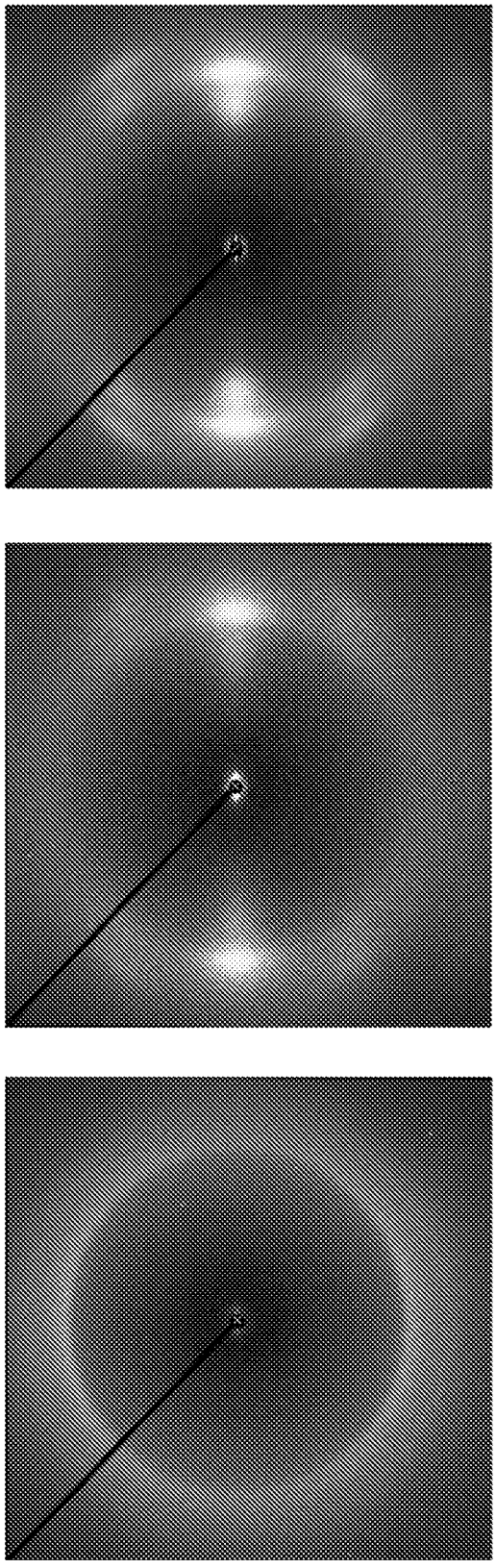


FIG. 5

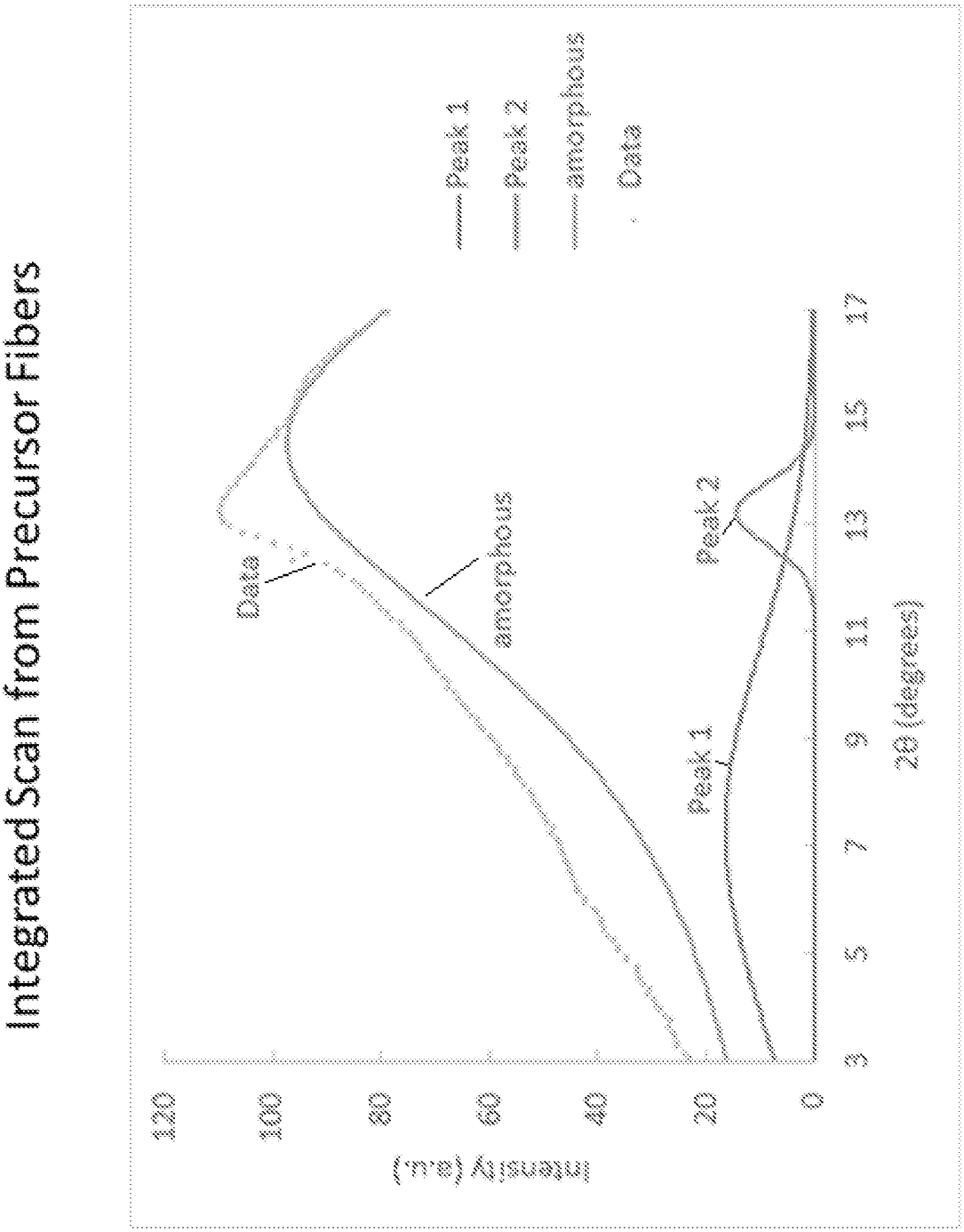

Integrated Scan from Precursor Fibers
Intensity (a.u.)
120
100
80
60
40
20
0
3
5
7
9
11
13
15
17
2θ (degrees)
Data
amorphous
Peak 1
Peak 2
Peak 1
Peak 2
amorphous
Data

FIG. 6A

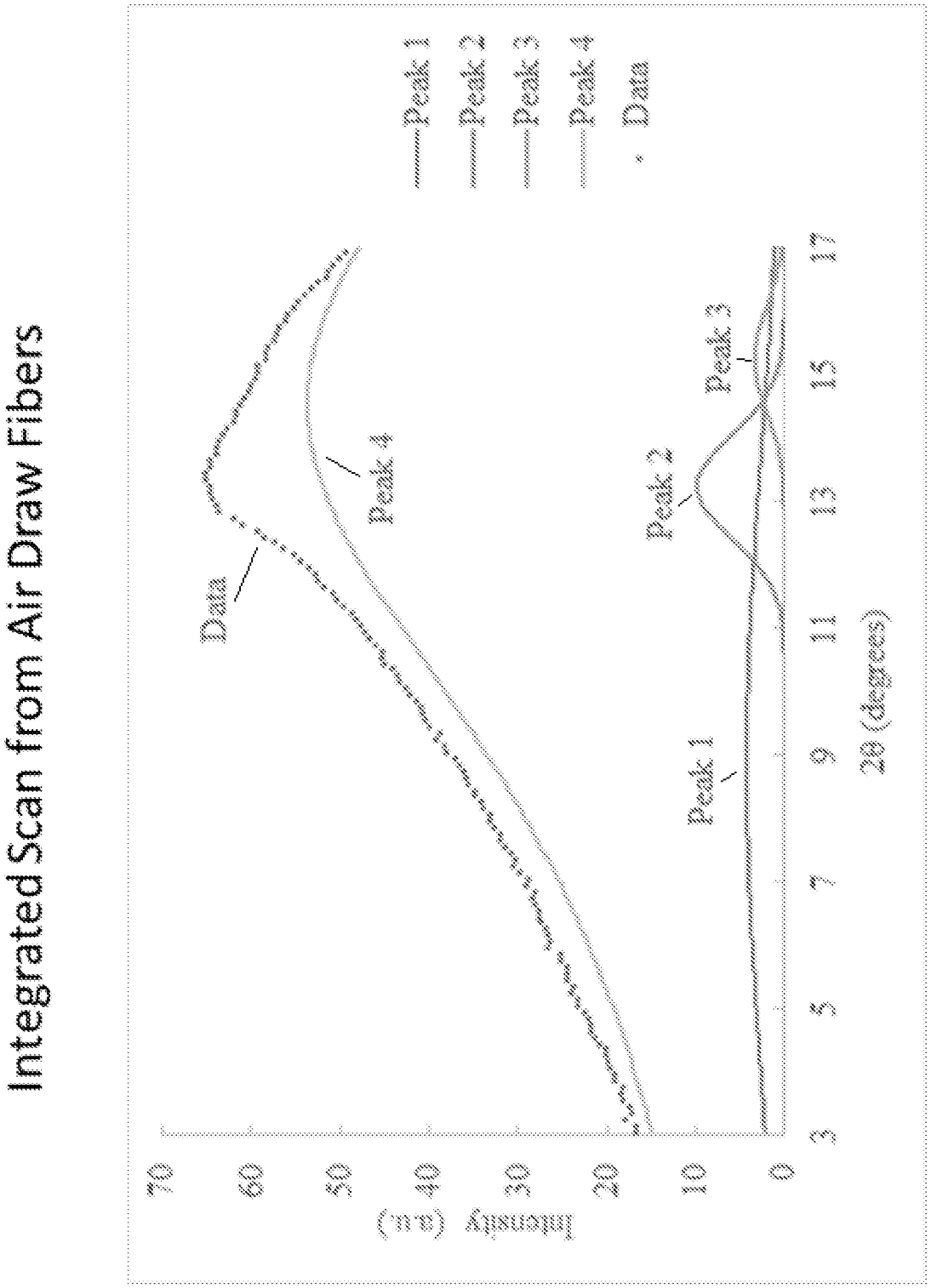

Integrated Scan from Air Draw Fibers
Intensity (a.u.)
70
60
50
40
30
20
10
0
3
5
7
9
11
13
15
17
2θ (degrees)
Data
Peak 4
Peak 1
Peak 2
Peak 3
Peak 1
Peak 2
Peak 3
Peak 4
Data

FIG. 6B

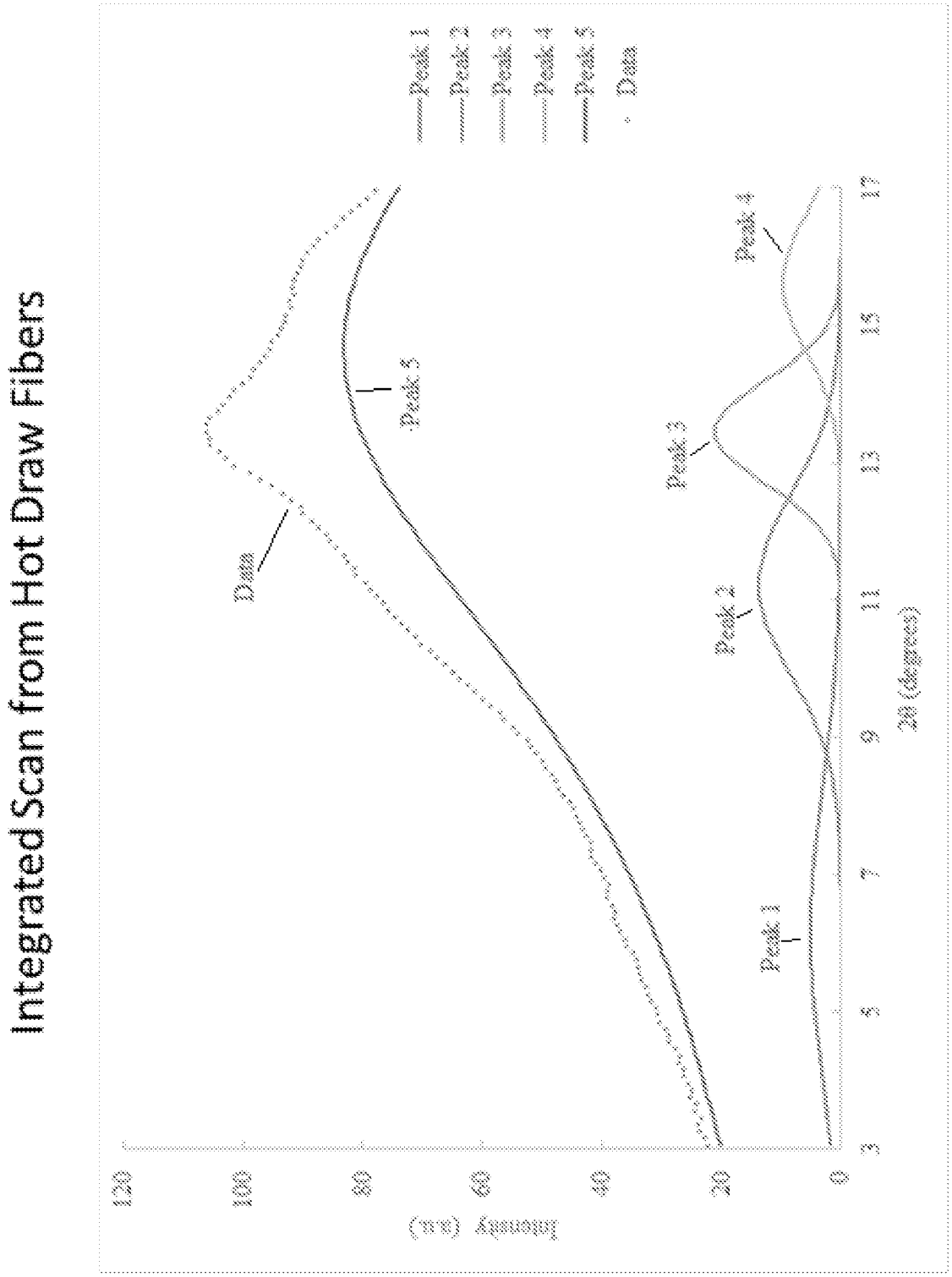

Integrated Scan from Hot Draw Fibers
Peak 1
Peak 2
Peak 3
Peak 4
Peak 5
Data
Peak 3
Data
Peak 4
Peak 3
Peak 2
Peak 1
Intensity (a.u.)
2θ (degrees)
120
100
80
60
40
20
0
3
5
7
9
11
13
15
17

FIG. 6C

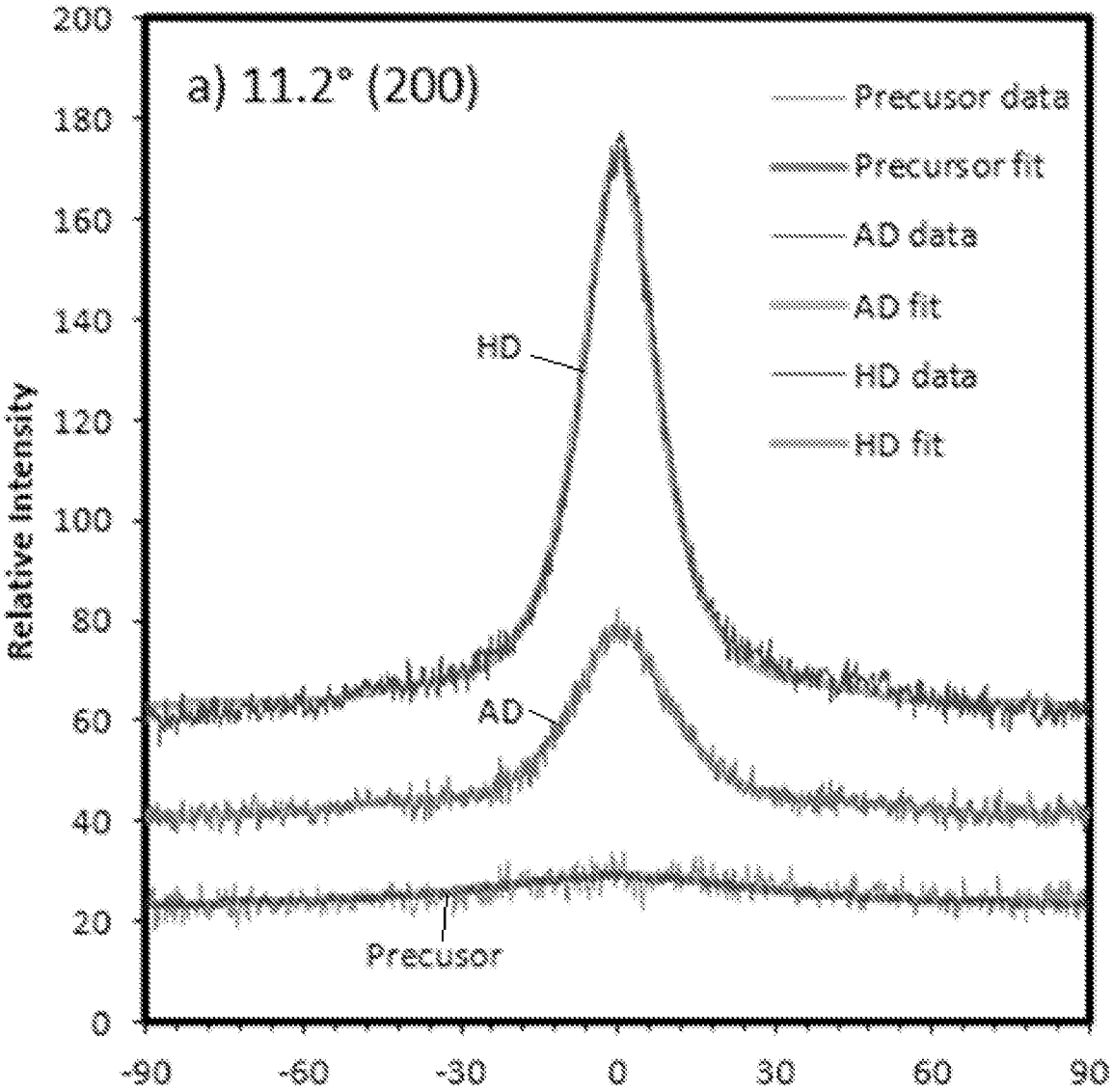

a) 11.2° (200)
Precusor data
Precursor fit
AD data
AD fit
HD data
HD fit
HD
AD
Precusor
Relative Intensity
200
180
160
140
120
100
80
60
40
20
0
-90
-60
-30
0
30
60
90

FIG. 7A

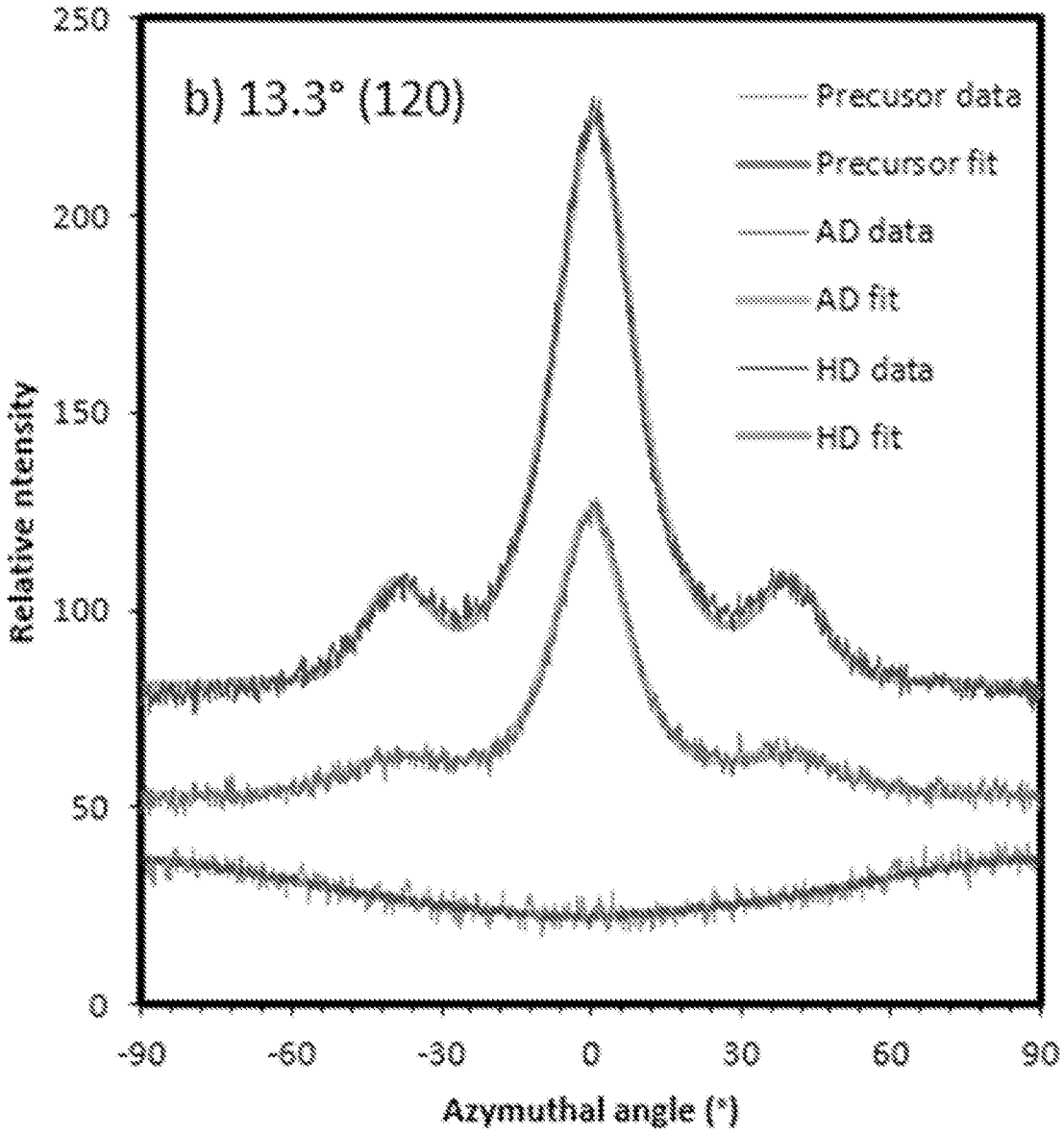

b) 13.3° (120)
Precusor data
Precursor fit
AD data
AD fit
HD data
HD fit
Relative ntensity
250
200
150
100
50
0
-90
-60
-30
0
30
60
90
Azymuthal angle (°)

FIG. 7B

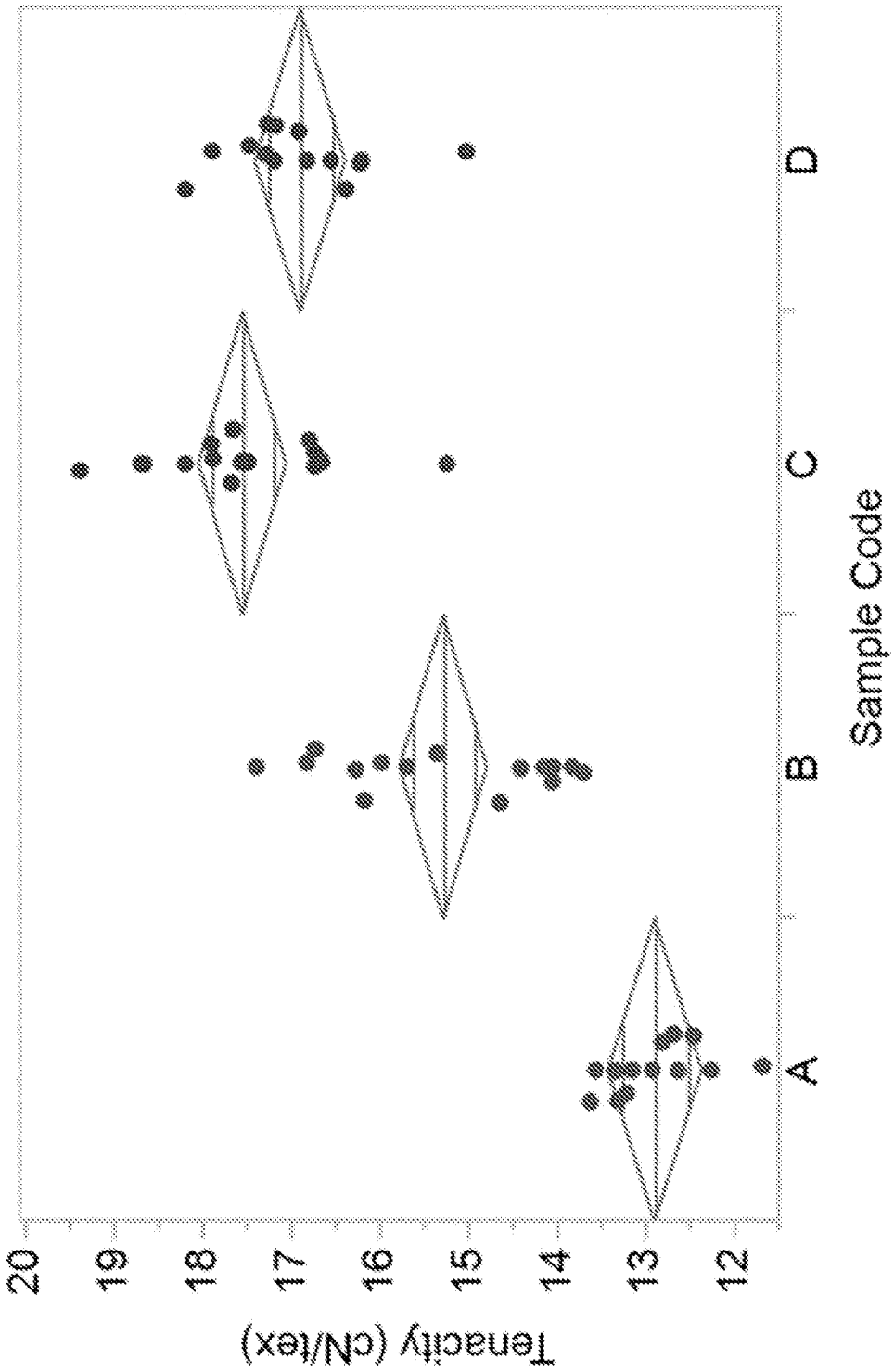


FIG. 8

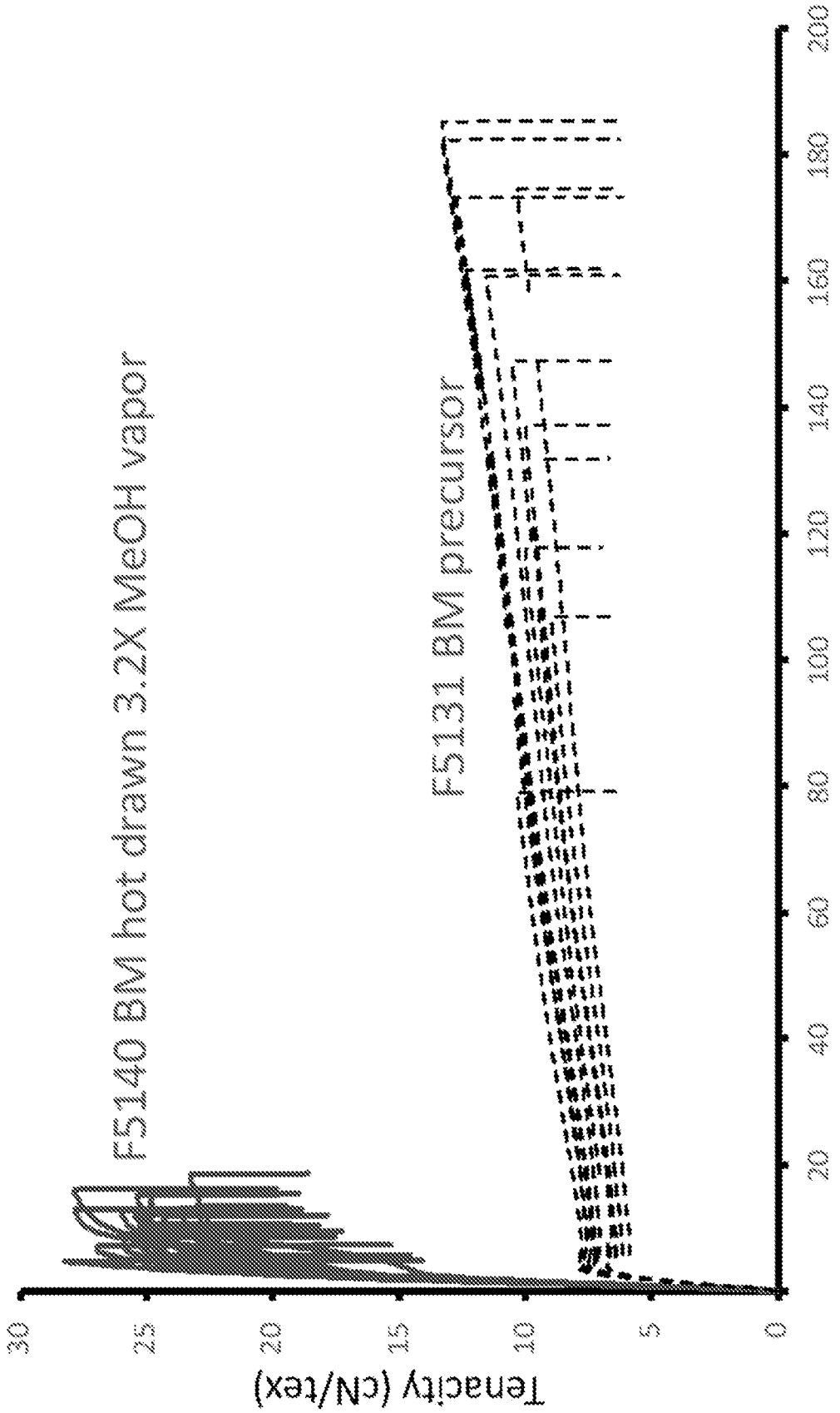

F5140 BM hot drawn 3.2X MeOH vapor
F5131 BM precursor
Tenacity (cN/tex)
Strain (%)
0
5
10
15
20
25
30
20
40
60
80
100
120
140
160
180
200

FIG. 9

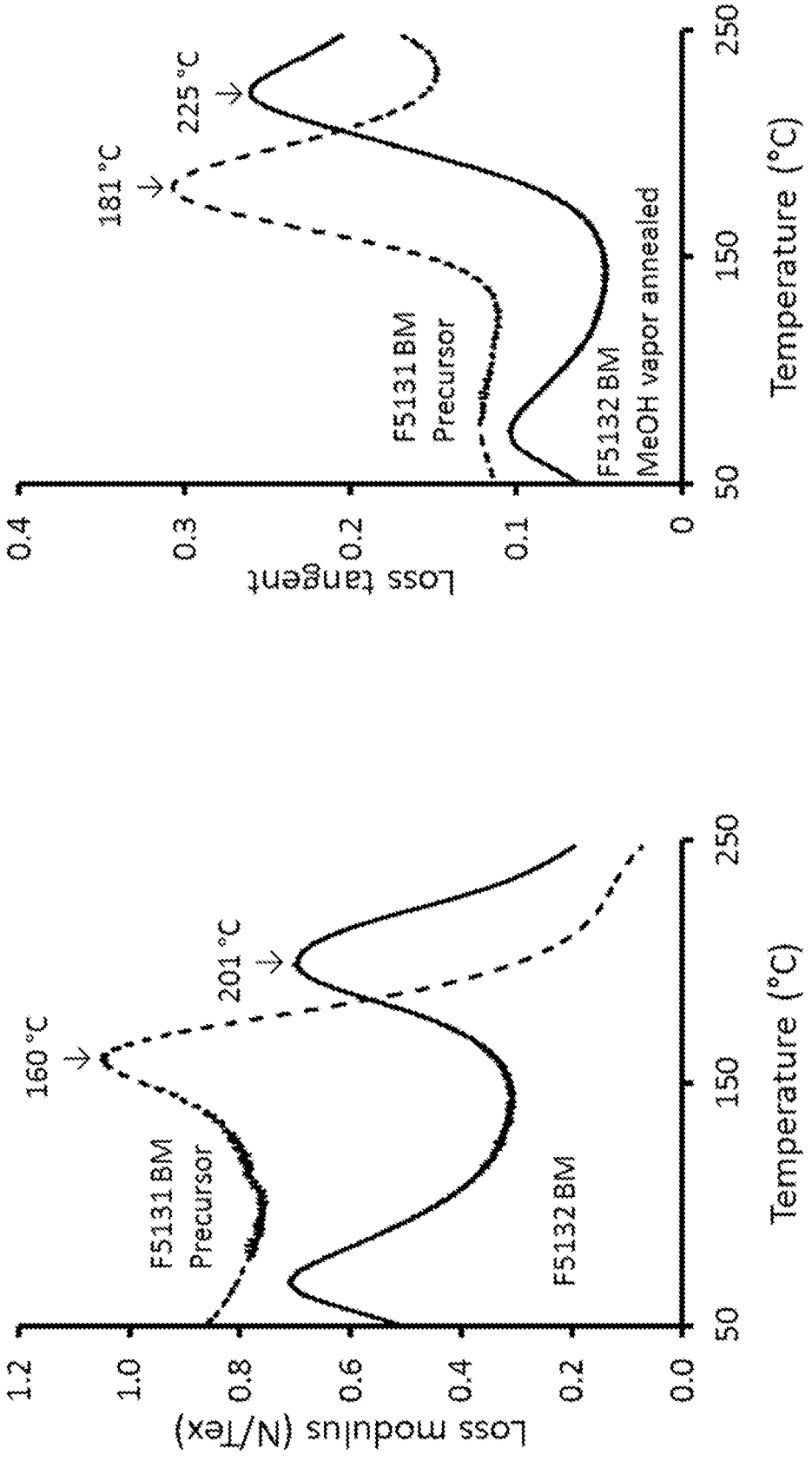

Loss tangent
0.4
0.3
0.2
0.1
0
181 °C
225 °C
F5131 BM
Precursor
F5132 BM
MeOH vapor annealed
50
150
250
Temperature (°C)
Loss modulus (N/Tex)
1.2
1.0
0.8
0.6
0.4
0.2
0.0
160 °C
201 °C
F5131 BM
Precursor
F5132 BM
50
150
250
Temperature (°C)

FIG. 10

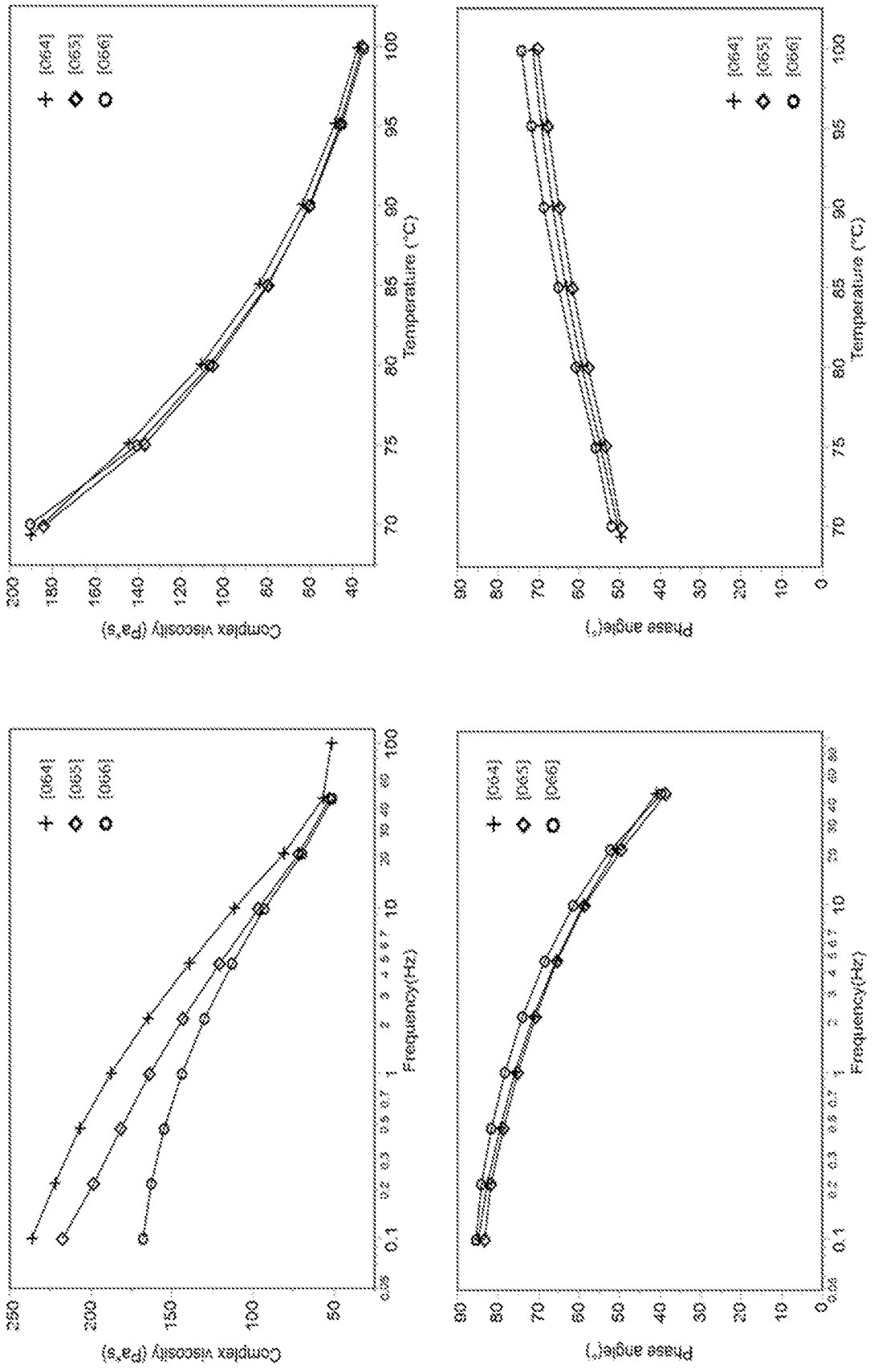

[064]
[065]
[066]
Complex viscosity (Pa*s)
Temperature (°C)
Phase angle(°)
Frequency(Hz)

FIG. 11

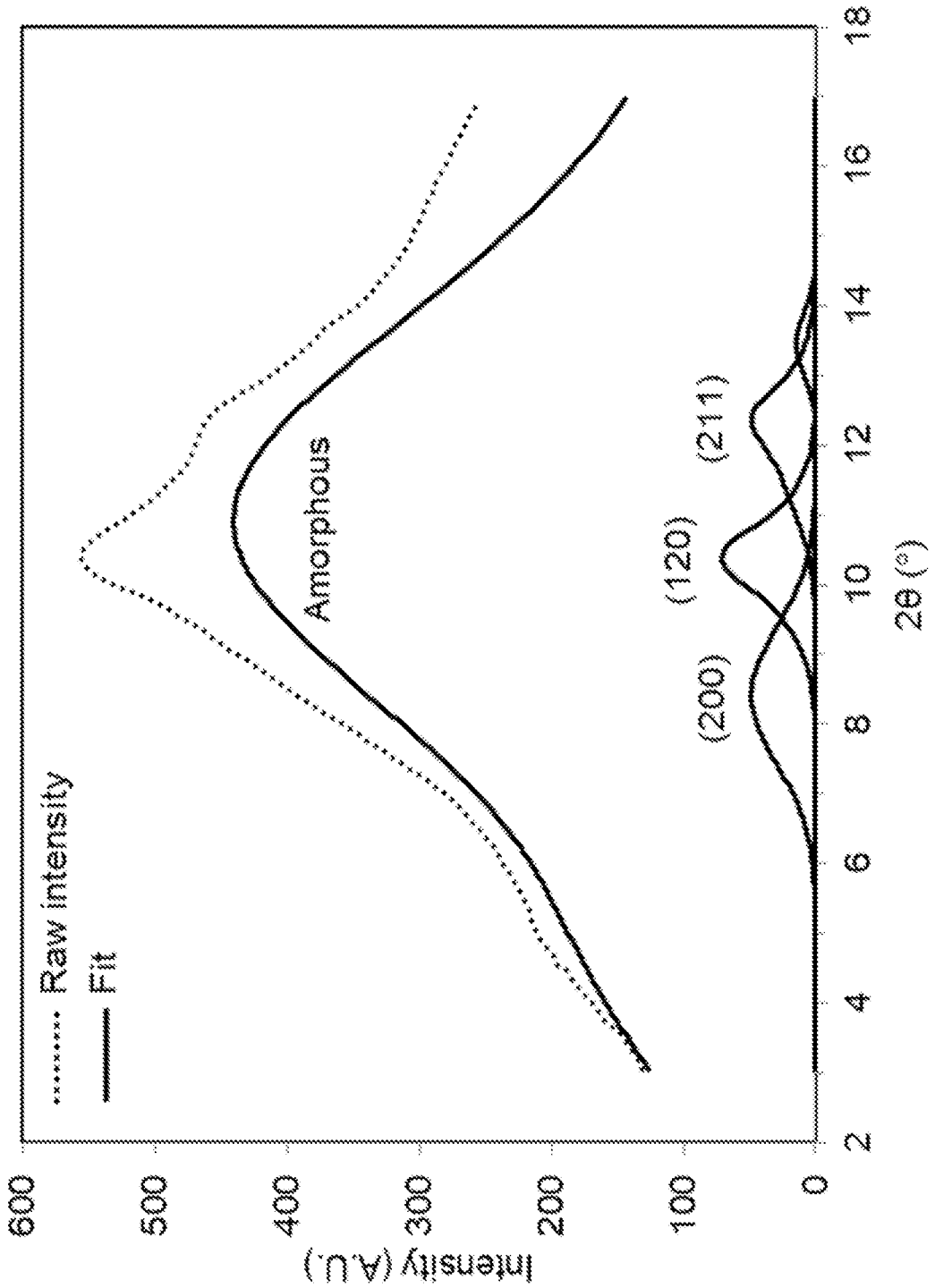

Raw intensity
Fit
Amorphous
(120)
(211)
(200)
Intensity (A.U.)
2θ (°)
600
500
400
300
200
100
0
2
4
6
8
10
12
14
16
18

FIG. 12

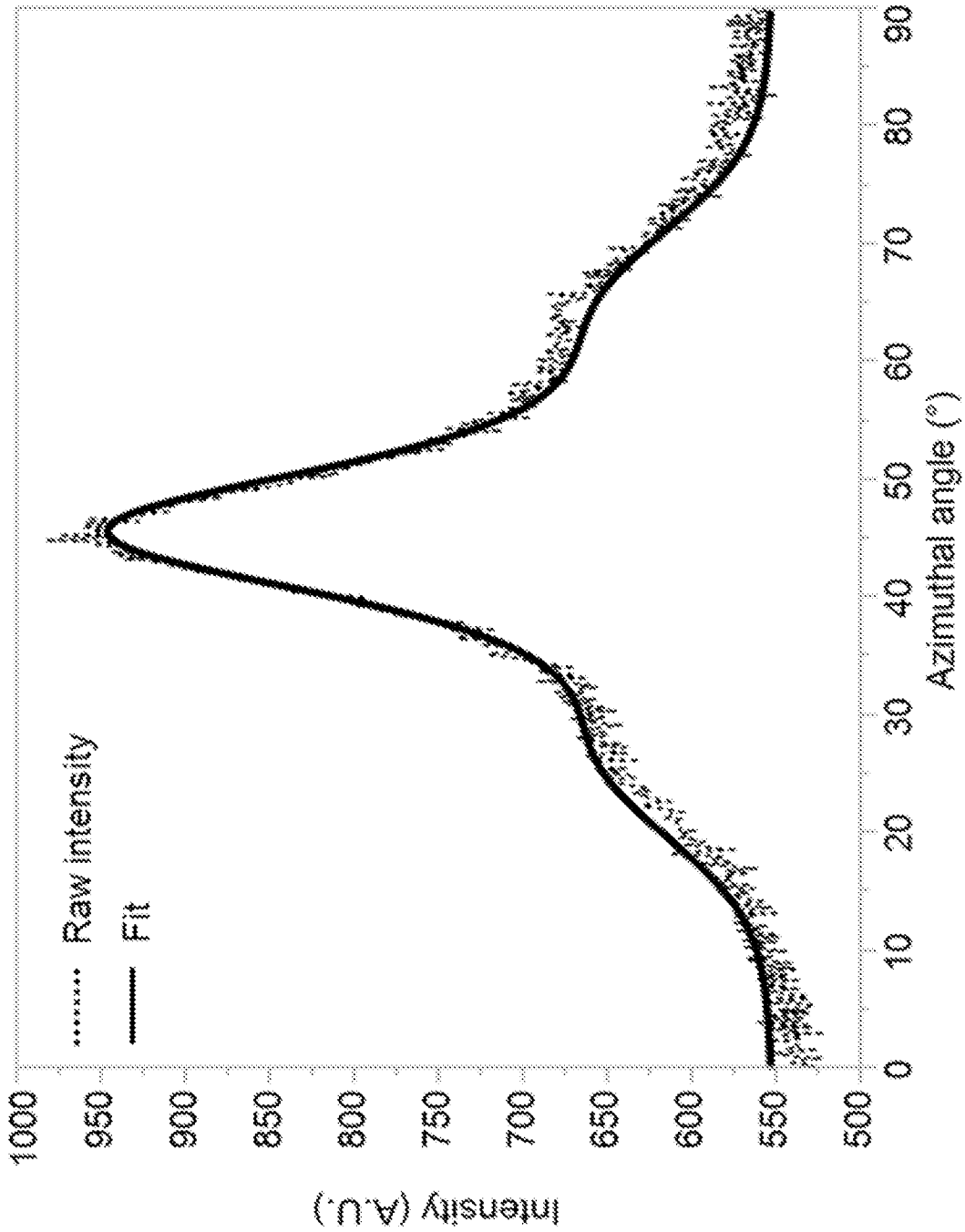

Raw intensity
Fit
Intensity (A.U.)
Azimuthal angle (°)
1000
950
900
850
800
750
700
650
600
550
500
0
10
20
30
40
50
60
70
80
90

FIG. 13

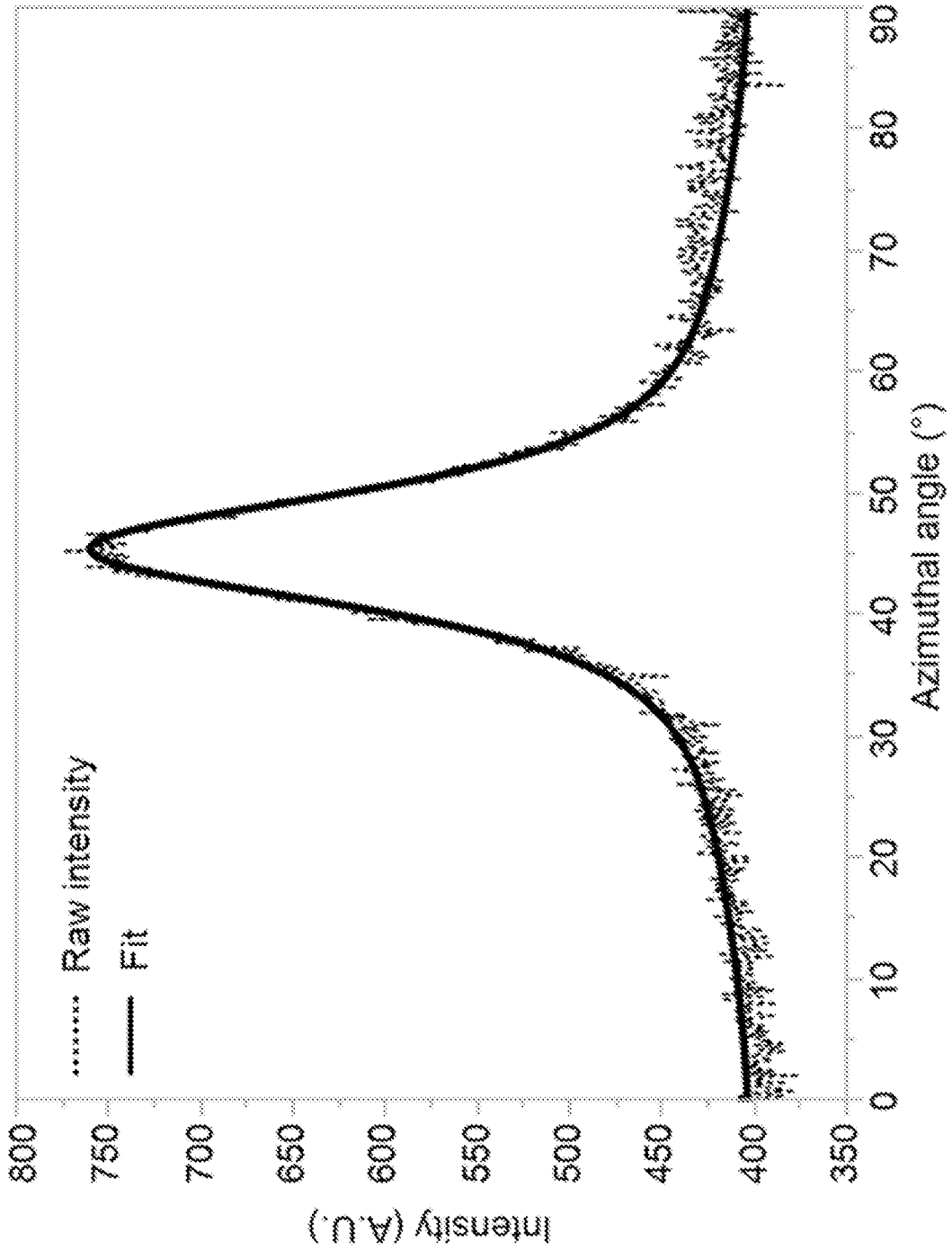

Raw intensity
Fit
Intensity (A.U.)
Azimuthal angle (°)
800
750
700
650
600
550
500
450
400
350
0
10
20
30
40
50
60
70
80
90

FIG. 14

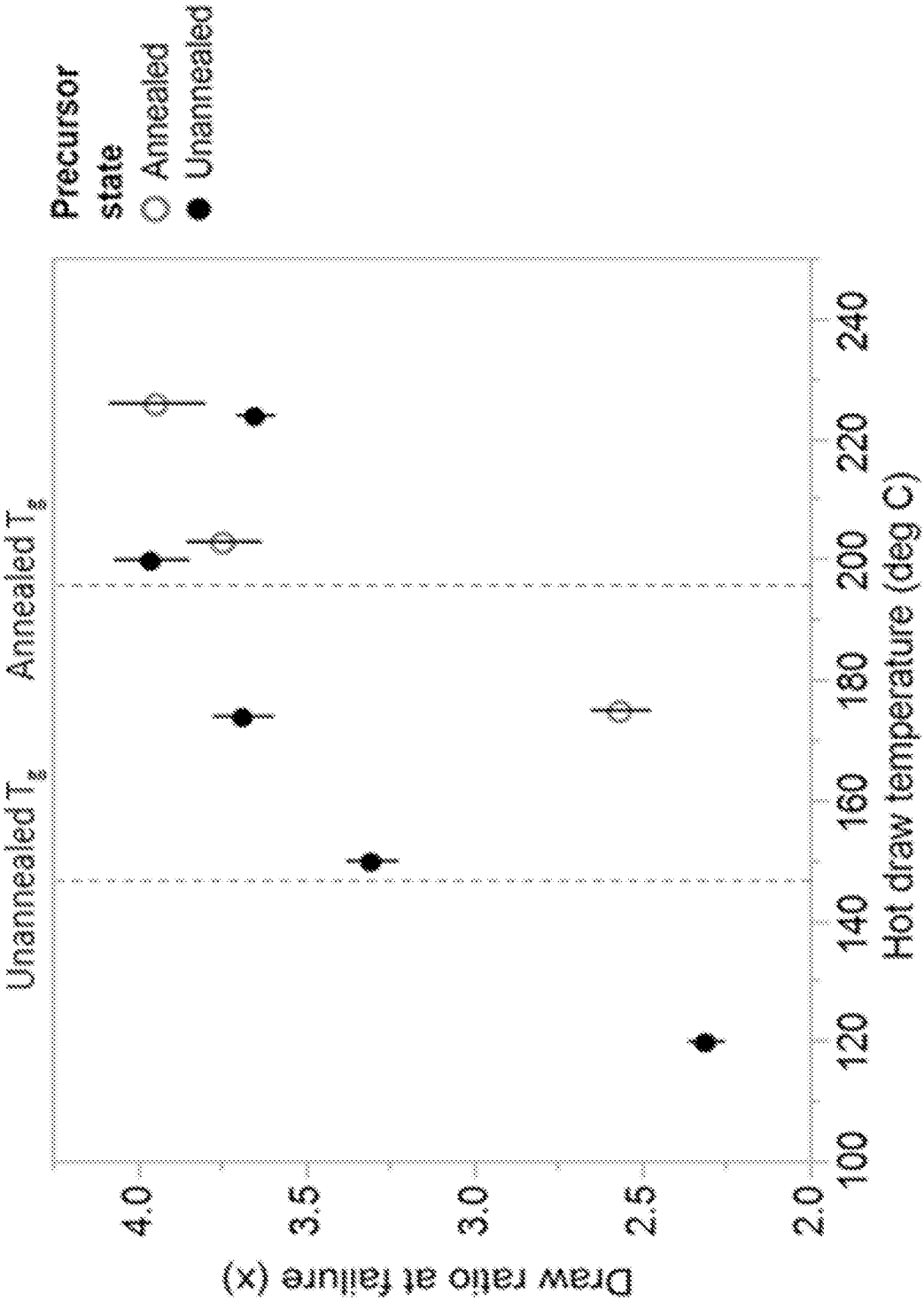

Precursor state
Annealed
Unannealed
Unannealed T_g
Annealed T_g
Draw ratio at failure (x)
Hot draw temperature (deg C)
2.0
2.5
3.0
3.5
4.0
100
120
140
160
180
200
220
240

FIG. 15

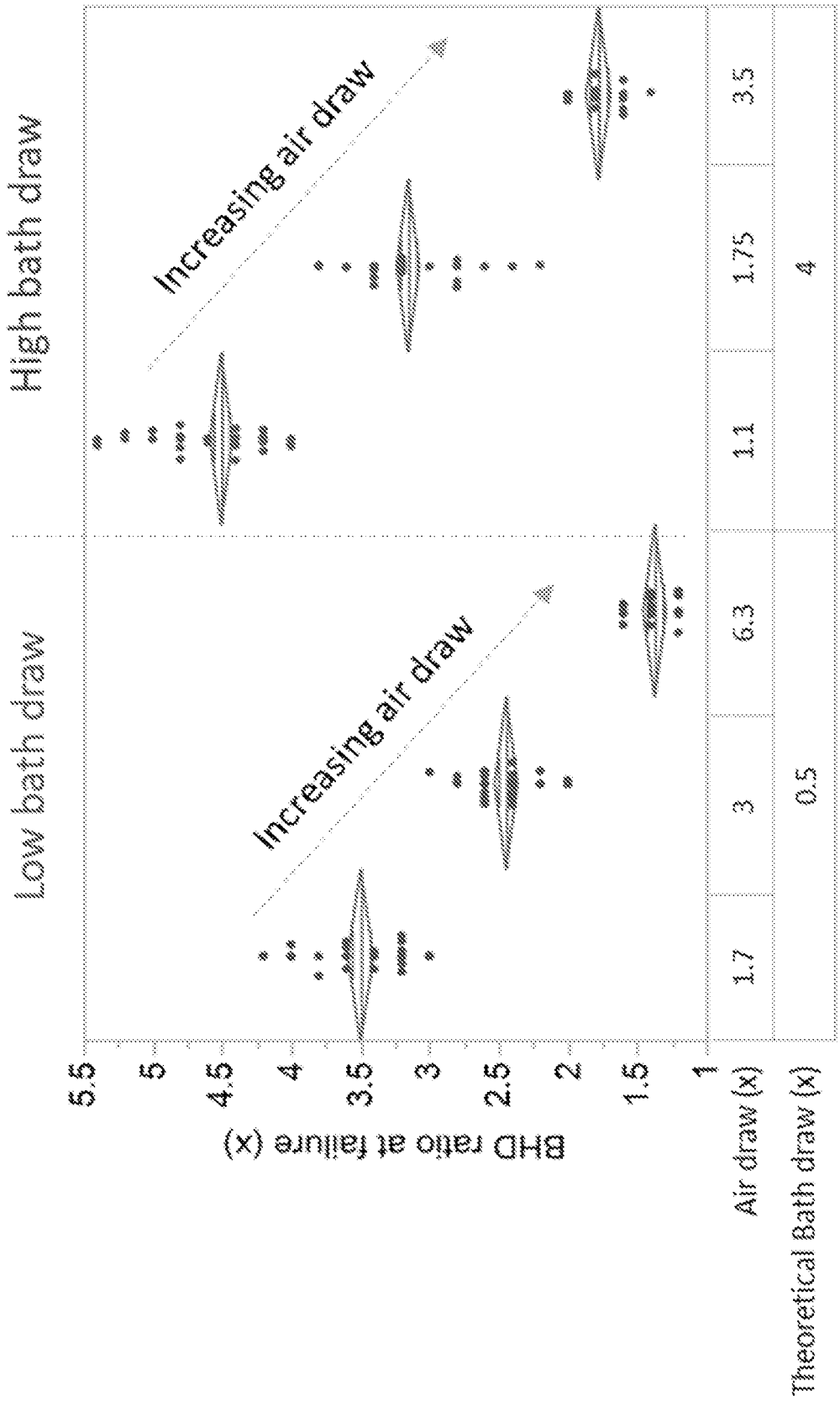

Low bath draw
High bath draw
Increasing air draw
Increasing air draw
BHD ratio at failure (x)
5.5
5
4.5
4
3.5
3
2.5
2
1.5
1
Air draw (x)
Theoretical Bath draw (x)
1.7
3
6.3
1.1
1.75
3.5
0.5
4

FIG. 16

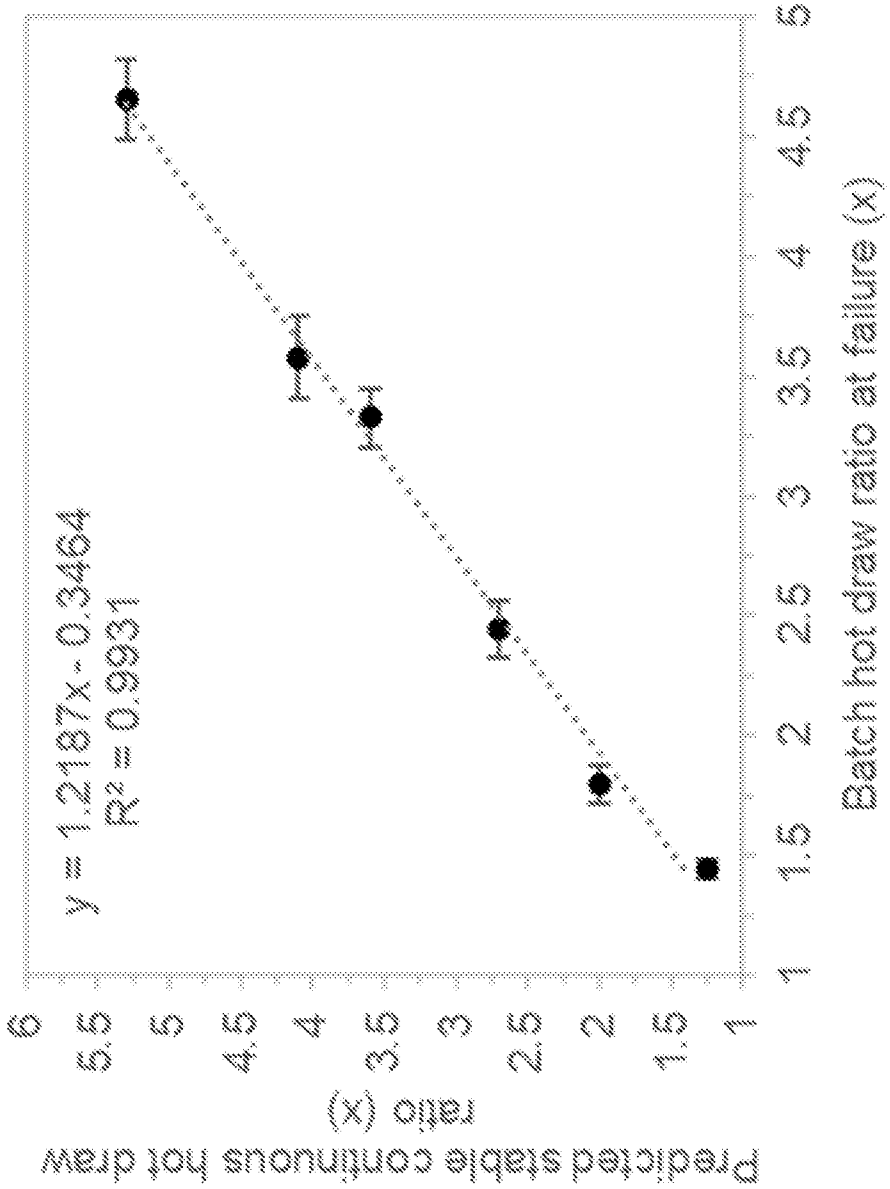

Predicted stable continuous hot draw ratio (x)
Batch hot draw ratio at failure (x)
y = 1.2187x - 0.3464
R² = 0.9931
1
1.5
2
2.5
3
3.5
4
4.5
5
5.5
6

FIG. 17

INTERNATIONAL SEARCH REPORT

International application No.
PCT/US18/52754

A. CLASSIFICATION OF SUBJECT MATTER

IPC - C12N 15/09; C07K 14/435; D01F 6/68, 4/02; D01D 5/24 (2018.01)

CPC - C12N 15/09; C07K 14/43518, 14/43586; D01F 6/68, 4/02; D01D 5/24

According to International Patent Classification (IPC) or to both national classification and IPC

B. FIELDS SEARCHED

Minimum documentation searched (classification system followed by classification symbols)
See Search History document

Documentation searched other than minimum documentation to the extent that such documents are included in the fields searched
See Search History document

Electronic data base consulted during the international search (name of data base and, where practicable, search terms used)
See Search History document

C. DOCUMENTS CONSIDERED TO BE RELEVANT

Category*	Citation of document, with indication, where appropriate, of the relevant passages	Relevant to claim No.
A	(MUNRO, T et al.) Investigation of Synthetic Spider Silk Crystallinity and Alignment via Electrothermal, Pyroelectric, Literature XRD, and Tensile Techniques. Macromolecular Materials and Engineering. April 2017, Epub 30 January 2017, Vol. 302, No. 4; pages 1-18; page 3, paragraph 6 – page 4, paragraph 2; page 6, paragraph 3; DOI: 10.1002/mame.201600480	1-5, 6/1-5, 7/6/1-5, 8/7/6/1-5
A	WO 2016/201369 A1 (BOLT THREADS, INC.) 15 December, 2016; paragraphs [0063], [0077]	1-5, 6/1-5, 7/6/1-5, 8/7/6/1-5
A	(PENG, Q et al.) Role of Humidity on the Structures and Properties of Regenerated Silk Fibers. Progress in Natural Science, 1 October 2015, Vol. 25, No. 5; pages 430-436; abstract; page 431, column 1, paragraph 3; page 431, column 2, paragraph 3; table 2; DOI: 10.1016/j.pnsc.2015.09.006	1-5, 6/1-5, 7/6/1-5, 8/7/6/1-5
P, X	WO 2018/053204 A1 (BOLT THREADS INC.) 22 March, 2018; whole document	1-5, 6/1-5, 7/6/1-5, 8/7/6/1-5

☐ Further documents are listed in the continuation of Box C. ☐ See patent family annex.

* Special categories of cited documents:
"A" document defining the general state of the art which is not considered to be of particular relevance
"E" earlier application or patent but published on or after the international filing date
"L" document which may throw doubts on priority claim(s) or which is cited to establish the publication date of another citation or other special reason (as specified)
"O" document referring to an oral disclosure, use, exhibition or other means
"P" document published prior to the international filing date but later than the priority date claimed
"T" later document published after the international filing date or priority date and not in conflict with the application but cited to understand the principle or theory underlying the invention
"X" document of particular relevance; the claimed invention cannot be considered novel or cannot be considered to involve an inventive step when the document is taken alone
"Y" document of particular relevance; the claimed invention cannot be considered to involve an inventive step when the document is combined with one or more other such documents, such combination being obvious to a person skilled in the art
"&" document member of the same patent family

Date of the actual completion of the international search	Date of mailing of the international search report
21 November 2018 (21.11.2018)	10 DEC 2018
Name and mailing address of the ISA/ Mail Stop PCT, Attn: ISA/US, Commissioner for Patents P.O. Box 1450, Alexandria, Virginia 22313-1450 Facsimile No. 571-273-8300	Authorized officer Shane Thomas PCT Helpdesk: 571-272-4300 PCT OSP: 571-272-7774

INTERNATIONAL SEARCH REPORT

International application No.
PCT/US18/52754

Box No. II Observations where certain claims were found unsearchable (Continuation of item 2 of first sheet)

This international search report has not been established in respect of certain claims under Article 17(2)(a) for the following reasons:

1. ☐ Claims Nos.:
because they relate to subject matter not required to be searched by this Authority, namely:

2. ☐ Claims Nos.:
because they relate to parts of the international application that do not comply with the prescribed requirements to such an extent that no meaningful international search can be carried out, specifically:

3. ☒ Claims Nos.: 9-36
because they are dependent claims and are not drafted in accordance with the second and third sentences of Rule 6.4(a).

Box No. III Observations where unity of invention is lacking (Continuation of item 3 of first sheet)

This International Searching Authority found multiple inventions in this international application, as follows:

1. ☐ As all required additional search fees were timely paid by the applicant, this international search report covers all searchable claims.

2. ☐ As all searchable claims could be searched without effort justifying additional fees, this Authority did not invite payment of additional fees.

3. ☐ As only some of the required additional search fees were timely paid by the applicant, this international search report covers only those claims for which fees were paid, specifically claims Nos.:

4. ☐ No required additional search fees were timely paid by the applicant. Consequently, this international search report is restricted to the invention first mentioned in the claims; it is covered by claims Nos.:

Remark on Protest

☐ The additional search fees were accompanied by the applicant's protest and, where applicable, the payment of a protest fee.

☐ The additional search fees were accompanied by the applicant's protest but the applicable protest fee was not paid within the time limit specified in the invitation.

☐ No protest accompanied the payment of additional search fees.